DOKUZ EYLÜL UNIVERSITY
GRADUATE SCHOOL OF NATURAL AND APPLIED SCIENCES

CATION ANALYSIS OF GEOTHERMAL WATER SAMPLES WITH ION CHROMATOGRAPHY AND SPECTROSCOPIC METHODS

by
Sibel KAÇMAZ

June, 2009
İZMİR

CATION ANALYSIS OF GEOTHERMAL WATER SAMPLES WITH ION CHROMATOGRAPHY AND SPECTROSCOPIC METHODS

A Thesis Submitted to the
Graduate School of Natural and Applied Sciences of Dokuz Eylül University
In Partial Fulfillment of the Requirements for the Master of Science of
Chemistry in Chemistry, Applied Chemistry Program

by
Sibel KAÇMAZ

June, 2009
İZMİR

M.Sc THESIS EXAMINATION RESULT FORM

We have read the thesis entitled **"CATION ANALYSIS OF GEOTHERMAL WATER SAMPLES WITH ION CHROMATOGRAPHY AND SPECTROSCOPIC METHODS"** completed by **SİBEL KAÇMAZ** under supervision of **ASSOC. PROFESSOR KADRİYE ERTEKİN** and we certify that in our opinion it is fully adequate, in scope and in quality, as a thesis for the degree of Master of Science.

Doç. Dr. Kadriye ERTEKİN

Supervisor

Prof. Dr. Ümran YÜKSEL	Doç. Dr. Elif SUBAŞI
(Jury Member)	(Jury Member)

Prof.Dr. Cahit HELVACI
Director
Graduate School of Natural and Applied Science

ACKNOWLEDGEMENTS

I would like to express sincere gratitude to my supervisor Associated Professor Kadriye Ertekin for providing the fascinating subject, for her valuable support during this thesis and for the great working conditions at our laboratory.

Funding for this research was provided by the TUBITAK (Multi-Disciplinary Earthquake Researches in High Risk Regions of Turkey Representing Different Tectonic Regimes – TURDEP Project) and Scientific Research Funds of Dokuz Eylul University.

I want to thank to Associated Professor Sedat İnan, Professor Zafer Akçığ, Associated Professor Mustafa Akgün, Assistant Professor Orhan Polat and Doctor Cemil Seyis for their valuable orientations.

I gratefully acknowledge that my personal funding was provided by the Scientific Research Council of Turkey (TUBITAK) (Multi-Disciplinary Earthquake Researches in High Risk Regions of Turkey Representing Different Tectonic Regimes– TURDEP Project) and Center for Earthquake Research (DAUM) of Dokuz Eylul University.

I also gratefully acknowledge the extensive helps of my colleagues Ph. D. student Merve Zeyrek, Ph. D. student Sibel Derinkuyu and M. Sc. student R.Erim Ongun during experimental studies and sampling respectively.

Finally, I want to thank to my parents and my sister Doctor Hülya Kaçmaz for their tolerant attitude to my working effort during the elaboration of this dissertation and for their incessant support during all the years of my studies.

Sibel KAÇMAZ

CATION ANALYSIS OF GEOTHERMAL WATER SAMPLES WITH ION CHROMATOGRAPHY AND SPECTROSCOPIC METHODS

ABSTRACT

This thesis consists of two complimentary chapters. In the first part, simultaneous ion chromatographic analysis of six cations (lithium, sodium, ammonium, potassium, magnesium, and calcium) in geothermal water samples was performed by ion chromatography method. Some validation tests and the optimum conditions for the determination of cations were studied. Analysis of the cations was performed by injection of samples to the chromatographic system after filtration and/or dilution. The precision and accuracy of the method were tested at three different concentration levels for each standard. Recovery studies were performed by adding standards into the geothermal water and drinking water samples. For geothermal water samples recovery tests was performed between two successive months. Precision was also assessed as the percentage relative standard deviation (%RSD) of both repeatability (within-day) and reproducibility (between-day and different concentrations) for geothermal water samples. SD and RSD values of 320 geothermal water samples acquired during 12 months were evaluated.

The second part consists of analysis of geothermal water samples by spectrophotometric method for Manganese (II), Zinc (II) and Copper (II). The indicator dyes namely [5-phenylazo-8-quinolinol (A-8) and 5-(4-clorophenylazo)-8-quinolinol (A–13)] were offered for the first time for absorption based analysis of Manganese (II), Zinc (II) and Copper (II). The indicator dyes were characterized in the different solvents of ethanol (EtOH), dichloromethane (DCM), tetrahydrofurane (THF) and Toluene/Ethanol (To: EtOH) mixture (80:20)) and in solid matrix of PVC. Maximum absorption wavelength (λabs) and molar extinction coefficients (ε) of the indicators were determined with UV-Vis spectrophotometer in all of the employed matrices. Acidity constant values of two different indicator dyes were calculated in ethanol (EtOH) and polyvinylchloride (PVC). Cross sensitivities of the indicator dyes to other cations and anions was also tested and evaluated.

Keywords: Ion chromatography, geothermal water analysis, chromatographic geothermal water analysis, cation analysis, UV-Vis spectroscopy, Manganese (II), Zinc (II) and Copper (II) analysis.

İYON KROMATOGRAFİ VE SPEKTROSKOPİK METOD İLE JEOTERMAL SU ÖRNEKLERİNDE KATYON ANALİZLERİ

ÖZ

Bu tez iki tamamlayıcı bölümden oluşmaktadır. Birinci bölümde jeotermal su örneklerinde altı katyonun (lityum, sodyum, amonyum, potasyum, magnezyum ve kalsiyum) eşzamanlı analizleri iyon kromatografi metoduyla gerçekleştirilmiştir. Bazı validasyon testleri ve katyonların analizi için optimum koşullar araştırılmıştır. Katyonların analizi filtrasyon ve/veya seyreltme işlemlerinden sonra örneklerin cihaza enjeksiyonu ile gerçekleştirilmiştir. Metodun kesinliği ve doğruluğu her bir standart için üç farklı konsantrasyon düzeyinde incelenmiştir. Geri kazanım çalışmaları standartların jeotermal su ve içme suyu örneklerine eklenmesiyle yapılmıştır. Yeraltı suyu örneklerinde geri kazanım testleri ardışık iki ay ara ile toplanan örnekler üzerinde gerçekleştirilmiştir. Yeraltı suyu örnekleri için kesinlik aynı zamanda gün içi ve günler arası tekrarlanabilirliğin % bağıl standart sapması (%RSD) olarak da araştırılmıştır. Standart sapma ve bağıl standart sapma değerleri on iki ay boyunca toplanan 320 adet jeotermal su örneğinde değerlendirilmiştir.

İkinci kısımda jeotermal su örneklerinde mangan(II), çinko(II) ve bakır(II) analizi spektrofotometrik metotla gerçekleştirilmiştir. [5-fenilazo-8-kinolinol (A-8) ve 5-(4-klorfenilazo)-8-kinolinol (A-13)] indikatör boyaları mangan(II), çinko(II) ve bakır(II) iyonlarının spektrofotometrik analizi için ilk kez önerilmiştir. İndikatör boyalar, etanol, diklorometan, tetrahidrofuran, toluen-etanol karışımı (80:20) çözücülerinde ve katı matriks olan polivinil klorür (PVC) de karakterize edilmiştir. İndikatör boyaların maksimum absorpsiyon dalga boyu (λabs) ve molar absorptivite katsayıları (ε) yukarıda söz edilen tüm matrikslerde UV-Vis spektrofotometresi ile belirlenmiştir. Boyar maddelerin asitlik sabitleri ile diğer metal katyonlarına ve anyonlara olan yanıtları da test edilip değerlendirilmiştir.

Anahtar Kelimeler: İyon kromatografi, jeotermal su analizi, kromatografik jeotermal su analizi, katyon analizi, UV-görünür bölge spektroskopisi, mangan(II), çinko(II), bakır(II) analizi.

CONTENTS **Page**

CHAPTER ONE

AN INTRODUCTION TO GEOTHERMAL WATER CHEMISTRY

Water may contain a wide variety and concentration of dissolved constituents. The simplest chemical parameters often quoted to characterize in water are:

1. Total dissolved solids (TDS) in parts per million (ppm) or milligrams per liter (mgL^{-1}). This gives a measure of the amount of chemical salts dissolved in the waters.

2. pH. The pH of a fluid is a measure of the acidity or alkalinity of the fluid. Neutral fluids have pH = 7 at room temperature. Acid fluids have pH values <7 and alkaline fluids have pH values >7

These two parameters can be measured in the field by use of a conductivity meter and a pH meter. The conductivity meter measures the TDS of a fluid by measuring its electrical conductivity (taken from geoheat.oit.edu/pdf/bulletin/bi015.pdf).

1.1 Chemical Character of Geothermal Water

The amount and nature of dissolved chemical species in geothermal fluids are functions of temperature and of the local geology. Lower-temperature resources usually have a smaller amount of dissolved solids than do higher temperature resources, although there are exceptions to this rule. TDS values range from a few hundred to more than 300.000 mg/L

The pH of geothermal resources ranges from moderately alkaline (8.5) to moderately acid (5.5). The dissolved solids are usually composed mainly of sodium (Na^{+}), calcium (Ca^{2+}), potassium (K^{+}), chlorine (Cl^{-}), silica ($Si0_2$), sulfate ($S0_4^{2-}$), and bicarbonate ($HC0_3^{-}$). Minor constituents include a wide range of elements with mercury (Hg^{2+}), fluorine (F^{-}), boron (B) and arsenic (As) being toxic in high enough concentrations and therefore, are of environmental concern. In general, each state has

regulations governing the use and disposal of waters that contain toxic or otherwise harmful constituents, and local regulations should always be consulted in planning the use of any geothermal resource. Dissolved gases usually include carbon dioxide (CO_2), hydrogen sulfide (H_2S), ammonia (NH_3) and methane (CH_4). Hydrogen sulfide (H_2S) is a safety hazard because of its toxicity to animals, including humans. Effective means have been and are still being developed to handle the scaling, corrosion, and environmental problems caused by dissolved constituents in geothermal fluids.

As geothermal fluids move through rocks, they react chemically with the rocks, which themselves are usually chemically complex. Certain minerals in the reservoir rocks may be selectively dissolved by the fluids while other minerals may be precipitated from solution or certain chemical elements from the fluid may substitute for certain other elements within a mineral. These chemical/mineralogical changes in the reservoir rocks may or may not cause volume changes, i.e., may or may not affect the permeability and porosity of the rocks. Obviously, if the mineral volume increases, it must be at the expense of open space in the rock, which caused a decrease in permeability. In locations where pressure, temperature, or rock chemistry change abruptly, minerals may be precipitated into the open spaces. This results in plugging of the plumbing system.

SiO_2 and $CaC0_3$ are the principal minerals usually involved. The solubility of $Si0_2$ decreases with a decrease in temperature, with pressure changes having very little effect. $Si0_2$ can be precipitated into open spaces such as fractures or pores in the rock in regions where the subsurface temperature changes abruptly and at the subsurface where hot springs discharge. Calcium carbonate has a retrograde solubility, i.e., it is more soluble at low temperatures than at high temperatures. Other carbonate species such as $MgC0_3$, as well as sulfate species such as $CaS0_4$, show similar retrograde solubility relationships with temperature. In addition, the solubility of carbonate minerals decreases rapidly with a decrease in the partial pressure of carbon dioxide. Thus, as fluids that are saturated with carbonate approach the surface, carbonate minerals such as $CaC0_3$ are deposited as a result of the loss of $C0_2$, which evolves

from the solution with the decrease in hydrostatic pressure (taken from geoheat.oit.edu/pdf/bulletin/bi015.pdf).

Most of the major, minor, trace constituents and organic compounds dissolved in geothermal water and information concerning ranges of concentration are given below (See Table 1.1).

Table 1.1 Dissolved constituents in geothermal water classified by relative abundance (taken from http://jan.ucc.nau.edu/~doetqp-p/courses/env302/lec35/LEC35.html)

Major constituents (> 5 mg/L)	
Cations	Anions
Magnesium	Bicarbonate
Calcium	Chloride
Sodium	Sulfate
Minor constituents (0.01 to 10.0 mg/L)	
Boron	Carbonate
Iron	Fluoride
Potassium	Nitrate
Strontium	

Trace constituents (< 0.1 mg/L)			
Aluminum	Antimony	Arsenic	Barium
Beryllium	Bismuth	Bromide	Cadmium
Cerium	Cesium	Chromium	Cobalt
Copper	Gallium	Germanium	Gold
Indium	Iodide	Lanthanum	Lead
Lithium	Manganese	Molybdenum	Nickel
Niobium	Phosphate	Platinum	Radium
Rubidium	Ruthenium	Scandium	Selenium
Silver	Thallium	Thorium	Tin
Titanium	Tungsten	Uranium	Vanadium
Yttrium	Zinc	Zirconium	

(taken from *(*faculty.kfupm.edu.sa/ES/shaibani/16-Dissolved%20Mass%20in%20GW.ppt)

Organic Compounds(shallow)	Organic Compounds(Deep)
Humic acid	Acetate
Fulvic acid	Propionate
Carbohydrates	
Amino acids	
Tannis	
Lignins	
Hyrocarbons	

1.2 Techniques for Chemical Analysis of Geothermal Water

Due to the diversity and complex nature of the samples; accurate analysis of geothermal waters has been an important issue for scientists and the determination of ions in complex matrices remained one of complicated areas of analytical chemistry. Numerous analytical techniques have been proposed for determination of cations in water samples, the most widely used are capillary electrophoresis (Antonio Jurado-Gonza´lez, Dolores Galindo-Rian˜o, & Garcı´a-Vargas, 2003; Motellier, Petit, & Decambox, 2000.), spectrophotometric (Nyman & Ivaska, *1995;* Fátima Barroso, Silva, Ramos, Oliva-Teles, Delerue-Matos, Goreti, Sales, & Oliveira, 2009.), atomic absorption spectrometry (AAS), and inductively coupled plasma-atomic emission spectrometry (ICP-AES) (Ozcan, & Yilmaz, 2005; Liu, Wu, Li, & Ga, 1999; Muller, 1999; Chakrapani, Murty, Mohanta, & Rangaswamy, 1998), Inductively coupled plasma – optical emission spectrometry / mass spectrometry (ICP-OES/MS), Inductively coupled plasma- mass spectrometry (ICP-MS), and Gas chromatography–mass spectrometry (GC-MS) (Otero-Roman´ı, Moreda-Pi˜neiro, Bermejo-Barrera, & Martin-Esteban, 2009; Afton, Kubachka, Catron, & Caruso, 2008; Fries, & Klasmeier, 2009), electrochemical (voltametric, ion-selective electrodes, amperometric, and coulometric), potentiometric and titration (Komy, 1993; Chen, & Adams, 1998; Mascini, 1971).

However these methods are sometimes difficult to apply for cation analysis because of some restrictions like large volume of sample needed, effect of the matrix and unsatisfactory selectivity.

Recently, some instrumental analytical methods for simultaneous analysis have been proposed. Ion chromatography (IC) is particularly useful for the separation, identification, and quantification of ions at the mg/L or μg/L level and offers good reproducibility, high sensitivity, selectivity and gives results in a short time (Ohta, & Tanaka, 1998; Wang, Wu, Chen, Lin, & Wu, 2008; Rong, Lim, & Takeuchi, 2007; Gros, Camões, Oliveira, Silva, 2008; Niedzielski, 2005; Vaaramaa, & Lehto, 2003).

CHAPTER TWO

ION CHROMATOGRAPHY

2.1 Introduction to Ion Chromatography

Ion chromatography (IC) is an established and popular technique for analyzing charged species. Complex mixture of anions, cations and transition metals can be separated and quantitated in a relatively short time. Separation can be done by ion exchange, ion exclusion, ion pairing or reversed-phase, using a column filled with specially designed ion exchange resin (taken from www.bioscreen.com/ pdf/tech%20bulletin %20ionchromatographybulletin.pdf).

Ion Exchange chromatography is probably the most frequently used chromatographic technique for the separation of different species. Table 2.1 gives some idea of the breadth of application of ion chromatography at the present time **(**Small, 1989).

Table 2.1 Types of Samples Analyzed by Ion Chromatography(taken from Small, 1989)

Acid rain	Ores
Analgesics	Pesticides
Chemicals	Pharmaceuticals
Detergents	Physiological fluids
Drinking water	Plating baths
Fermentation broths	Protein hydrolysates
Fertilizers	Pulping liquors
Foods and beverages	Soil and plant extracts
High-purity water	Waste water

The determination of ionic species in solution is a classical analytical problem with a variety of solutions. In the field of cation analysis alternative fast and sensitive analytical methods (AAS, ICP, polarography, and others) have been available for a

long time. Conventional wet-chemical methods such as titration, photometry, gravimetry, turbidimetry, and colorimetry are all labor-intensive, time-consuming, and occasionally troublesome. In contrast, ion chromatography offers the following advantages (Weiss, 2004): speed, sensitivity, selectivity, simultaneous detection and stability of the separator columns.

2.2 Classification in IC

Ion exchange chromatography or ion chromatography (IC) is a subdivision of HPLC (Eith, Kolb, Seubert, & Viehweger, 2001). Four types of high performance liquid chromatography (HPLC):

- Partition
- Adsorption (liquid-solid)
- **İon exchange**
- Size exclusion or gel

An older, more general definition is for defining ion chromatography: **"Ion chromatography includes all rapid liquid chromatography separations of ions in columns coupled online with detection and quantification in a flow through detector."** (Schwedt, & Fresenius, 1985). This definition characterizes ion chromatography irrespective of the separating mechanism and detection method while at the same time distinguishing it from classical ion exchange. The following separation principles apply in ion chromatography: ion exclusion, ion pair formation, ion exchange.

Chromatography methods are defined by the chief separation mechanism used. Today ion exchange chromatography is simply known as ion chromatography (IC), while ion pair chromatography (IPC) and ion exclusion chromatography (IEC) are regarded as being more specialized applications (Eith, Kolb, Seubert, & Viehweger, 2001).

2.2.1 Ion-Exclusion Chromatography (HPICE)

(High Performance Ion Chromatography Exclusion)

Ion exclusion chromatography (IEC) is mainly used for the separation of weak acids or bases (Weiß, 1991; Haddad, & Jackson, 1990). The greatest importance of IEC is for the analysis of weak acids such as carboxylic acids, carbohydrates, phenols or amino acids. Figure 2.1 shows the separation principle of IEC using an R - COOH carboxylic acid as an example (Eith, Kolb, Seubert, & Viehweger, 2001).

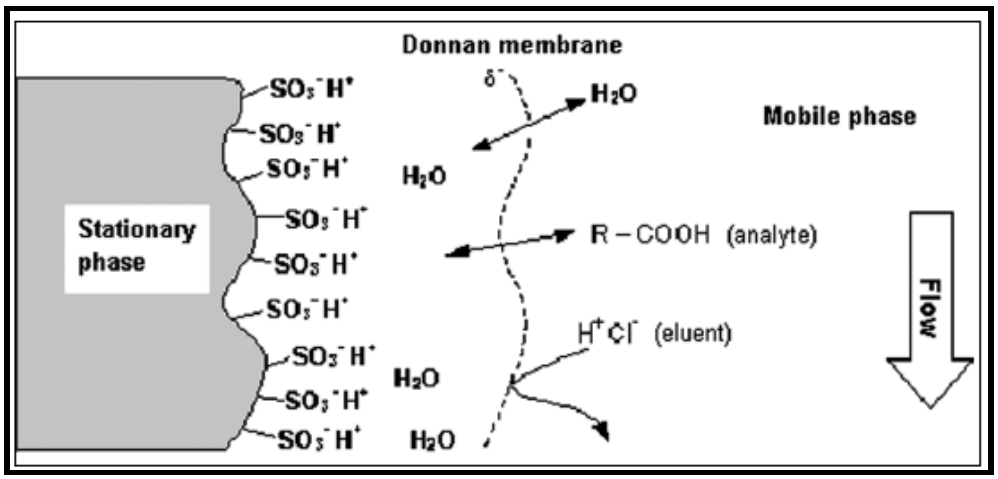

Figure 2.1 Donnan exclusion as the separation principle in ion exclusion chromatography (IEC) (taken from www.metrohmpeak.com/ pdf/8_792_5003_practical. Pdf)

The separation mechanism in ion-exclusion chromatography is governed by Donnan exclusion, steric exclusion, sorption processes and, depending on the type of separator column, by hydrogen bonding. A high-capacity, totally sulfonated cation exchange material based on polystyrene/divinylbenzene is employed as the stationary phase. In case hydrogen bonding should determine selectivity, significant amounts of methacrylate are added to the styrene polymer. Ion-exclusion chromatography is particularly useful for the separation of weak inorganic and organic acids from completely dissociated acids which elute as one peak within the void volume of the column. In combination with suitable detection systems, this separation method is also useful for determining amino acids, aldehydes, and alcohols (Weiss, 2004).

2.2.2 Ion-Pair Chromatography (MPIC)

(Mobile Phase Ion Chromatography)

With the aid of ion pair chromatography it is possible to separate the same analytes as in ion exclusion chromatography, but the separation mechanism is completely different. The stationary phases used are completely polar reversed phase materials such as are used in distribution chromatography. A so-called ion pair regent is added to the eluents; this consists of anionic or cationic surfactants such as tetraalkylammonium salts or n-alkylsulfonic acids. Together with the oppositely charged analyte ions the ion pair reagents form an uncharged ion pair, which can be retarded at the stationary phase by hydrophobic interactions. Separation is possible because of the formation constants of the ion pairs and their different degrees of adsorption. Figure 2.2 shows a simplified static ion exchange model in which it is assumed that interactions with the analytes only occur after adsorption of the ion pair reagent at the stationary phase (Eith, Kolb, Seubert, & Viehweger, 2001).

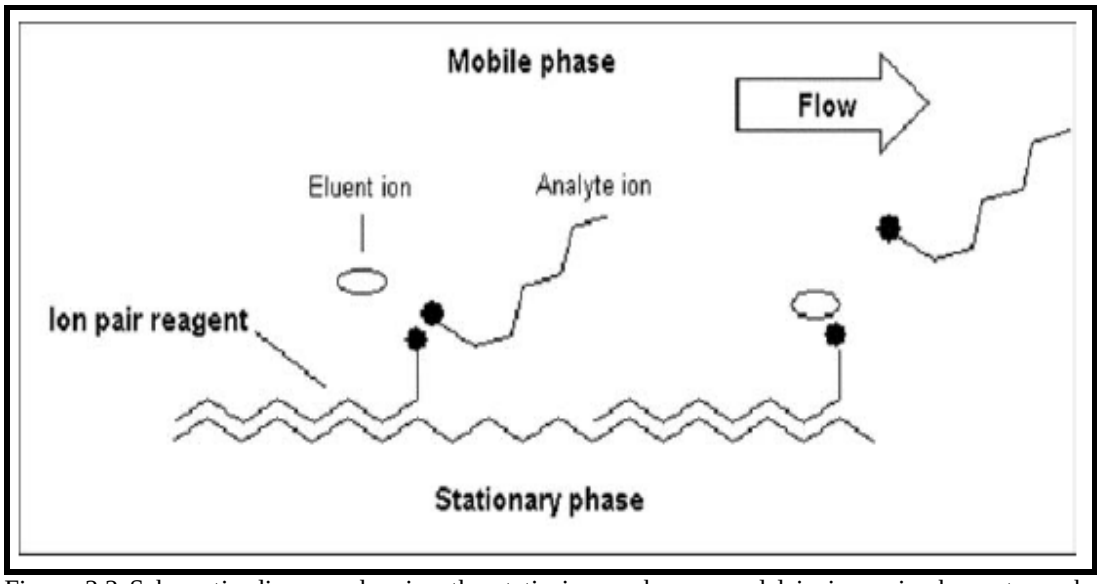

Figure 2.2 Schematic diagram showing the static ion exchange model in ion pair chromatography (MIPC). The separation principle applies to both anions and cations (taken from www.metrohmpeak.com/ pdf/8_792_5003_practical. Pdf)

2.2.3 Ion-Exchange Chromatography (HPIC)

(High Performance Ion Chromatography)

Ion exchange chromatography (IC) is based on a stoichiometric chemical reaction between ions in a solution and a normally solid substance carrying functional groups which can fix ions as a result of electrostatic forces. In the simplest case in cation chromatography these are sulfonic acid groups, in anion chromatography quaternary ammonium groups.

In theory ions with the same charge can be exchanged completely reversibly between the two phases. The process of ion exchange leads to a condition of equilibrium. The side towards which the equilibrium lies depends on the affinity of the participating ions to the functional groups of the stationary phase. Figure 2.3 is a schematic diagram showing the Exchange processes for cations and anions. The analyte ions are marked A, the eluent ions competing with them for the exchange positions with E (Eith, Kolb, Seubert, & Viehweger, 2001).

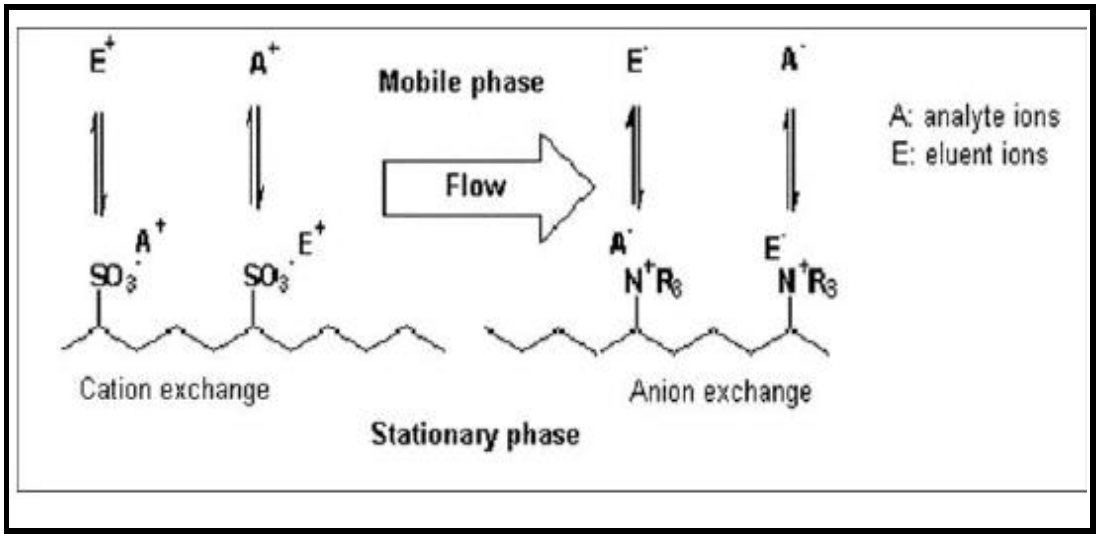

Figure 2.3 Schematic diagram showing the ion exchange process in ion chromatography. Left: cation exchange, right: anion exchange (taken from www.metrohmpeak.com/ pdf/8_792_5003_practical. Pdf)

2.3 The theory of Ion Chromatographic Separation and Detection

Separation in ion exchange chromatography depends upon the reversible adsorption of charged solute molecules to immobilized ion exchange groups of opposite charge (taken from sbio.uct.ac.za/sbio/documentation/ ion_exchange _chromatography.pdf).

For example, ions can be separated on a cation-anion exchange resin columns with a dilute solution as the eluent (mobile phase). Introduction of the sample causes ions to be taken up in a band (zone) near the top of the column by ion exchange (Fritz, & Gjerde, 2000).

Both of ions of mobile phase and sample components in ionic composition compete with each other for attaching to the opposite charge resin. The sample ions bind to the counter ions of the resin. While the ions which strongly tied up to the resin retain inside the column for long time; neutral or unavailable charged ions move faster down and leave the column first (Fritz, & Gjerde, 2000).

The major requirements of systems used in modern ion chromatography can be summarized as follows:

1. An efficient cation- or anion-exchange column with as many theoretical plates as possible.
2. An eluent that provides reasonable differences in retention times of sample ions.
3. A resin-eluent system that attains equilibrium quickly so that kinetic peak broadening is eliminated or minimized.
4. Elution conditions such that retention times are in a convenient range-not too short or too long.
5. An eluent and resin those are compatible with a suitable detector (Fritz, & Gjerde, 2000).

2.3.1 Mechanism of Separation

Most ion-exchanged experiments are performed in four main stages: (taken from http://www.rmpr.cnrs.fr/j1pr/5__techniques_de_purification/ion_exchange.swf).

- Equilibration
- Sample application and wash
- Elution and Regeneration
- Detection

Equilibration; To perform a separation, the eluent is first pumped through the system until equilibrium is reached, as evidenced by a stable baseline. The time needed for equilibrium to be reached may vary from a couple of minutes to an hour or longer, depending on the type of resin and eluent that is used. During this step the ion-exchange sites will be converted to the E^+ form: Resin-Q^- $\mathbf{E}^+$ (See Figure 2.4).

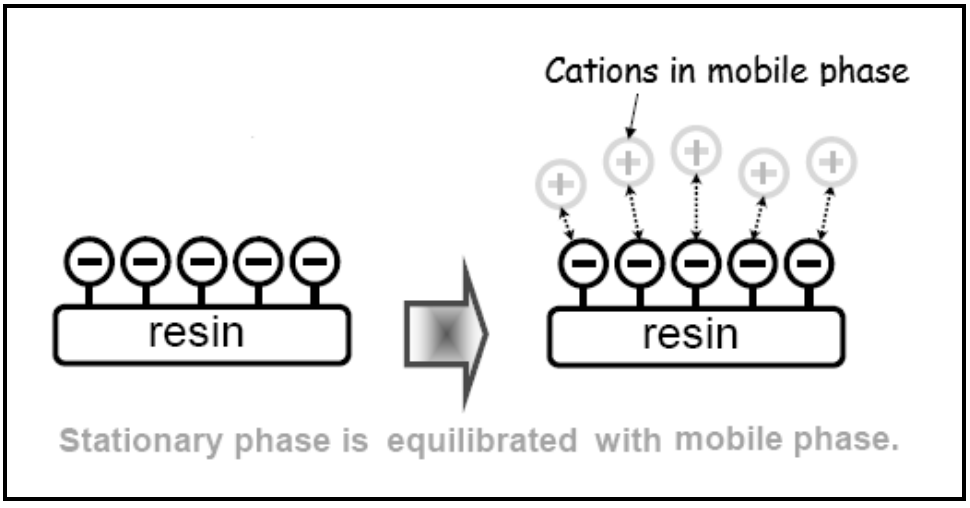

Figure 2.4 Equilibration (taken from www.thairohs.org/index.php?)

Sample application and wash; An analytical sample can be injected into the system as soon as a steady baseline has been obtained. A sample containing cations A_1^+, A_2^+, A_3^+.....A_i^+ undergoes ion-exchange with the exchange sites near the top of the chromatography column (Fritz, & Gjerde, 2000) (See Figure 2.5).

$$\mathbf{A_1}^+ \; + \; \text{Resin-Q}^- \mathbf{E}^+ \rightarrow \text{Resin-Q}^- \text{A}_1^+ \; + \; \text{E}^+$$

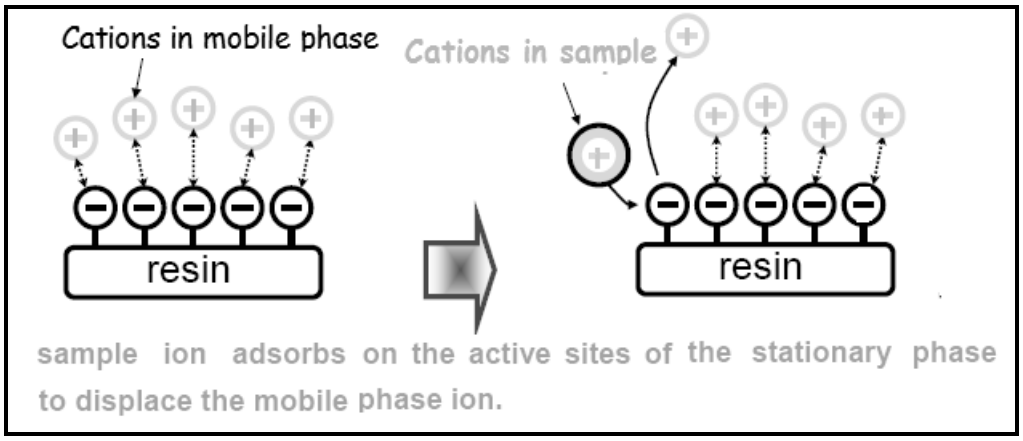

Figure 2.5 Sample applications (taken from www.thairohs.org/index.php*?)*

If the total anion concentration of the sample happens to be exactly the same as that of the eluent being pumped through the system, the total ion concentration in the solution at the top of the column will remain unchanged. However, if the total ion concentration of the sample is greater than that of the eluent, the concentration of E^+ will increase in the solution at the top of the column due to the exchange reaction shown above (Figure 2.6). This zone of higher E^+ concentration will create a ripple effect as the zone passes down the column and through the detector. This will show up as the first peak in the chromatogram, which is called the injection peak.

A sample of lower total ionic concentration than that of the eluent will create a zone of lower E^+ concentration that will ultimately show up as a negative injection peak. The magnitude of the injection peak (either positive or negative) can be used to

estimate the total ionic concentration of the sample compared with that of the eluent. Sometimes the total ionic concentration of the sample is adjusted to match that of the eluent in order to eliminate or reduce the size of the injection peak. The intensity of the injection peak may give an idea regarding the concentration of the analyte. In case of a small injection peak, the analyte concentration can be concluded as high.

Conversely, a high injection peak can be indicator of a small analyte concentration on an ion chromatogram (Fritz, & Gjerde, 2000).

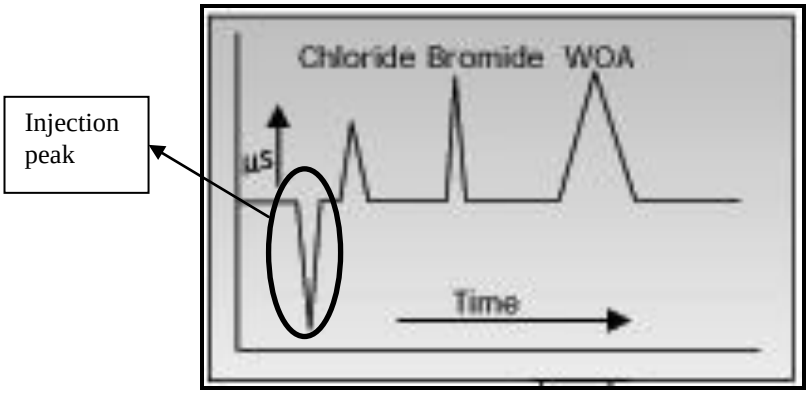

Figure 2.6 The injection peak (taken from http://www.residues.com/ion_chromatography.html)

Behind the zone in the column due to sample injection, the total cation concentration in the column solution again becomes constant and is equal to the E^+ concentration in the eluent. However, continuous ion exchange will occur as the various sample cations compete with E^+ for the exchange sites on the resin. As eluent, containing E^+ continues to be pumped through the column, the sample cations will be pushed down the column. The separation is based on differences in the ion-exchange equilibrium of the various sample cations with the eluent cation, E^+. Thus, if sample ion A_1^+ has a lower affinity for the resin than ion A_2^+, then A_1^+ will move at a faster rate through the column than A_2^+ (Fritz, & Gjerde, 2000).

Elution and Regeneration; In the elution step, pumping eluent through the column results in multiple ion-exchange equilibria along the column in which the sample ions and eluent ions compete for ion-exchange sites next to the Resin-Q^- groups (See Figure 2.7).

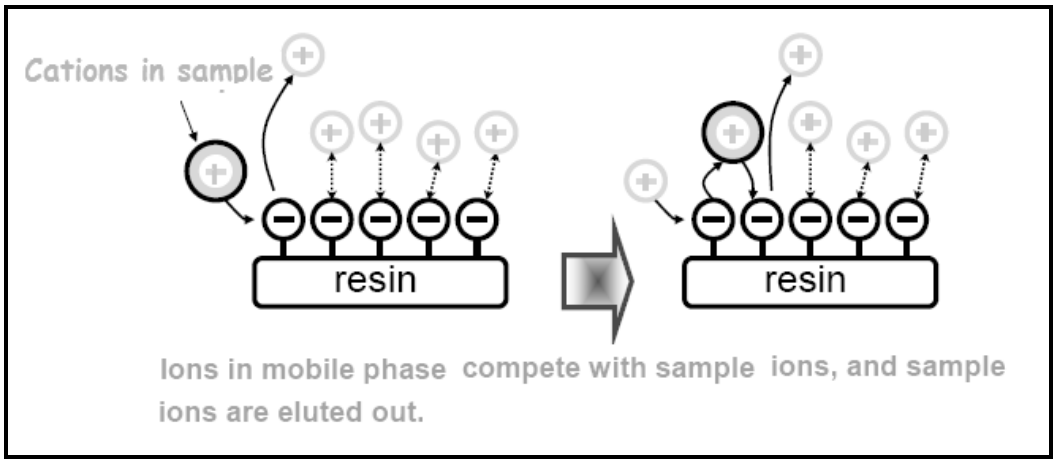

Figure 2.7 Elution (taken from www.thairohs.org/index.php?)

Elution:	Cl^-E^+ + Resin-Q^-	→	Resin-Q^-E^+ + Cl^-
A_1:	$Cl^-A_1^+$ + Resin-Q^-E^+	→	Resin-$Q^-A_1^+$ + Cl^-E^+
A_2:	$Cl^-A_2^+$ + Resin-Q^-E^+	→	Resin-$Q^-A_2^+$ + Cl^-E^+

The net result is that both A_1^+ and A_2^+ move down the column. If A_1^+ has a greater affinity for the Q^- sites than A_2^+ has, the A_1^+ moves at a slower rate Due to their differences in rate of movement, A_1^+ and A_2^+ are gradually resolved into separate zones or bands (Fritz, & Gjerde, 2000). The solid phase in each of these zones contains some E^+ as well as the sample ion, A_1^+ or A_2^+. Likewise, the liquid phase contains some E^+ as well as A_1^+ or A_2^+. The total anionic concentration (A_1^+ + E^+ or A_2^+ + E^+) is equal to that of the eluent in each zone (Fritz, & Gjerde, 2000).

Detection; Continued elution with eluent causes the sample ions to leave the column and pass through a small detector cell. If a conductivity detector is used, the conductance of all of the cations, plus that of the anions will contribute to the total conductance. If the total ionic concentration remains constant, how can a signal be obtained when a sample cation zone passes through the detector? The answer is that the equivalent conductance of A_1^+ and A_2^+ is much lower than that of E^+. The net result is a decrease in the conductance measured when the A_1^+ and A_2^+ zones pass through the detector (Fritz, & Gjerde, 2000).

The total ionic concentration of the initial sample zone was higher than that of the eluent. This zone of higher ionic concentration will be displaced by continued pumping of eluent through the column until it passes through the detector. This will cause an increase in conductance and a peak in the recorded chromatogram called an injection peak. If the total ionic concentration of the injected sample is lower than that of the eluent, an injection peak of lower conductance will be observed. The injection peak can be eliminated by balancing the conductance of the injected sample with that of the eluent. Strasburg et al. studied injection peaks in some detail **(**Strasburg, Fritz, Berkowitz, & Schmuckler, 1989).

In suppressed cation chromatography, the effluent from the ion exchange column comes into contact with an anion-exchange device (Anex-OH^-) just before the liquid stream passes into the detector.

The background conductance of the eluent entering the detector is thus very low because virtually all ions have been removed by the suppressor unit. However, when a sample zone passes through the detector, the conductance is high due to the conductance of the A_1^+ or A_2^+ and the even higher conductance of the OH^- associated with the cation (Fritz, & Gjerde, 2000).

2.4 Ion-Exchange selectivity and Equilibria

2.4.1 Selectivity of Ion Exchange Chromatography

Selectivity and retention time depends on; valence of ions, radius of hydrated ions, polarization of ions, concentration of the mobile phase, Column temperature and pH of the mobile phase (taken from www.thairohs.org/index.php?).

1. *Valence of ions:* Polyvalent ions are much more strongly held than singly charged species and retention time increases with increasing ionic charge (See Figure 2.8).

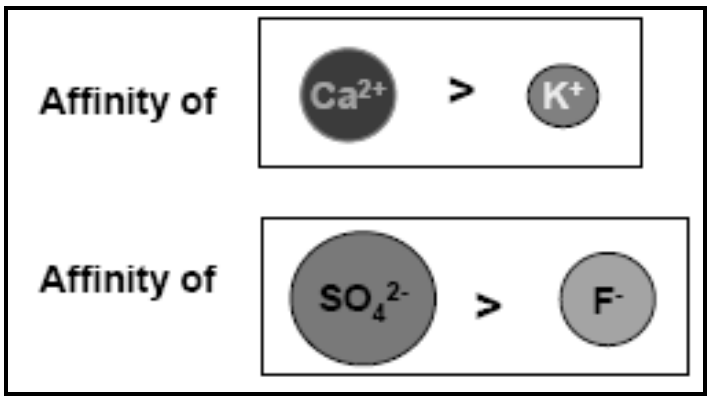

Figure 2.8 Effect of ionic charge (taken from www.thairohs.org/index.php?)

2. *Radius of hydrated ions:*

- The true radius of the ion in solution is the hydrated radius, which is the effective size of an ion or a molecule plus its associated water molecules in solution
- Larger radius of naked ion → more diffuse electric charge → fewer water molecules surrounding the ion
- Greater ion charge → increased solvent attraction → greater the hydrated radius (taken from www.thairohs.org/index.php?) (See Figure 2.9).

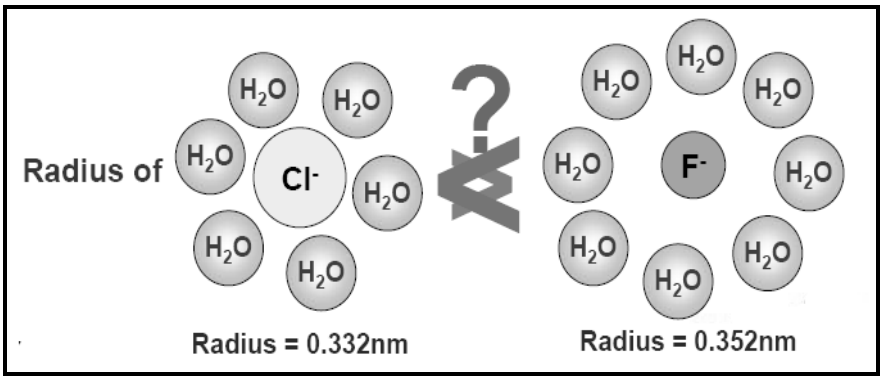

Figure 2.9 Effect of Radius of hydrated ions (taken from www.thairohs.org/index.php?)

- Retention time increases with decreasing hydrated ionic radius, and increasing naked ionic radius (See Figure 2.10).

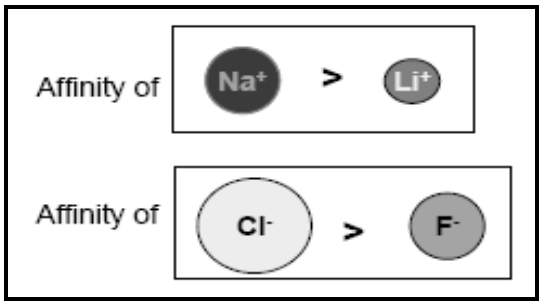

Figure 2.10 Effect of Radius of hydrated ions. (taken from www.thairohs.org/index.php*?)*

3. Polarization of ions: Ion which can be polarized easily has longer retention (See Figure 2.11).

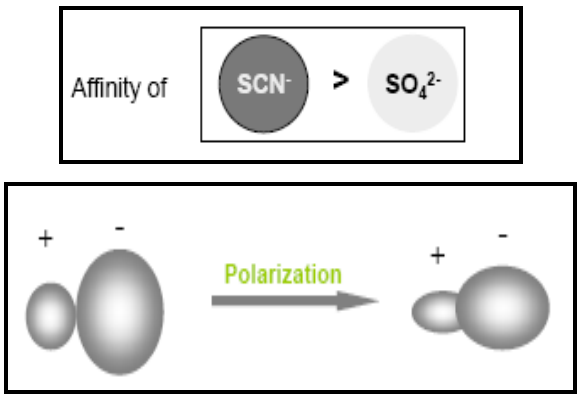

Figure 2.11 Effect of Radius of Polarization. (taken from www.thairohs.org/index.php?)

4. Concentration of the mobile phase: increase of mobile phase concentration → increase the ion concentration → reduces the retention time of sample ions.

5. Column temperature: An increase in temperature, reduces the viscosity of the mobile phase, increase in theoretical plate number, and reduces retention time.

6. pH of the mobile phase: **pH < 4**: Undissociated weak cation exchanger , **pH □ 8**: Dissociated weak cation exchanger and **4< pH< 8**: Partly dissociated weak cation exchanger (taken from www.thairohs.org/index.php*?)* (See Figure 2.12).

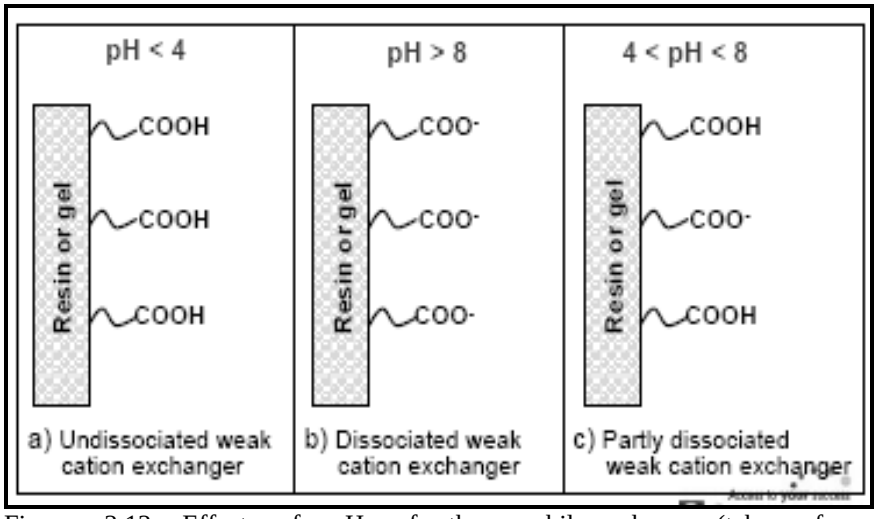

Figure 2.12 Effect of pH of the mobile phase. (taken from www.thairohs.org/index.php?)

2.4.2 Ion-Exchange Equilibria

Ion-exchange processes are based upon exchange equilibria between ions in solution and ions of like sign on the surface of an essentially insoluble, high-molecular-weight solid. Natural ion exchangers, such as clays and zeolites, have been recognized and used for several decades. Synthetic ion-exchange resins were first produced in the mid-1930s for water softening, water deionization, and solution purification. The most common active sites for cation exchange resins are the sulfonic acid group —$S0_3$~H^+, a strong acid, and the carboxylic acid group —COO~H^+, a weak acid. Anionic exchangers contain quaternary amine groups — N

$(CH_3)_3^+ OH^-$ or primary amine groups $—NH_3^+ OH^-$; the former is a strong base and the latter a weak one.

When a sulfonic acid ion exchanger is brought in contact with an aqueous solvent containing a cation M^+, exchange equilibria is set up that can be described by

$$\underset{\text{resin}}{n\ RSO_3^- H^+} + \underset{\text{solution}}{M^{+n}} \rightarrow \underset{\text{resin}}{(RSO_3^-)_n M^{n+}} + \underset{\text{solution}}{n\ H^+} \qquad (2.1)$$

where $RS0_3{\sim}H^+$ represents one of many sulfonic acid groups attached to a large polymer molecule. Similarly, a strong base exchanger interacts with the anion A^- as shown by the reaction (Skoog, & Leary, 1992).

$$\underset{\text{resin}}{n\ RN(CH_3)_3^+ OH^-} + \underset{\text{solution}}{A_n^-} \rightarrow \underset{\text{resin}}{[RN(CH_3)_3^+]_n A_n^-} + \underset{\text{solution}}{n\ OH^-} \qquad (2.2)$$

As an example of the application of the mass-action law to ion-exchange equilibria, we will consider the reaction between a singly charged ion B^+ with a sulfonic acid resin held in a chromatographic column. Initial retention of B^+ ions at the head of the column occurs because of the reaction

$$RS0_3\text{-}H^+_{(s)} + B^+_{(aq)} \rightarrow RSO_3\text{-}B^+_{(s)} + H^+_{(aq)} \qquad (2.3)$$

Here, the (s) and (aq) emphasize that the system contains a solid and an aqueous phase. Elution with a dilute solution of hydrochloric acid shifts the equilibrium in Equation 2.3 to the left causing part of the B^+ ions in the stationary phase to be transferred into the mobile phase. These ions then move down the column in a series of transfers between the stationary and mobile phases (Skoog, & Leary, 1992).

The equilibrium constant K_{cx} for the exchange reaction shown in Equation 2.3

takes the form

$$\frac{[RSO_3^-B^+]_s \times [H^+]_{aq}}{[RSO_3^-H^+]_s \, x [B^+]_{aq}} = K_{ex} \qquad (2.4)$$

Here, $[RSO_3^-B^+]_s$ and $[RSO_3^-H^+]_s$ are concentrations (strictly activities) of B^+ and H^+ in the solid phase. Rearranging yields;

$$\frac{[RSO_3^-B^+]_s}{[B^+]_{aq}} = K_{ex} \times \frac{[RSO_3^-H^+]_s}{[H^+]_{aq}} \qquad (2.5)$$

During the elution, the aqueous concentration of hydrogen ions is much larger than the concentration of the singly charged B^+ ions in the mobile phase. Furthermore, the exchanger has an enormous number of exchange sites relative to the number of B^+ ions being retained. Thus, the overall concentrations $[H^+]_{aq}$ and $[RSO_3\text{-}H^+]_s$ are not affected significantly by shifts in the equilibrium 2.3. Therefore, when $[RSO_3^-H^+]_s >> [RSO_3^-B^+]_s$ and $[H^+]_{aq} >> [B^+]_{aq}$ the right-hand side of Equation 2.5 is substantially constant, and we can write

$$\frac{[RSO_3^-B^+]_s}{[B^+]_{aq}} = K = \frac{C_s}{C_m} \qquad (2.6)$$

Note that K_{ex} in Equation 2.4 represents the affinity of the resin for the ion B^+ relative to another ion (here, H^+). Where K_{ex} is large, a strong tendency exists for the solid phase to retain B^+; where K_{ex} is small, the reverse obtains. By selecting a common reference ion such as H^+, distribution ratios for different ions on a given type of resin can be experimentally compared. Such experiments reveal that polyvalent ions are much more strongly held than singly charged species, within a given charge group. However, differences appear that are related to the size of the hydrated ion as well as to other properties.

Thus, for a typical sulfonated cation exchange resin, values for K_{ex} decrease in the order

$$\mathbf{Tl^{+} > Ag^{+} > Cs^{+} > Rb^{+} > K^{+} > NH_4^{+} > Na^{+} > H^{+} > Li^{+}}$$

For divalent cations, the order is

$$\mathbf{Ba^{2+} > Pb^{2+} > St^{2+} > Ca^{2+} > Ni^{2+} > Cd^{2+} > Cu^{2+} > Co^{2+} > Zn^{2+} > Mg^{2+} > UO^{2+}}$$

For anions, K ex for a strong base resin decreases in the order

$$\mathbf{SO_4^{2-} > C_20_4^{2-} > I^{-} > N0_3^{-} > Br^{-} > Cl^{-} > HC0_2^{-} > CH_3CO_2^{-} > OH^{-} > F^{-}}$$

This sequence is somewhat dependent upon type of resin and reaction conditions and should thus be considered only approximate (Skoog, & Leary, 1992).

2.5 The Ion Chromatographic System

The basic principles of ion chromatography are very simple. A suitable ion-exchange column is used in conjunction with auxiliary equipment typical of liquid chromatography (Fritz, & Gjerde, 2000).

The hardware requirement for an IC include a supply of eluent(s), a high pressure pump(with pressure indicator) to deliver the eluent, an injector for introducing the sample into the eluent stream and onto the column, a column to seperate the sample mixture into individual components, an optional oven to contain the column, a chemical suppressor that selectively enhances detection of the sample ions while suppressing the conductivity of the eluent, a detector to measure the analyte peaks as elute from the column and a data system for collecting and organizing the chromatograms and data (Fritz, & Gjerde, 2000) (See Figure 2.13).

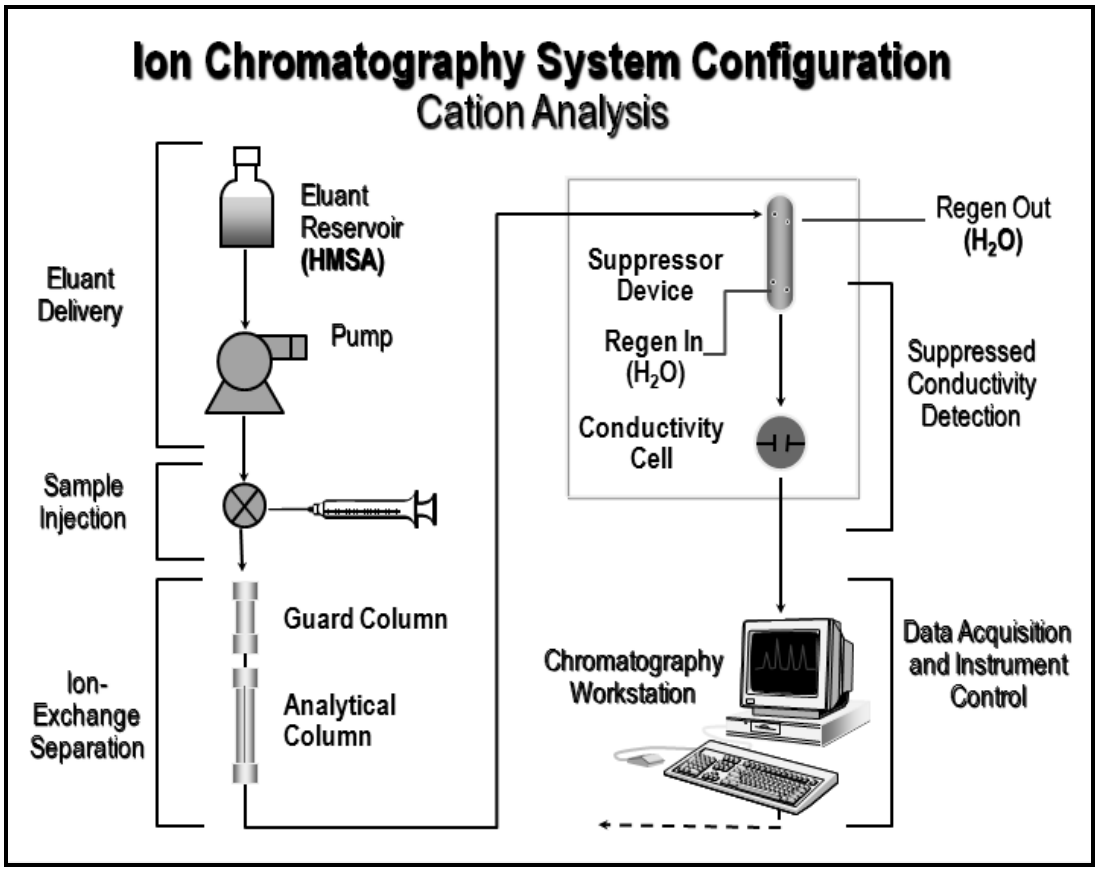

Figure 2.13 A typical IC system (taken from Dionex)

Before running a sample, the ion chromatography system is calibrated using a standard solution. By comparing, the data obtained from a sample to that obtained from the known standard, sample ions can be identified and quantitated. The data collection system, typically a computer running chromatography software, produces a chromatogram (a plot of the detector output vs. time). The chromatography software converts each peak in the chromatogram to a sample concentration and produces a printout of the results (Dionex, 2007).

2.5.1. Eluent Delivery

Eluent, a liquid that helps to separate the sample ions, carries the sample through the ion chromatography system (Dionex, 2007).

2.5.2. Pump

The pump pushes the eluent and sample through the guard and separator columns. (Dionex, 2007).

2.5.3. İnjection System

The injection system may be manual or automated, but both rely on the injection valve. An injection valve is designed to introduce precise amounts of sample into the sample stream. The variation is usually less than 0.5 % precision from injection to injection. Figure 2.14 schematically represents the valve. It is a 6-port and 2-position device; one position is load and the other is injected. In the load position, the sample from the syringe or auto sampler vial is pushed into the injection loop. The loop may be partially filled (partial loop injection) or completely filled (full loop injection) (Fig. 2.14). Typical loop sizes are 10-200 µL (Fritz, & Gjerde, 2000).

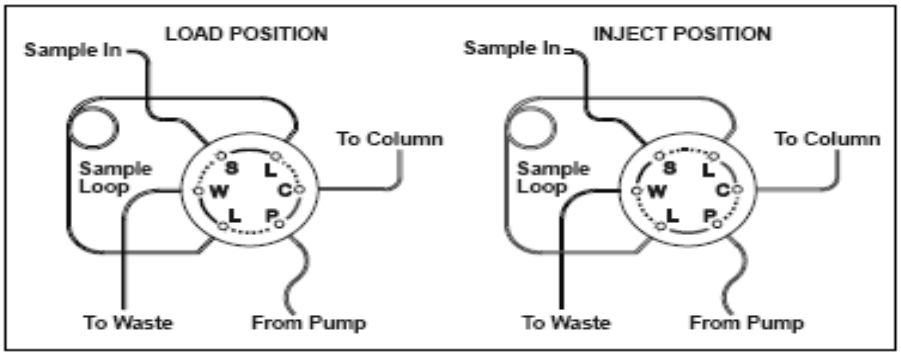

Figure 2.14 Injection valve flow schematics (taken from Dionex)

2.5.4 Column Oven

The column heater provides temperature control for the separator and guard column. The heater temperature can be set to between 30 °C and 60 °C and it must be set at least 5 °C above the ambient temperature. Temperature is monitored via a thermistor mounted in the heater block (Dionex, 2007). The column oven is optional. Most IC separations are not dependent on the use of an oven. Nevertheless, an oven can be quite useful for high-sensitivity work. Conductivity is proportional to

temperature. There is about a 2 % change in conductance per °C change in temperature. Conductivity detectors have temperature control, temperature compensation, or both. An oven can help to keep the temperature of the fluid, before the conductivity cell is reached, constant; this can help decrease the detector noise and decrease the detection limit of the instrument (Fritz, & Gjerde, 2000).

2.5.5 Column

In Ion chromatography, complex mixtures of anions or cations can usually be seperated on a separator column that contains anion-exchange or cation-exchange resin.

A typical column used in ion chromatography might be 150 x 4.6 mm although columns as short as 50 mm in length or as long as 250 mm are also used. The column is carefully packed with a spherical anion or cation-exchange resin with a particle diameter of 5 or 10 μm (Fritz, & Gjerde, 2000).

2.5.6 Ion-Exchange Resins

Ion exchangers are the most widely used stationary phase agents in IC. Cation and anion exchangers are solid particulate metarials with negatively and positively charged functional groups, respectively, arranged to interactions with ions in the surrounding liquid phase (See Figure 2.15).

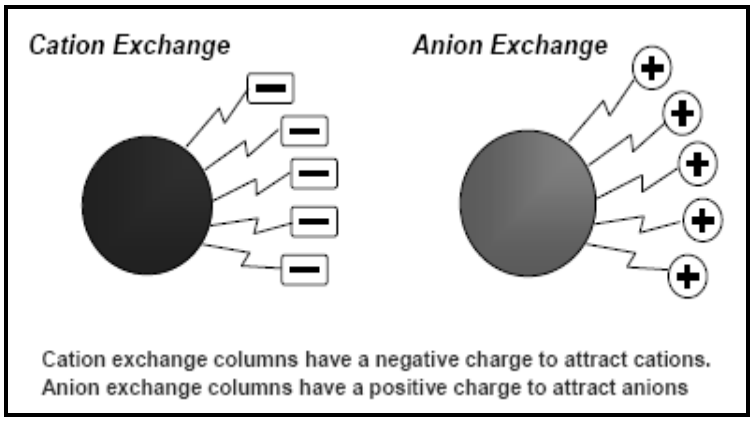

Figure 2.15 Cation-Anion exchanger (taken from (www.forumsci.co.il/ hplc/ic_pharm.pdf)

The most common types of cation and anion exchangers functionalized with sulfonic acid groups and quaternary ammonium groups, were shown in Figure 2.16.

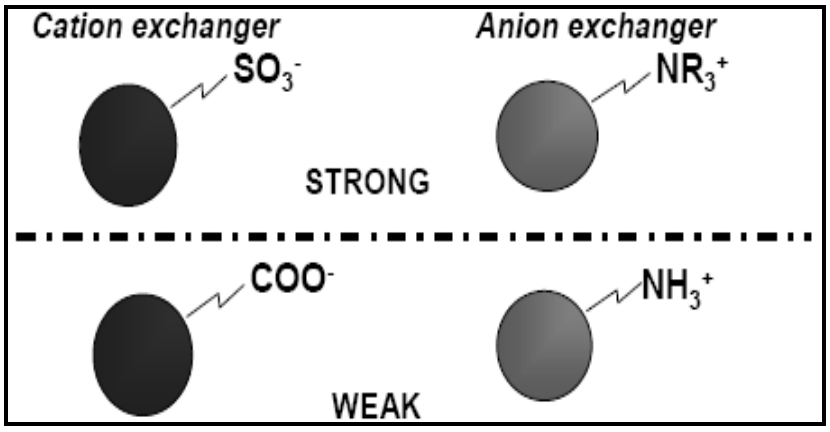

Figure 2.16 Cation-Anion exchanger (taken from (www.forumsci.co.il/hplc/ic_pharm.pdf)

An ion exchanger comprises three important elements: an insoluble matrix, which may be organic or inorganic; fixed ionic sites, either attached to or an integral part of the matrix; and, associated with these fixed ions. The attached groups are often referred to as functional groups. The associated ions are called the counterions. They are mobile throughout the ion exchanger and most importantly have the ability to exchange with others of like charge when placed in contact with a solution containing such. It is this latter property that gives these metarials their name **(**Small, 1989).

As well as having this fundamental property, ion exchangers, if they are to be useful in IC, should also have the following properties:

- The ability to exchange their ions rapidly.
- Good chemical stability over a wide pH range.
- Good chemical strenght and resistance to osmotic shock.
- Resistance to deformation when packed in a column and subjected to the flow of the mobile phase.

A variety of metarials have been used as matrices on which to anchor the ionic sites

of an ion exchanger. In modern IC the two most widely used are silica and organic polymers based on styrene. The excellent chemical stability of the organic –based ion exchange resins gives them a distinct advantage over the pH-sensitive, silica-based materials in many applications **(**Small, 1989).

How a stationary phase is built? Figure 2.17 shows that Composition of the stationary phase.

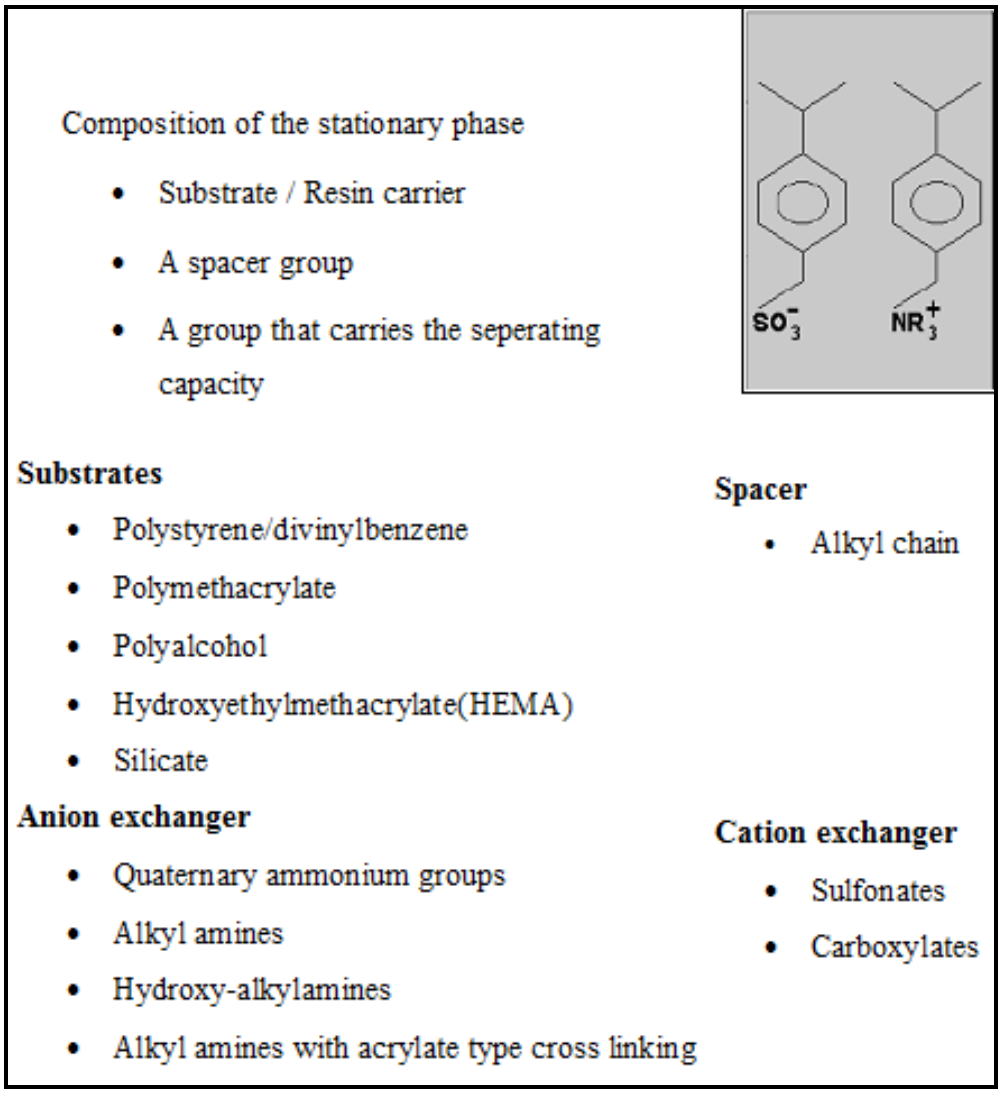

Figure 2.17 Composition of the stationary phase (taken from http://www.metrohm.com.cn/administrator/resource/upfile/ic_theory_20041011_e.pdf)

Table 2.2 shows that Strong and weak functional groups on typical synthetic ion-exchange materials.

Table 2.2 Functional groups on typical synthetic ion-exchange materials (taken from www.forumsci.co.il/hplc/ic_pharm.pdf)

CATION EXCHANGERS		ANION EXCHANGERS	
TYPE	FUNCTIONAL GROUP	TYPE	FUNCTIONAL GROUP
Sulfonic acid	$-SO_3^-H^+$	Quaternary amine	$-N(CH_3)_3^+OH^-$
Carboxylic acid	$-COO^-H^+$	Quaternary amine	$-N(CH_3)_2(EtOH)^+$
Phosphonic acid	$PO_3^-H^+$	Tertiary amine	$-NH(CH_3)_2^+OH^-$
phosphinic acid	$HPO_2^-H^+$	Secondary amine	$-NH_2(CH_3)_2^+OH^-$
Phenolic	$-O^-H^+$	Primary amine	$-NH_3^+OH^-$
Arsonic	$-HAsO_3^-H^+$		
Selenonic	$-SeO_3^-H^+$		

2.5.6.1 Substrate and Cross-Linking

A variety of polymeric substrates can be used in ion-exchange synthesis, including polymers of esters, amides, and alkyl halides. But resins based on styrene-divinylbenzene copolymers are probably the most widely used ion exchangers. The polymer is schematically represented in Fig. 2.18. The resin is made up primarily of polystyrene; however, a small amount of divinylbenzene is added during the polymerization to "cross-link" the resin. This cross-linking confers mechanical stability upon the polymer bead and also dramatically decreases the solubility of the polymer by increasing the molecular weight of the average polymer chain length. Typically, 2 to 25 % weight of the cross-linking compound is used for microporous resins and up to 55 % weight cross-linking for macroporous resins. In many cases, the resin name will indicate the cross-linking of the material (Fritz, & Gjerde, 2000).

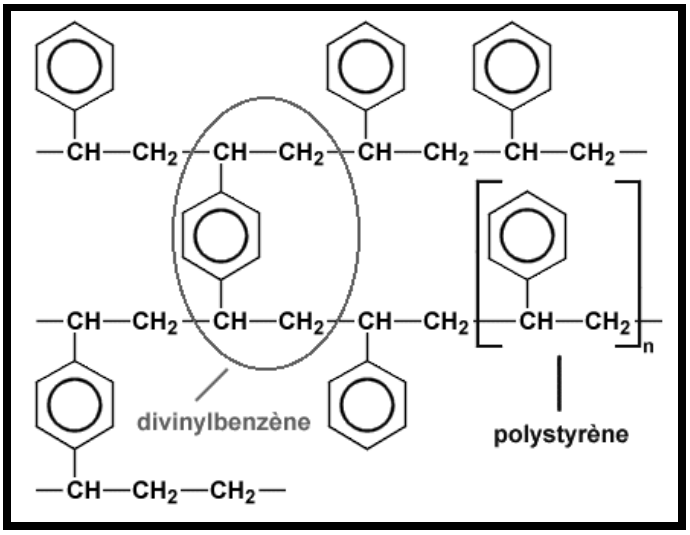

Figure 2.18 Schematic representation of a styrene-divinylbenzene copolymer.

The divinylbenzene "cross-links" the linear chain of the styrene polymer. A high percentage of divinylbenzene produces a more rigid polymer bead.

2.5.6.2 Chemical Functionalization

Ion exchangers are created by chemically introducing suitable functional groups into the polymeric matrix. In a few instances, monomers are functionalized first, and then they are polymerized into beads. An attractive feature of the aromatic copolymer used in many ion exchangers is that it can be modified easily by a wide variety of chemical reactions. More recently, some ion-exchange substrates have been polymers of esters (polymethacrylate) or amides. The reaction solvent is important in ion-exchange synthesis. In many cases, gel substrates must first be swollen in the reaction solvent to achieve complete functionalizalion of the resin. The reaction solvent does not appear to be as critical in ion-exchange synthesis of macroporous substrates. Their surface is already "exposed" and ready to be converted to an ion exchanger (Fritz, & Gjerde, 2000).

Weak-acid cation-exchange resins that contain a carboxylic acid ion-exchange group are sometimes used. However, the most popular type of cation exchanger is made by introducing a sulfonic acid functional group. Resins with the sulfonic acid

group are said to be strong acid ion exchangers. Sulfonation reactions are performed by treating the polystyrene resin with concentrated sulfuric acid. Alternatively, the beads can be reacted with chlorosulfonic acid to produce a sulfonyl chloride group. The sulfonyl chloride group is then hydrolyzed to the acid.

Presumably, the later reaction effects a more uniform placement of the ionogenic groups. This is because the chlorosulfonic acid reagent is dissolved in an organic solvent. The solvent swells the bead, allowing free access of the chlorosulfonic acid to the aromatic rings. Concentrated sulfuric acid is more polar. Sulfonation with this reagent occurs first on the bead surface and then moves progressively toward the center of the bead. Even though this product is not as homogeneous, resins prepared with concentrated sulfuric acid are more popular for ion chromatography. The $-SO3^-$ anionic group that is produced is chemically bound to the resin and its movement is thus severely restricted. However, the H^+ counterion is free to move about and can be exchanged for another cation. When a solution of sodium chloride is brought into contact with a cation exchange resin in the hydrogen ion form, the following exchange reaction occurs: (Fritz, & Gjerde, 2000).

2.5.6.3 Categories According to Pore Diameter

2.5.6.3.1 Microporous Resins. The starting material for cation- and anion-exchange "polymer" resins can be classified either as microporous or macroporous. Most classical work has been done with microporous ion-exchange resins. Microporous substrates are produced by a suspension polymerization in which styrene and divinylbenzene are suspended in water as droplets. The monomers are kept in suspension in the reaction vessel through rapid, uniform stirring. Addition of a catalyst such as benzoyl peroxide initiates the polymerization. The resulting beads are uniform and solid but are said to be microporous. The size distribution of the beads is dependent on the stirring rate, that is, faster stirring produces smaller beads. The beads swell but do not dissolve when placed in common hydrocarbon solvents. After the resin is functionalized (the ion-exchange functional groups are attached to the polymer), the bead is considerably more polar. Depending on the relative number

of functional groups, polar solvents such as water will now swell the ion-exchange resin. However, nonpolar solvents will tend to dehydrate the bead and cause it to shrink.

Tire extent of ion-exchange resin hydration will also depend on the ionic form of the resin. Ion-exchange resin beads with very little cross-linking are soft and tend to swell or shrink excessively when converted from one ionic form to another.

However, the amount of cross-linking used in resin synthesis is still based on a compromise of resin performance. Microporous polystyrene resins usually contain about 8 % divinylbenzene. Gel-type resins with a high cross-linking tend to exclude larger ions, and the diffusion of ions of ordinary dimensions within the gel may be slower than might be desired. Resins with cross-linking lower than about 2 % are too soft for most column work (Fritz, & Gjerde, 2000).

2.5.6.3.2 Macroporous Resins. Macroporous resins (sometimes called macroreticular resins) are prepared by a special suspension polymerization process. Again, as with microporous resins, the polymerization is performed while the monomers are kept as a suspension of a polar solvent. However, the suspended monomer droplets also contain an inert diluent that is a good solvent for the monomers, but not for the material that is already polymerized. Thus, resin beads are formed that contain pools of diluent distributed throughout the bead matrix. After polymerization is complete, the diluent is washed out of the beads to form the macroporous structure. The result is rigid, spherical resin beads that have a high surface area (Fritz, & Gjerde, 2000).

Rather than using an inert solvent to precipitate the copolymer and form the pores, the polymerization may be carried out in the presence of an inert solid agent such as finely divided calcium carbonate to create the voids within the bead. Later, the solid is also extracted from the copolymer. Both of these polymerization processes create large (although probably different) inner pores. The average pore diameter can be varied within the range of 20 A to 500 A (Fritz, & Gjerde, 2000).

The final resin bead structure of a macroreticular resin contains many hard micro-spheres interspersed with pores and channels. Because each resin bead is really made up of thousands of smaller beads (something like a popcorn ball), the surface area of macroporous resins is much higher than that of microporous resins. A gel resin has a (calculated) surface area of less than 1 m^2/g. However, macroporous resin surface areas range from 25 to as much as 800 m^2/g.

Macroporous resins are remarkably rigid because of the large amounts of cross-linking agents normally used in the synthesis. Such resins are particularly advantageous for performing ion-exchange chromatography in organic solvents since changing solvent polarity does not swell or shrink the resin bed as it might for a gel-type resin. But the high cross-linking does not inhibit the ion-exchange process as it does in gel resins because the resins have pores and channels that are easily penetrated by the ions (Fritz, & Gjerde, 2000).

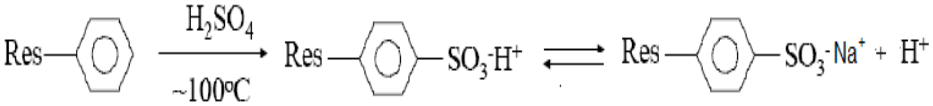

2.5.6.4 Cation Exchangers

Most of the cation exchangers used in IC fall into two major categories: sulfonated resins, sometimes called "strong-acid" exchangers, and resins with carboxylic acid groups, sometimes called "weak-acid" exchangers. The ion exchangers used in IC have a much lower exchange capacity than those intended for commercial applications such as the removal of calcium and magnesium ions from hard water (Fritz, & Gjerde, 2000).

2.5.6.4.1 Sulfonated Resins. Low-capacity cation-exchange resins are obtained by superficial sulfonation of styrene-divinylbenzene copolymer beads. The resin beads are treated with concentrated sulfuric acid and a thin layer of sulfonic acid groups is formed on the surface. The final capacity of the resin is related to the thickness of the

layer and is dependent on the type of resin, the bead diameter, and the temperature and time of contact with the sulfuric acid. Typical capacities range from 0.005 to 0.1 mequiv/g.

It can be easily appreciated that, compared to a conventional cation-exchange resin, the diffusion path length is reduced because the unreacted, hydrophobic resin core restricts analyte cations to the resin surface. This results in faster mass transfer of the cations and consequently in improved separations. Also, because of the rigidity of the resin core, there is less tendency for the bead to compress. This means that higher flow rates (at relatively low back pressures) can be used than would be passible with conventional resins. Superficially functionalized resins are stable over the pH range of 1 to 14 and swelling problems are minimal. The selectivity of the superficial cation-exchange resins for ions is similar to that observed for conventional resins (Fritz, & Gjerde, 2000).

2.5.6.4.2 Weak-acid Cation Exchangers. Owing to their differences in selectivity, it is often difficult to find conditions for separation of cations of different positive charge on a sulfonated resin column. Eluents that provide good separation of monovalent cations are too weak to elute diva lent cations in a reasonable time. There is now a trend to use weak-acid cation exchange columns. These materials contain carboxylic acid functional groups, or in some cases mixed carboxylic acid and phosphonic acid groups. At more acidic pH values these groups are gradually converted from the ionic to the molecular form and thus their ability to retain sample cations is diminished. By adjusting the operating pH to an appropriate value it becomes possible to separate a wider variety of cations in a single run (Fritz, & Gjerde, 2000).

Morris and Fritz (1992) described the preparation and chromatographic applications of two weak-acid resins that are easily synthesized, and carry the exchange group on the cross-linking benzene ring of the resin or on a short spacer arm from the ring. The first resin was prepared by reaction of a cross-linked polystyrene resin with succinic anhydride in a Friedel-Crafts reaction, aluminum chloride catalyst. The carboxyl groups are connected to the resin benzene rings by a

three-carbon atom spacer arm: $-COCH_2CH_2CO_2H$. The second cation exchanger was prepared by reaction of the resin with phenylchloroformate to give a phenyl ester attached to the resin benzene rings: $-CO-OC_6H_5$. The ester groups were then hydrolyzed by refluxing for 1 hour in a sodium hydroxide-ethanol solution to give the sodium salts of the carboxylate. The exchange capacity of resin I was 0.60 mequiv/g and that of resin II was 0.39 mequiv/g. Resin II in particular gave excellent separations of divalent metal cations with a complexing eluent (Fritz, & Gjerde, 2000).

2.5.6.4.3 Pellicular Resins. These anion-exchange resins have a surface layer of quaternary ammonium latex on a surface-sulfonated substrate. By adding a second coating layer of sulfonated latex beads, the outer layer of the resin consists of latex beads with exposed sulfonate groups. These groups undergo cation exchange with sample and eluent cations in IC. A schematic representation for these cation exchangers is:

$$Resin\text{-}S0_3\text{-}(N^+R_3 \text{ latex } N^+R_3)\ (S0_3^-\text{-latex-}\ S0_3^-)$$

A diagram of such a resin indicates that the sulfonated latex beads are of larger diameter than the quaternized beads (See Fig. 2.19). (Fritz, & Gjerde, 2000).

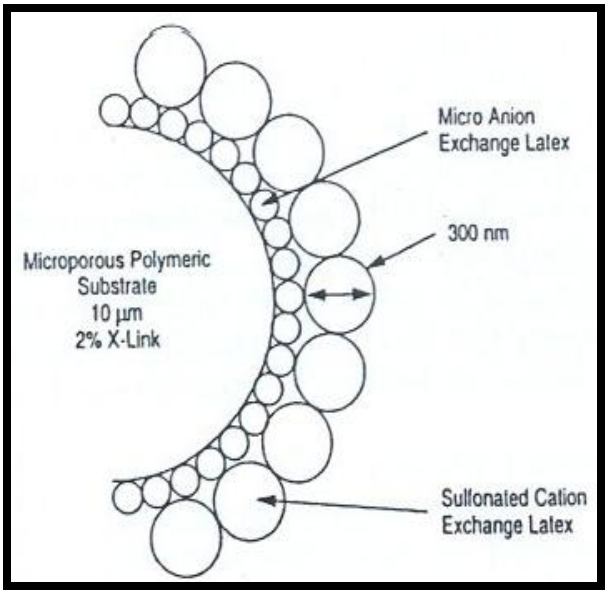

Figure 2.19 Schematic representation of lonPac CS3, a latex-coaled pellicular strong-acid cation exchanger (Courtesy Dionex Corp).

2.5.6.4.4 Silica-based cation exchangers. Several of the earlier cation exchangers contained groups such as -(CH_2)3C_6H_4SO3- attached to spherical silica particles, but these no longer find much use in IC (Fritz, & Gjerde, 2000).

2.5.7 Suppressor

The suppressor reduces the eluent conductivity and enhances the conductivity of the sample ions, thereby increasing detection sensitivity (Dionex, 2007).

2.5.7.1 Fiber Suppressors (Stevens, Davis, & Small, 1981)

The fiber suppressor was the first device based on the use of an ion-exchange membrane. It consisted of a long, hollow fiber made of a semi-permeable ion-exchange material. Column effluent containing zones of separated sample ions passed through the hollow center of the fiber. Here the sodium counter ion was exchanged for H^+ from the membrane. The outside of the hollow fiber was bathed in an acidic solution, allowing for continual replacement of the H^+ as the effluent passed through. The main advantage of this design was that it permitted continuous operation of the IC system. Band broadening in this suppressor was less than with the large packed-bed devices but was still significant. Fiber suppressors were also limited in their ability to suppress flow rates above 2 mL/min or eluents above 5 mM concentration (Fritz, & Gjerde, 2000).

2.7.7.2 Membrane Suppressors (Stillian, 1985)

A flat membrane suppressor from Dionex, known as the Micro-Membrane Suppressor (MMS) had a much higher capacity and lower dead volume than previous devices and was able to operate around the clock with minimal attention. The MMS includes two regenerant compartments and one eluent compartment separated by ion exchange membranes. The eluent flow channel and the regenerant flow channels are defined by gasketed ion exchange screens. The regenerant flow direction is opposite to the eluent flow direction (Dionex, 2007).

The internal design of the MMS is shown in Fig. 2.20.

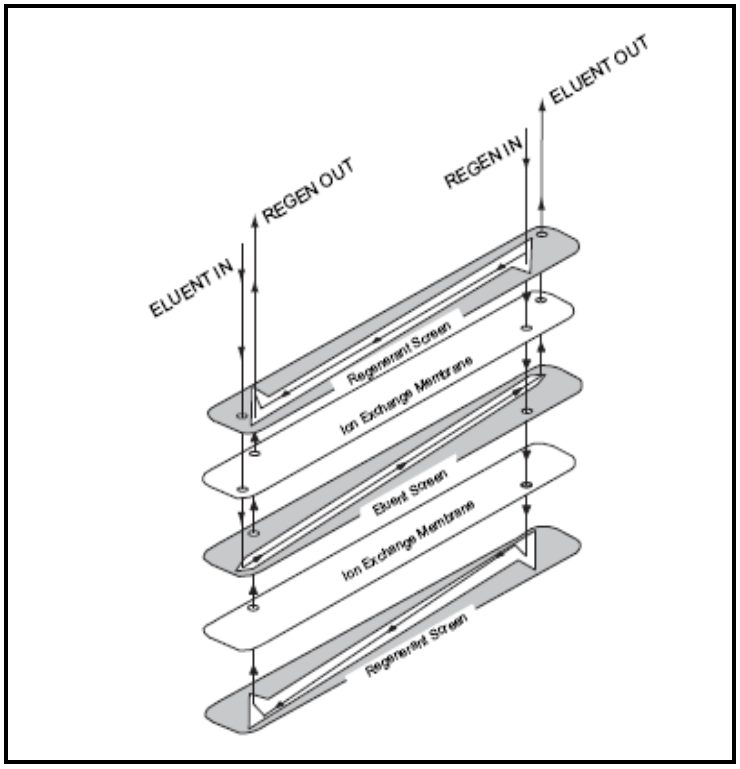

Figure 2.20 Internal design of the micro membrane suppressor (taken from http://www.dionex.com/en-us/columns-accessories/accessories-suppressors/cons5339.html)

Two semi-permeable ion-exchange membranes are sandwiched between three sets of ion-exchange screens. The eluent screen is of fine mesh to promote the suppression reaction while occupying a very low volume. The ion-exchange membranes on either side of this screen define the eluent chamber. There are two ion-exchange regenerant screens that permit tortuous flow of the regenerant solution towards the membranes. These screens provide a reservoir for suppressing ions without having a counter ion present (Fritz, & Gjerde, 2000).

Flow pattern for the cation suppressor is shown in Fig. 2.21.

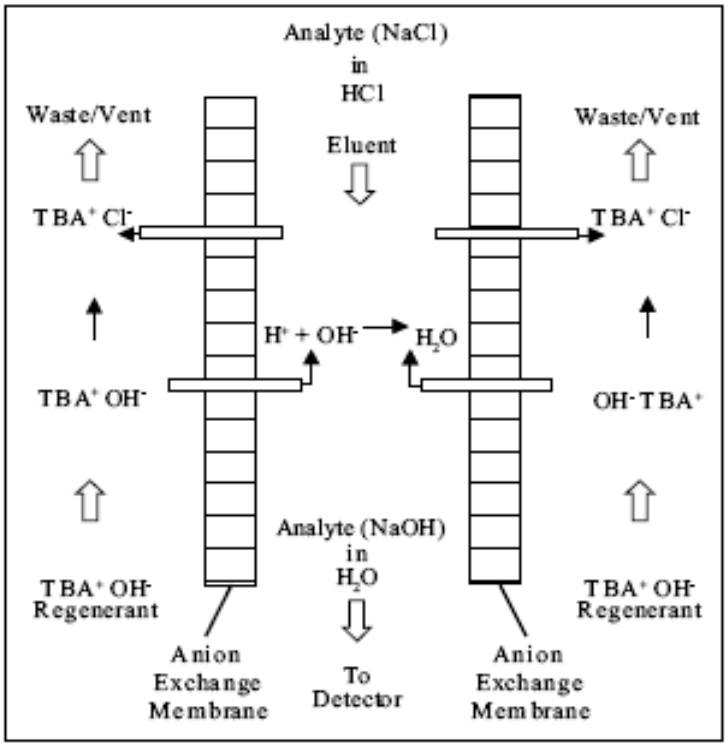

Figure 2.21 Chemical Suppression with the Cation MicroMembrane Suppressor taken from http://www.dionex.com/en-us/columns-accessories /accessories-suppressors/cons5339.html

Membrane and Screen Configuration in the MircoMembrane Suppressors

The regenerant channels are flushed with a regenerant that supplies hydronium or hydroxide ions that are required for the suppression reaction. The ion exchange membranes provide the transport pathway for the hydroxide ions into the eluent channel while providing a transport pathway for the chloride or MSA ions out of the eluent channel. The regenerant channel is fitted with unfunctionalized neutral regenerant screens that facilitate excellent transport of ions to and from the ion exchange membranes without any retention in the regenerant channel. The net result is suppression or conversion of the eluent from a highly conductive form to a weakly conductive form and conversion of most analytes into highly conductive forms. For example, hydrochloric acid eluent is converted to water and the analyte, sodium chloride, is converted to sodium hydroxide. Thus sodium chloride is detected as the highly conductive NaOH form against a low conductivity water background.

Chemical Suppression is a neutralization reaction and selective desalting process carried out across the anion exchange membranes. Hydroxide ions in the chemical regenerant cross the membranes and combine with the eluent cations, in this case hydronium ions, to form water. At the same time, eluent anions, in this case chloride ions, cross the membranes into the regenerant stream replacing the hydroxide ions (Dionex, 2007).

2.7.7.3 Electrolytic Suppressors (Strong, & Dasgupta, 1989)

The ideal way to regenerate a suppressor for IC is to electrolyze water to produce the H^+ or OH^- needed. In this device, a platinum wire-filled tube made of a Nafion cation-exchange membrane is inserted into another, larger Nafion tube and coiled into a helix. The helical assembly is inserted within an outer jacket packed with granular conductive carbon. An alkaline eluent, for example, NaOH or Na_2C0_3, flows in the annular channel between the two membranes and pure water flows through the inner membrane and the outer jacket countercurrent to the direction of eluent flow. A DC voltage (3 to 8 V) is applied across the carbon bed and the platinum wire. Sodium ions in the eluent migrate to the cathode compartment resulting in water as the suppressed eluent. Up to 500 μL/min of sodium hydroxide could be suppressed effectively with a membrane 50 cm in length. The band dispersion was 106 μL for a 20 μL sample.

In 1992 Dionex introduced a commercial electrochemical suppressor called a Self Regeneration Suppressor, or SRS (Henshall, Rabin, Statler, & Stilian, 1992). The internal design is similar to the membrane suppressor, but the regenerating ion (H^+ for anion chromatography) is produced by electrolysis of water. This allows the use of very low flow rates for regenerant water and avoids the use of independent chemical feed needed for earlier suppression devices (Fritz, & Gjerde, 2000). The SRS ULTRA II includes two regenerant compartments and one eluent compartment separated by ion Exchange membranes. Regenerant flow channels and an eluent flow channel are defined by the membrane. The eluent flows countercurrent to the regenerant. Electrodes are placed along the length of the regenerant channels. When

an electrical potential is applied across the electrodes, water from the regenerant channels is electrolyzed, supplying regenerant hydroxide ions (OH-) in the CSRS ULTRA II for the neutralization reaction. The membrane allows hydroxide ions to pass into the eluent chamber resulting in the conversion of the electrolyte of the eluent to a weakly ionized form. Eluent counter ions (anions in cation exchange) are simultaneously passed into the regenerant chamber to maintain charge balance. The eluent suppression process is illustrated for cation exchange in Figure 2.22. As shown in Figure 2.22, the water regenerant undergoes electrolysis to form hydrogen gas and hydroxide ions in the cathode chamber while oxygen gas and hydronium ions are formed in the anode chamber. Anion Exchange membranes allow hydroxide ions to move from the cathode chamber into the eluent chamber to neutralize hydronium ions. Anions in the eluent, such as methane sulfonate, attracted by the electrical potential applied to the anode, move across the membrane into the anode chamber to maintain electric neutrality with the hydronium ions at the electrode (Dionex, 2007).

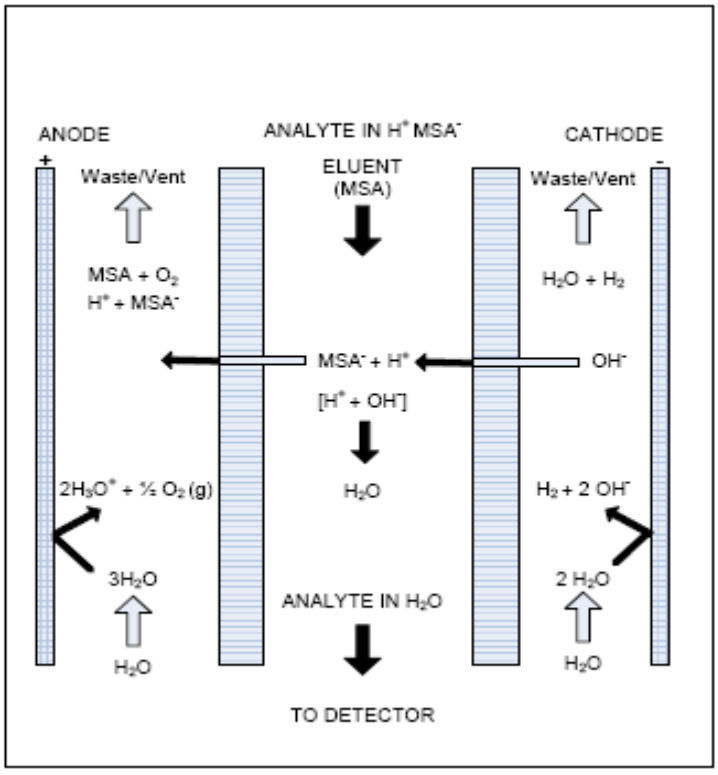

Figure 2.22 Mechanism of suppression for the Cation Self - Regenerating Suppressor (taken from http://www.dionex.com/en-us/columns-accessories/accessoriessuppressors/cons5339.html

2.5.8 Detectors

Several types of detectors used in ion chromatographic analysis along with a brief description. In IC, the detector must be able to "pick out or see" sample ions in the presence of the eluent ions.

There are several methods that can be employed to make this possible. One is to choose a detector that wills response only to the sample ions of interest, but not the eluent ions. Another method is to use indirect detection. This is where the eluent has a background signal and the presence of samples ions cause a decrease in eluent ions through a replacement process. The detector looks for the absence of eluent ions when the sample ion peak elutes and a decreasing signal is detected (Fritz, & Gjerde, 2000).

2.5.8.1 Conductivity Detectors

Conductivity is the ability of a solution containing a salt to conduct electricity across two electrodes. The ability of the solution to conduct is directly proportional to the salt content and the mobility of the individual anions and cations. As the ionic character of a molecule is increased, the conductivity increases. Small, mobile ions conduct quite readily and to a much greater extent than large bulky ions. For example, hydroxide anion is small and mobile and will conduct much better than proprionate anion which larger and bulkier. The relative conductances of ions are shown in Table 2.3 (Fritz, & Gjerde, 2000).

Table 2.3 Limiting equivalent ionic conductances in aqueous solution at 25 °G Units: ohm-^{1} cm^{2} equiv"^{1}

Anions	r	Cations	r
OH^-	198	H^+	350
F^-	54	Li^+	39
Cl^-	76	Na^+	50
Br^-	78	K^+	74
I^-	77	NH_4^+	73
NO_3-	71	Mg^{2+}	53
$HC0_3$-	45	Ca^{2+}	60
Formate	55	Sr^{2+}	59
Acetate	41	Ba^{2+}	64
Propionate	36	Zn^{2+}	53
Benzoate	32	Hg^{2+}	53
SCN-	66	Cu^{2+}	55
$s0_4^{2}$-	80	Pb^{2+}	71
$C0_3^{2}$-	72	Co^{2+}	53
$C_20_4^{2}$-	74	Fe^{3+}	68
$Cr0_4^{2}$-	85	La^{3+}	70
PO_4^{3}-	69	Ce^{3+}	70
$Fe(CN)_6^{3-}$	101	$CH_3HN_3^+$	58
$Fe(CN)_6^{4-}$	111	$N(Et)_4^+$	33

Molecular substances such as solvents (water and methanol) and solutions of non-ionized organic acids do not conduct electricity and are not detected by conductivity. The portion of a weak acid that does ionize results in a contribution to the conductivity signal. The ionic form of the weak acid depends on pH. A weak acid with a pKa larger than about six cannot be detected with suppressed conductivity detection because all anions are converted to the acid form by the suppressor. Because of high sensitivity and reduced background noise, the most common form of conductivity detection is with the use of suppressors. The advantage of this detection method is simplicity in instrument design and operation and the ability to detect salts of weak acids. There is a number of IC users who employ non-suppressed, direct or indirect conductivity detection where the separation column is connected directly to the conductivity cell (Fritz, & Gjerde, 2000).

2.5.8.2 Ultraviolet-Visible Detectors

There are several reasons why a spectrophotometric detector is a useful detector for monitoring ion-exchange separations. It is selective, yet its selectivity can be changed simply by changing the wavelength monitored by the detector. Versatility of the detector can be increased by adding a color-forming reagent to the eluent or the column effluent. The fundamental law under which ultraviolet-visible (UV-VIS) detectors operate is the Lambert-Beer law. It can be stated in the following form:

$$A = \varepsilon b C$$

A is the absorbance of a species of concentration C, and with an absorptivity ε, in a cell of length b. Concentration is usually in molar concentration and the path length is measured in cm. The term (molar) absorptivity has units that are the inverse of the C and ε units. This leaves a dimensionless; it is usually described in terms of absorbance units. A detector set to a certain sensitivity.

The Lambert-Beer equation is useful for choosing conditions for the separation and detection of ions. The eluent ions should have a low absorptivity and the sample ions should have reasonably high absorptivity. In a special case of indirect detection, this should be reversed. In this case, the eluent has an absorption signal and the sample is detected by a decrease of the background signal (Fritz, & Gjerde, 2000).

2.5.8.3 Electrochemical Detectors

Electrochemical detectors are sometimes divided into the groups of potentiometric, amperometric and conductometric detectors, that is, according to the three parameters of electric measurements. Potentiometric detectors measure voltage, amperometric measure current and conductometric measure resistance.

Conductometric detectors respond to all ions, but the other detectors respond only to certain electroactive ions (Fritz, & Gjerde, 2000).

The potentiometric detector operates on the same principles as ion-selective electrodes. An indicating electrode measures a change in the potential in the presence of certain sample ions. Hershcovitz, Yarnitsky, & Schmuckler (1982), explored the use of potentiometric-type detectors for ion chromatography.

Amperometric detectors are some of the most selective and sensitive detectors used to monitor ion chromatography separations. They are selective because they operate on the principles of oxidation or reduction of substances at an electrode. The potential needed to induce electrolysis differs for each ion (Fritz, & Gjerde, 2000).

Other advantages of electrochemical detection include a wide range of detector response (four to five orders of magnitude) and small cell dead volumes (as low as 1 μL). The detectors are simple, inexpensive, and rugged. Their main disadvantage is that they are sometimes difficult to use. Detectors are sensitive to the eluent flow rate and pH (Fritz, & Gjerde, 2000).

2.5.8.4 Refractive Index Detection

Extensive work has been performed with refractive index (R_I) detection for ion chromatography (Chrompack, 1981; Buytenhuys, 1981; Haddad, & Heckenberg, 1982). The refractive index detector can be considered to be a universal detector because any salt (or acid or base) added to water will cause a change in refractive index of the solvent. The differences in refractive index can be measured as the sample ions pass through the detector window replacing some of the eluent ions and changing the refractive index. Depending on the relative change, the peak may be increasing or decreasing. The detector has been used for both anion and cation separations with good results (Fritz, & Gjerde, 2000).

The refraction index of solution increases with the molecular weight (and concentration) of the solute dissolved in the solution. Organic ions usually cause a greater change than inorganic ions in the refractive index of a solution. Refractive index detection allows extremely wide latitude in the selection of the eluent type, eluent

pH and the ionic strength. In principle, refractive index detection can be substituted for conductance or UV absorption detection in many separations (Fritz, & Gjerde, 2000).

2.5.9 Suppressed Cation Chromatography

Suppression provides a simple, yet elegant way to reduce the background conductance of the eluent and at the same time to enhance the conductance of sample ions. In its original form, a second ion-exchange-column was placed between the separator column and the conductivity cell (Small, Stevens, & Bauman, 1975). With suppressed conductivity detection, an acidic cationic eluent is used to separate the sample cations. The column effluent with zones of separated cations passes directly into the suppressor unit containing an anion-exchange membrane in the hydroxide form. The eluent cation is neutralized and the counteranions associated with the sample metal ions are exchanged for the more highly conducting hydroxide ion (Fritz, & Gjerde, 2000).

Eluent:

$$\mathbf{H^+}MSA^- + Resin\text{-}NR_3^+\mathbf{OH^-} \rightarrow Resin\text{-}NR_3^+MSA^- + \mathbf{H_2O}$$

Eluent — Suppressor — Suppressor — Suppressed

(Highly Conductive)

Sample:

$$\mathbf{X^+}MSA^- + Resin\text{-}NR_3^+\mathbf{OH^-} \rightarrow Resin\text{-}NR_3^+MSA^- + \mathbf{X^+OH^-}$$

Analyte — Suppressor — Suppressor — Basic form of Analyte (Highly Conductive)

The background conductivity is very low after the eluent passes through the suppressor unit; theoretically it is that of pure water. The equivalent conductance of sample ions is high; it is the sum of conductances of the alkali metal cation and the hydroxide counter ion (Fritz, & Gjerde, 2000).

For example, if a dilute nitric acid (1 mM $H^+NO_3^-$) eluent is used and sodium (Na^+) and potassium (K^+) sample ions are to be separated, the following reactions take place in the suppressor unit:

Eluent:

$$\mathbf{H^+}NO_3^- + \text{Resin-}NR_3^+\mathbf{OH^-} \rightarrow \text{Resin-}NR_3^+NO_3^- + \mathbf{H_2O}$$

Sample:

$$\mathbf{Na^+}\ NO_3^- + \text{Resin-}NR_3^+\mathbf{OH^-} \rightarrow \text{Resin-}NR_3^+\ NO_3^- + \mathbf{Na^+OH^-}$$

$$\mathbf{K^+}\ NO_3^- + \text{Resin-}NR_3\text{+}\ \mathbf{OH^-} \rightarrow \text{Resin-}NR_3^+\ NO_3^- + \mathbf{K^+OH^-}$$

SAMPLE = 0.1mM NaNO3; 0.1mM KNO3 ELUENT = 1 mM HNO_3

GE = 0

$GS = (\lambda_{H+} + \lambda_{NO3-}) \times C_E + (\lambda_{Na+} + \lambda_{OH-}) \times C_S$

GS = (350 +71) x 0 + (50+198) x 0.1 = 25 µS

ΔG_{S-E} = GS - GE

ΔG = 25 – 0 = **25 µS**

GE = 0

$GS = (\lambda_{H+} + \lambda_{NO3-}) \times C_E + (\lambda_{K+} + \lambda_{OH-}) \times C_S$

GS = (350 +71) x 0 + (74+198) x 0.1 = 27.2 µS

ΔG_{S-E} = GS - GE

ΔG = 27.2 – 0 = **27.2 µS**

An increase in conductivity is observed when the sample cation elutes.

C_E = Eluent concentration (mM)

C_S = Sample concentration (mM)

λ_X = Equivalent conductance of X (µS/ mM)

GE = Background conductance of eluent, $GE = (\lambda_{H+} + \lambda_{X-}) \times C_E$

GS = Conductance in the sample band, $GS = (\lambda_{H+} + \lambda_{X-}) \times C_E + (\lambda_{C+} + \lambda_{X-}) \times C_S$

ΔG_{S-E} = Sample signal

2.5.10 Non-suppressed Cation Chromatography

With modern columns and dilute solutions of a strong acid as the eluent, cations may be separated and detected by direct conductivity. Non-suppressed ion chromatography employs a conventional liquid chromatographic system with a conductivity detector cell connected directly to the outlet end of an ion-exchange separation column. No suppressor unit is required. The successful development of this method was made possible by three principal innovations:

(1) The use of an anion- or cation-exchange resin of very low capacity (initially 0.007 to 0.04 m equiv/g).

(2) An eluent with a low ionic concentration and hence a low conductivity.

(3) An eluting ion in the eluent that has a significantly lower equivalent conductance than the analyte ions (Fritz, & Gjerde, 2000).

The basis for direct conductivity detection is that the highly conductive H^+ (equivalent conductance = 350 S cm^2 $equiv^{-1}$) in the eluent is partially replaced by a cation of lower conductance when a sample zone passes through the detector.

For example, the equivalent conductance of Na^+ and K^+ is 50 and 74 S cm^2 $equiv^{-1}$, respectively.

$$Na^+ (50\ [S*cm^2/eqiv]) < H^+ (350[S*cm^2/eqiv])$$

$$K^+ (74[S*cm^2/eqiv]) < H^+ (350[S*cm^2/eqiv])$$

The decrease in conductance on an equivalent basis can be calculated as follows:

Background: $H^+ + NO_3^- = 350 + 71 = 421$ (S cm^2 $equiv^{-1}$).

Sample peaks: $Na^+ + NO_3^- = 50 + 71 = 121$, a decrease of 300;

$K^+ + NO_3^- = 74 + 71 = 145$, a decrease of 276.

SAMPLE = 0.1mM NaNO3; 0.1mM KNO3 ELUENT = 1 mM HNO_3

$GE = (\lambda_{H+} + \lambda_{NO3-)} \times C_E$

GE = (350 +71) x 1 = 421 µS

$GS = (\lambda_{H+} + \lambda_{NO3-}) \times C_E + (\lambda_{Na+} + \lambda_{NO3-}) \times C_S$

GS = (350 +71) x 0.9 + (50+71) x 0.1 =391 µS ΔG_{S-E} = GS - GE

ΔG_{S-E} = 391 - 421 = **-30 µS**

$GE = (\lambda_{H+} + \lambda_{NO3-)} \times C_E$

GE = (350 +71) x 1 = 421 µS

$GS = (\lambda_{H+} + \lambda_{NO3-}) \times C_E + (\lambda_{K+} + \lambda_{NO3-}) \times C_S$

GS = (350 +71) x 0.9 + (74+71) x 0.1 =393.4 µS ΔG_{S-E} = GS - GE

ΔG_{S-E} = 393.4 - 421 = **-27.6 µS**

A decrease in conductivity is observed when the sample cation elutes.

The change in conductivity, AG, is actually slightly greater with non-suppressed conductivity. However, the noise is much higher in the non-suppressed detection mode. Noise may be defined as the random signal that results from chemical background (conductance in this case) temperature fluctuations, hydraulics and electronics. It was found that noise is proportional to background conductivity. Pump noise and detector/electronic noise also increase with increased background conductivity. Temperature control is critical for direct detection and slightly improves suppressed detection.

A major difference between the two detection modes is that detection limits for alkali metal ions were 12-21 times lower with suppressed detection. (Barreto, Bao, Pohl, & Riviello. 1999). Nevertheless, cations may be separated and quantified with direct detection down to fairly low concentrations. Another advantage is that the eluent remains acidic and metal does not precipitate as easily as it might in the high pH environment of the suppressor (See Figure 2.23).

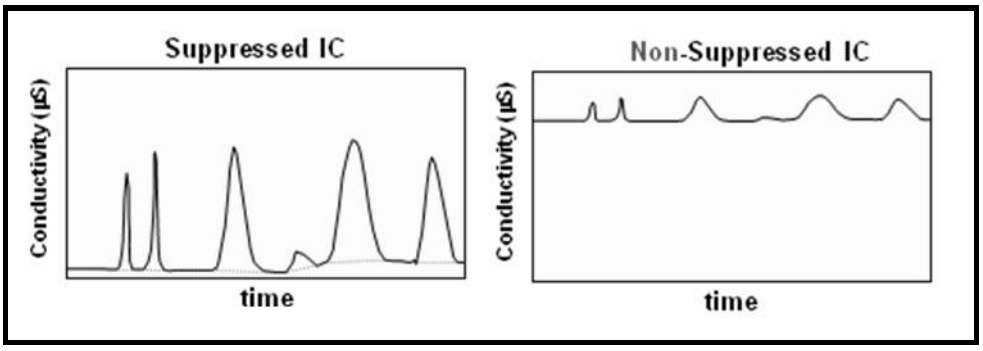

Figure 2.23 The differences between suppressed and non-suppressed type.

CHAPTER THREE

EXPERIMENTAL STUDIES WITH ION CHROMATOGRAPHY

A single-column method for the simultaneous determination of common cations (lithium, sodium, ammonium, potassium, magnesium, and calcium) in geothermal waters were separated and analyzed by means of ion chromatography using an elution with 20 mM methane sulfonic acid as mobile phase, a cation-exchange column and the suppressed conductivity detector.

This work was aimed to investigate if ion chromatography was a proper tool for meausuring the concentration of major cations in geothermal water samples as well as to determine standard stability of the method. The experimental procedure involved choise of cloumn type, eluent concentration and flow rate, and dilution ratio and integration parameters. Most of these parameters were selected based upon litreature referances personal experience and operates manuals of Dionex.

Ion chromatography is normally use for analysing low concentrations of samples. The direct measuerant of highly concentrated solitions like geothermal water samples without any dilutions proses result in a poor resolution in ion chromatography. Therefore the proper dilution ratio should be optimized both for standards and geothermal water samples.

3.1 Instrument

All systems and components for ionic analysis were from Dionex (Sunnyvale, CA, USA). The hardware used for these analyses consisted of an ICS-1000 ion chromatograph equipped with an isocratic pump, a conductivity detector, a self-regenerating suppressor (CSRS ultra II 4mm), an AS40 auto sampler and a column heater. Eluent flow rates were set at 1 mL/min with an injection volume of 25μL. All measurements were made at 30 ◦C. An Ion Pac® CG12A (50mm×4mm I.D.) guard column and an Ion Pac® CS12A (250mm×4mm I.D) analytical column were used to

separate the cations. The current of the suppressor was set at 59 mA to give a background conductivity of 1.5-2 μs. The complete operating conditions and the composition of the eluent used by the ion chromatography system during the chromatographic runs were summarized in Table 3.1.

Table 3.1 Operating Conditions

IC	
Ion-Chromatographic Unit	Dionex ICS-1000 IC
Pump	GP50 Gradient Pump
Guard Column	IonPac® CG12A Guard, 50mm×4mm I.D
Column	IonPac® CS12A Analytical, 250mm×4mm I.D
Column Temperature	30 ◦C
Suppressor	CSRS Ultra II 4mm
Suppressor Current	59 mA
Eluent	20mM Methanesulfonic acid
Eluent Source	Dionex EluGen® EGC Cartridge
Flow-Rate	1 mL/min
Detector	Dionex DS6 Heated Conductivity Cell
Cell Temperature	35 ◦C
Injection Volume	25μL
Run Time	12.5 min
Background Conductance	≈1.5-2 mS
Back Pressure	≈1050 psi
Data Management	Chromeleon® 6.5 Chromatography Workstation
Auto Sampler	AS-40

3.2 Reagents

Deionized water, generated by a Milli-Q deionized water unit that had a resistance better than 18.2 MΩcm, was used for the preparation of all the solutions and eluents.

Certified reference cations standard (CRS) solution of Dionex (Lithium 49.9 ±0.4 mgL^{-1}, Sodium 203 ±2 mgL^{-1}, Ammonium 251 ±5 mgL^{-1}, Potassium 506 ±5 mgL^{-1}, Magnesium 252 ±2 mgL^{-1}, Calcium 509 ±5 mgL^{-1}) were used throughout the study. All chemicals were of analytical reagent grade unless otherwise specified.

3.3 Preparation of the Solutions

All the solutions were prepared with deionized water (Milli-Q, USA). The standard solutions of six cations (as chloride salts) were prepared daily by serial dilution of certified reference cation standard (CRS) solution of Dionex.

Methansulfonic acid (1 M) was obtained from DIONEX and used for the mobile phase. The mobile phase was prepared daily before use. For preparing 20 mM eluent, 20 mL methansulfonic acid added to the volumetric flask and finally diluted to 1000 mL by water.

3.4 Pretreatment of Samples

The method was applied to the determination of cations in geothermal water samples. The geothermal water samples were taken from Pamukkale Antique Pool and Bölmekaya, Denizli, Turkey.

To avoid accidental contamination of the samples, the samples were collected to polyethylene collectors on daily basis. Then they were filtered with Pionex/Millipore/Sartorius through a filter with a pore diameter 0.45 μm to polyethylene bottles at 25 ^{0}C. In laboratory conditions prior to injection samples were kept under refrigeration at 4 ^{0}C.

3.5 Analysis of Six Cation Standards

The cation standards were analyzed with ion exchange chromatography method employing guard (CG12A (4x50 mm)) and analytical columns (CS12A (4x250 mm)) of DIONEX with Carboxylic/Phosphonic acid functional groups, respectively. Characteristics of the analytical and guard columns were given below (See Table 3.2).

Table 3.2 IonPac CS12A/CS12A packing specifications (taken from dionex)

IonPac CS12A/CG12A Packing Specifications					
Column	Particle Diameter µm	Substrate[a] X-linking %	Column Capacity meq/column	Functional Group	Hydrophobicity
CS12A 4 x 250 mm	8.5	55	2.8	Carboxylic/ Phosphonic acid	Med-low
CG12A 4 x 50 mm	8.5	55	0.56	Carboxylic/ Phosphonic acid	Med-low

Three different concentration levels of the employed standards were shown in Table 3.3.

Table 3.3 Three different concentration levels of the employed standards

Peak Name	Amount Std.1 (mgL^{-1})	Amount Std.2 (mgL^{-1})	Amount Std.3 (mgL^{-1})
Lithium	0.84	4.25	8.39
Sodium	3.41	17.29	34.14
Ammonium	4.22	21.38	42.21
Potassium	8.51	43.10	85.09
Magnesium	4.24	21.46	42.38
Calcium	8.56	43.35	85.59

Optimum conditions: mobile phase; 20 mM of methanesulfonic acid, 1 mL/ min eluent flow rate, 950 – 1050 psi column pressure, 30 ^{0}C of column temperature, 35 ^{0}C of detector temperature, 59 mA of suppressor current. Retention times of standards were measured between 3.6–12.4 min. under optimized working conditions. The peaks of the standards were sharp, symmetrical, well shaped, Gaussian type and well separated. The resolution throughout the chromatogram was satisfactory. The chromatogram of the cation standards were shown in Figure 3.1.

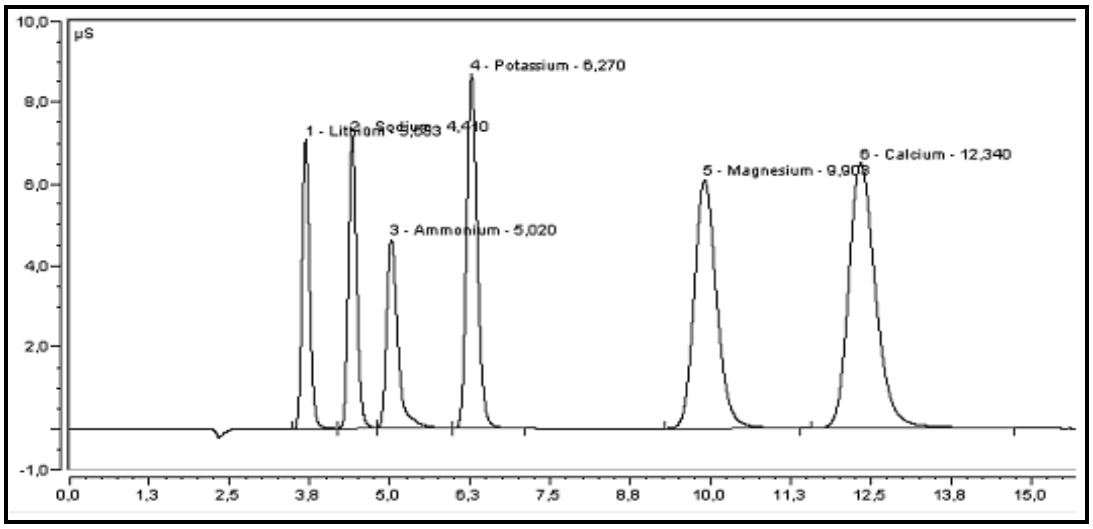

Figure 3.1 IC chromatogram of the standards (Lithium, sodium, ammonium, potassium, magnesium, and calcium) acquired at optimum working conditions

The calibration plot of each standard consists of three different concentration levels and six concentration points. In all cases, the quadratic fit was employed for the acquired data since it has been statistically significant and suggested by the litreature (Tartari, Marchetto, & Mosello, 1995) for the employed concentration levels (See Figure 3.2).

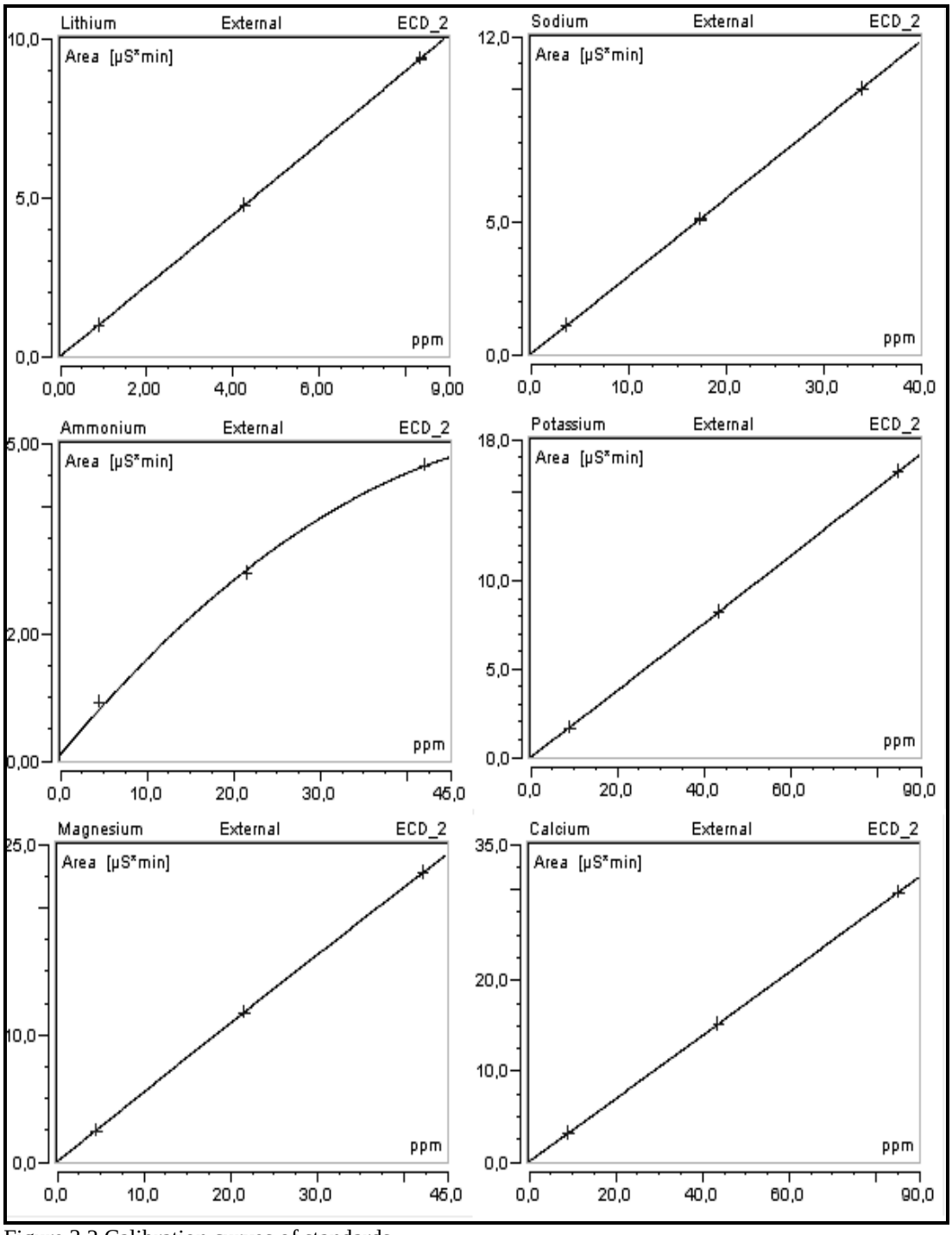

Figure 3.2 Calibration curves of standards

Table 3.4 shows regression coefficient and relative standard deviation values of the calibration plots of 6 different cation standards. ‘’0QOff’’ refers quadratic and originated fit. Except that of ammonium, all other cations exhibited quite good regression coefficients; > % 99.999.

Table 3.4 Regression coefficient and relative standard deviation values of the calibration plots of 6 cation standards

Peak Name	Calibration Type	Calibration Points	Relative Standart Deviation %	Regression Coefficient %
Lithium	0QOff	6	0.19	99.9996
Sodium	0QOff	6	0.17	99.9997
Ammonium	A0QOff	6	4.18	99.7011
Potassium	0QOff	6	0.17	99.9997
Magnesium	0QOff	6	0.15	99.9997
Calcium	0QOff	6	0.13	99.9998
AVERAGE:		6	0.83	99.9499

Table 3.5 Shows the employed standards for the calibration plot of cations in terms of concentration (mgL^{-1}), Peak Area (µs*min) and Peak Height (µs). From Table 3.5 it can be conculeded that the peak area and peak hight values are in correlation with the concentrations of the calibration standards for chosen concentration range.

Table 3.5 Six concentrations of cations employed for the calibration plot in (mgL^{-1}), Peak Area (μs*min) and Peak Height (μs)

	Lithium	Sodium	Ammonium	Potassium	Magnesium	Calcium
Concentration (mgL^{-1})	0.8288	3.4428	5.1118	8.4255	4.1993	8.4879
	0.8295	3.4067	5.1180	8.4199	4.2041	8.4928
	4.2527	17.2772	20.9308	43.1031	21.4735	43.3774
	4.2545	17.2937	20.9144	43.1509	21.4788	43.3755
	8.3898	34.1664	42.4541	85.1041	42.3515	85.5705
	8.3907	34.1075	42.4053	85.0572	42.3936	85.6024
Peak Area (μs*min)	0.9010	1.0408	0.9209	1.5607	2.2843	2.8822
	0.9017	1.0300	0.9219	1.5596	2.2869	2.8839
	4.7005	5.1434	3.0062	8.0923	11.6334	14.8744
	4.7025	5.1483	3.0044	8.1014	11.6362	14.8737
	9.3215	10.0256	4.7398	16.0371	22.5903	29.3997
	9.3225	10.0088	4.7373	16.0282	22.6120	29.4107
Peak Height (μs)	6.6724	6.9967	4.5466	8.0441	5.6584	5.9374
	6.6786	6.9304	4.5451	8.0508	5.6631	5.9486
	34.3422	34.2821	12.6847	41.7451	28.1120	29.7122
	34.3363	34.2821	12.6828	41.7527	28.1081	29.7055
	66.2726	65.5295	18.6176	82.4946	52.8820	55.6063
	66.2299	65.4256	18.5738	82.4133	52.9504	55.5684

Chromatographic system-suitability parameters (asymmetry (EP), resolution and plate number (N) values) were determined for six different calibration points. Table 3.6 reveals retention time, peak area, relative peak area, peak width, peak height, asymmetry, resolution and plate number values for six different calibration points. From Table 3.6 it can be concluded that retention times of six cation standards are in correlation for six different concentration points.

The peak area of each cation standard was increased as concentration rose as expected.

Peak asymmetry (EP) is a factor regarding with peak symmetry and its value should be around 10 % of the peak height. A peak asymmetry value of 1-1.05 points out excellent peak symmetry. Where the asymmetry values between 1.2-2 are acceptable, the higher ones are being unacceptable. The asymmetry values of high concentrations of lithium and sodium exhibited an excellent peak symmetry. All other measured asymmetry values were acceptable for the employed calibration ranges (See Table 3.6).

The resolution of a column provides a quantitative measure of its ability to separate two analyte. A resolution value of 1.5 means essentially complete separation of peaks whereas a resolution of 0.75 does not. The resolution values were calculated with respect to Ca^{2+} and were found to be 3.22, 2.24, 4.05, 7.72 and 3.44 for Li^{+}, Na^{+}, NH_4^{+}, K^{+} and Mg^{2+} respectively. From Table 3.6 it can be concluded that the resolution performance of the column was very satisfactory in all cases (See Table 3.6).

The efficiency of chromatographic columns increases as the number of plates (N) becomes greater and the plate height becomes smaller. Efficiencies in terms of plate numbers can vary from a few hundred to several hundred thousand. Plate number of N>2000 is a desirable value. In our case number of plates are 4853, 5651, 4370, 6685, 3886 and 4201 for Li^{+}, Na^{+}, NH_4^{+}, K^{+}, Mg^{2+} and Ca^{2+} respectively which are quite good for all calibration points (See Table 3.6).

Table 3.6 Retention time(min), peak area(μS*min), relative peak area(%), peak width(min), peak height(μS), asymmetry(EP), resolution and plate number(N) values for six different calibration points.

First point of calibration

Peak Name	Ret. Time (min)	Area (μS*min)	Rel. Area %	Peak Width (min)	Height (μS)	Asym. (EP)	Resol.	Plates (N)
Li^+	3.660	0.9010	9.39	0.21	6.672	1.14	3.22	4853
Na^+	4.370	1.0408	10.85	0.23	6.997	1.11	2.24	5651
NH_4^+	4.967	0.9209	9.60	0.30	4.547	1.52	4.05	4370
K^+	6.183	1.5607	16.27	0.30	8.044	1.14	7.72	6685
Mg^{2+}	9.760	2.2843	23.82	0.63	5.658	1.14	3.44	3886
Ca^{2+}	12.117	2.8822	30.05	0.75	5.937	1.19	n.a.	4201

Second point of calibration

Peak Name	Ret. Time (min)	Area (μS*min)	Rel. Area %	Peak Width (min)	Height (μS)	Asym. (EP)	Resol.	Plates (N)
Li^+	3.660	0.9017	9.41	0.21	6.679	1.13	3.22	4853
Na^+	4.370	1.0300	10.75	0.23	6.930	1.11	2.25	5664
NH_4^+	4.967	0.9219	9.62	0.30	4.545	1.52	4.05	4370
K^+	6.183	1.5596	16.27	0.30	8.051	1.15	7.72	6710
Mg^{2+}	9.757	2.2869	23.86	0.63	5.663	1.14	3.44	3880
Ca^{2+}	12.113	2.8839	30.09	0.75	5.949	1.20	n.a.	4193

Third point of calibration

Peak Name	Ret. Time (min)	Area (μS*min)	Rel. Area %	Peak Width (min)	Height (μS)	Asym. (EP)	Resol.	Plates (N)
Li^+	3.670	4.7005	9.91	0.22	34.342	1.08	3.19	4763
Na^+	4.380	5.1434	10.84	0.24	34.282	1.07	2.14	5595
NH_4^+	4.984	3.0062	6.34	0.34	12.685	1.75	3.76	3612
K^+	6.174	8.0923	17.05	0.30	41.745	1.16	7.41	6652
Mg^{2+}	9.687	11.6334	24.52	0.65	28.112	1.26	3.18	3575
Ca^{2+}	11.957	14.8744	31.35	0.79	29.712	1.45	n.a.	3730

Fourth point of calibration

Peak Name	Ret. Time (min)	Area (µS*min)	Rel. Area %	Peak Width (min)	Height (µS)	Asym. (EP)	Resol.	Plates (N)
Li^+	3.670	4.7025	9.91	0.22	34.336	1.07	3.18	4751
Na^+	4.380	5.1483	10.85	0.24	34.282	1.07	2.14	5581
NH_4^+	4.984	3.0044	6.33	0.34	12.683	1.75	3.77	3618
K^+	6.177	8.1014	17.07	0.30	41.753	1.15	7.40	6646
Mg^{2+}	9.687	11.6362	24.51	0.65	28.108	1.26	3.18	3572
Ca^{2+}	11.957	14.8737	31.34	0.79	29.706	1.46	n.a.	3730

Fifth point of calibration

Peak Name	Ret. Time (min)	Area (µS*min)	Rel. Area %	Peak Width (min)	Height (µS)	Asym. (EP)	Resol.	Plates (N)
Li^+	3.680	9.3215	10.12	0.22	66.273	1.01	3.13	4544
Na^+	4.394	10.0256	10.88	0.24	65.529	1.01	2.10	5443
NH_4^+	5.007	4.7398	5.15	0.35	18.618	1.71	3.61	3348
K^+	6.177	16.0371	17.41	0.31	82.495	1.15	7.04	6609
Mg^{2+}	9.610	22.5903	24.52	0.67	52.882	1.42	2.93	3257
Ca^{2+}	11.814	29.3997	31.92	0.84	55.606	1.76	n.a.	3211

Sixth point of calibration

Peak Name	Ret. Time (min.)	Area (µS*min)	Rel. Area %	Peak Width (min.)	Height (µS)	Asym. (EP)	Resol.	Plates (N)
Li^+	3.680	9.3225	10.12	0.22	66.230	1.01	3.13	4544
Na^+	4.394	10.0088	10.86	0.24	65.426	1.01	2.09	5443
NH_4^+	5.004	4.7373	5.14	0.36	18.574	1.73	3.61	3333
K^+	6.174	16.0282	17.40	0.31	82.413	1.16	7.05	6602
Mg^{2+}	9.607	22.6120	24.55	0.67	52.950	1.43	2.93	3263
Ca^{2+}	11.807	29.4107	31.93	0.84	55.568	1.78	n.a.	3199

Table 3.7 shows expected retention times, windows, experimentally measured average retention times, relative retention times, standard deviation and relative standard deviations of the six cation standards. For three different concentrations, double injections were performed. Therefore, the retention times were extracted from six measurements for each standard. Relative retention times were measured with respect to K^+. The calculation of relative retention time (RRT) for Li^+ is as follows. RRT values of other standards were calculated similarly.

$$RRT = \frac{t_{standard}}{t_{referance}} \qquad RRT = \frac{3.700}{6.270} \qquad RRT = 0.5901$$

RRT: Relative Retention Time, $t_{standard}$: Real retention time of standard, $t_{reference}$: Real retention time of standards which used as a reference.

Table 3.7 Expected retention time (min), Windows (± min), average retention time, standard deviation (SD, min, n=6), relative standard deviation (%RSD) and relative retention time of the employed cation standards.

Peak Name	Ret. Time (min.)	Windows (± min.)	Ave. Retention time	SD (min.) (n=6)	RSD %	Rel. Ret. Time (RRT)
Lithium	3.700	0.160 AG	3.670	0.0089	0.25	0.59
Sodium	4.430	0.163 AG	4.381	0.0107	0.24	0.71
Ammonium	5.060	0.160 AG	4.985	0.0172	0.35	0.81
Potassium	6.270	0.230 AG	6.178	0.0041	0.07	**1.00**
Magnesium	9.800	1.500 AG	9.685	0.0671	0.69	1.56
Calcium	12.500	2.000 AG	11.961	0.1362	1.14	1.99

Precision simply can be determined by replicating a measurement. In this work, precision of the retention times was evaluated with six replicate measurements for each standard. Average retention times were found to be 3.670, 4.381, 4.985, 6.178, 9.685 and 11.961 min. for lithium, sodium, ammonium, potassium, magnesium and calcium, respectively. Except that of calcium their standard deviations were in the range of 0.0041 – 0.0671 min. which is less than 1 %, only calcium exhibited a RSD % value of 1.14 which is also accaptable.

3.6 Method Validation Studies

In this work the method was validated in accordance with the ICH guideline, Validation of Analytical Procedures: Text and Methodology Q2 (R1), in terms of system suitability, analytical performance parameters; repeatability, intermediate precision, reproducibility, and stability (International Conference on Harmonization, Validation of Analytical Procedures, 2005).

Accuracy. The accuracy of an analytical method is one of the key features of validation. A few alternative methods have been proposed for the assessment of the accuracy which is the use of certified reference materials, the comparison of the proposed method with a reference one and the use of recovery assays on samples (Gonzalez, Herrador, & Agustin, 1998). The average recovery should be in the range of 99–101 %.

In this work, recovery studies were performed by adding standards in to the geothermal water samples and drinking water. The precision and accuracy of the method were tested at three different concentration levels for each standard. Table 2.10 shows dilution ratio of added standarts and added concentrations of six different cation standards in mgL^{-1}.

For geothermal water samples recovery tests was performed between two successive months. Additionally, the accuracy was also defined as the difference between the calculated amount and the specified amount for the selected certified reference standard (CRS) and expressed as RSD%. The geothermal water samples were treated with added different concentrations of certified reference standards(CRS), which were diluted in the ratio of 1:40, 1:25 and 1:20 (See Table 3.8).

Table 3.8 Three different concentration levels for the added standards

Standard Name	I. Concentration (mgL^{-1}) (1/40 dilute)	II. Concentration. (mgL^{-1}) (1/25 dilute)	III. Concentration (mgL^{-1}) (1/20 dilute)
Lithium	1.25	2.00	2.50
Sodium	5.08	8.12	10.15
Ammonium	6.28	10.04	12.55
Potassium	12.65	20.24	25.30
Magnesium	6.30	10.08	12.60
Calcium	12.73	20.36	25.45

3.6.1 Recovery Studies with Geothermal Water Samples

Table 3.9, 3.10 and 3.11 shows recovery values (%) of six cations for two different months and three different dilution ratios. The column "Found" in Table 3.9, 3.10 and 3.11 is the average of three-injections. Amounts of the added certified reference standards (CRS) were kept in the range of calibration limits.

In geothermal water samples, the deviations in recovery values (%) were less than 10 %, except that of ammonium. However, in all cases ammonium exhibited considerable deviations extending up to 20 %. This can be attributed to the interference of ammonium with sodium. According to literature information ammonium is extremely difficult to analize in samples of very dissimilar concentration ratios of sodium-to-ammonium since these two cations have similar selectivities for stationary phases (Wang, Wu, Chen, Lin, & Wu, 2008).

Drinking water samples exhibited excellent recovery values with respect to geothermal water samples. This can be referred to the rich heavy metal content of geothermal water samples, which is a strongly possible reason for interferences (See Table 3.12).

Table 3.9 Cation concentrations, recovery, relative standard deviation (% RSD) and % recovery values for geothermal water samples collected from Bölmekaya in April 29, 2008 and june 26, 2008 respectively. Certified reference standards were diluted 1:40 with pure water

29-04-2008

Ion	Real Concn. (mgL^{-1})	Found (mgL^{-1})	Added (mgL^{-1})	Recovery (mgL^{-1})	RSD (%) (n =3)	Recovery (%)
Lithium	0.0703	1.3227	1.2557	1.2524	0.26	99.74
Sodium	24.9149	29.6019	5.1084	4.6870	8.25	91.75
Ammonium	---	7.6039	6.3163	7.6039	-20.39	120.39
Potassium	10.9173	23.8307	12.7333	12.9134	-1.41	101.41
Magnesium	73.9612	80.2909	6.3415	6.3297	0.19	99.81
Calcium	80.3932	93.4622	12.8088	13.0690	-2.03	102.04

26-06-2008

Ion	Real Concn. (mgL^{-1})	Found (mgL^{-1})	Added (mgL^{-1})	Recovery (mgL^{-1})	RSD (%) (n =3)	Recovery (%)
Lithium	0.0703	1.3266	1.2508	1.2563	-0.44	100.44
Sodium	24.0588	28.7942	5.0882	4.7354	6.93	93.07
Ammonium	---	7.5893	6.2914	7.5893	-20.63	120.63
Potassium	10.8368	23.8461	12.6830	13.0093	-2.57	102.57
Magnesium	74.9782	81.3916	6.3164	6.4134	-1.54	101.54
Calcium	144.6197	157.8147	12.7582	13.1950	-3.42	103.42

Table 3.10 Cation concentrations, recovery, relative standard deviation (% RSD) and % recovery values for geothermal water samples collected from Bölmekaya in April 29, 2008 and june 26, 2008 respectively. Certified reference standards were diluted 1:25 with pure water

29-04-2008

Ion	Real Concn. (mgL^{-1})	Found (mgL^{-1})	Added (mgL^{-1})	Recovery (mgL^{-1})	RSD (%) (n =3)	Recovery (%)
Lithium	0.0703	2.0851	2.0314	2.0148	0.82	99.18
Sodium	24.9149	32.395	8.2641	7.4801	9.49	90.51
Ammonium	---	11.8811	10.2182	11.8811	-16.27	116.27
Potassium	10.9173	31.596	20.5993	20.6787	-0.39	100.39
Magnesium	73.9612	84.0301	10.2589	10.0689	1.85	98.15
Calcium	80.3932	101.1516	20.7214	20.7584	-0.18	100.18

26-06-2008

Ion	Real Concn. (mgL^{-1})	Found (mgL^{-1})	Added (mgL^{-1})	Recovery (mgL^{-1})	RSD (%) (n =3)	Recovery (%)
Lithium	0.0703	2.1288	2.0702	2.0585	0.57	99.43
Sodium	24.0588	31.9719	8.4219	7.9131	6.04	93.96
Ammonium	---	12.0318	10.4133	12.0318	-15.54	115.54
Potassium	10.8368	32.0273	20.9926	21.1905	-0.94	100.94
Magnesium	74.9782	85.4537	10.4548	10.4755	-0.20	100.20
Calcium	144.6197	166.0328	21.117	21.4131	-1.40	101.40

Table 3.11 Cation concentrations, recovery, relative standard deviation (% RSD) and % recovery values for geothermal water samples collected from Bölmekaya in April 29, 2008 and june 26, 2008 respectively. Certified reference standards were diluted 1:20 with pure water

29-04-2008

Ion	Real Concn. (mgL^{-1})	Found (mgL^{-1})	Added (mgL^{-1})	Recovery (mgL^{-1})	RSD (%) (n =3)	Recovery (%)
Lithium	0.0703	2.5981	2.5382	2.5278	0.41	99.59
Sodium	24.9149	34.2844	10.3255	9.3695	9.26	90.74
Ammonium	---	14.5528	12.7671	14.5528	-13.99	113.99
Potassium	10.9173	36.7258	25.376	25.8085	-1.70	101.70
Magnesium	73.9612	86.4753	12.8179	12.5141	2.37	97.63
Calcium	80.3932	106.1721	25.8902	25.7789	0.43	99.57

26-06-2008

Ion	Real Concn. (mgL^{-1})	Found (mgL^{-1})	Added (mgL^{-1})	Recovery (mgL^{-1})	RSD (%) (n =3)	Recovery (%)
Lithium	0.0703	2.6371	2.5602	2.5668	-0.26	100.26
Sodium	24.0588	35.2712	10.415	11.2124	-7.66	107.66
Ammonium	---	14.7518	12.8777	14.7518	-14.55	114.55
Potassium	10.8368	37.0993	25.9606	26.2625	-1.16	101.16
Magnesium	74.9782	87.7349	12.929	12.7567	1.33	98.67
Calcium	144.6197	168.9871	26.1146	24.3674	6.69	93.31

Table 3.12 Cation concentrations, recovery, relative standard deviation (% RSD) and % recovery values for two parallel drinking water samples. Certified reference standards were diluted 1:25 with pure water

Sample 1

Ion	Real Concn. (mgL^{-1})	Found (mgL^{-1})	Added (mgL^{-1})	Recovery (mgL^{-1})	RSD (%) (n =3)	Recovery (%)
Lithium	---	1.0287	1.0167	1.0287	-1.18	101.18
Sodium	1.6011	5.7425	4.1359	4.1414	-0.13	100.13
Ammonium	---	6.222	5.1139	6.2220	-21.67	121.67
Potassium	0.5587	10.8493	10.3092	10.2906	0.18	99.82
Magnesium	0.5802	5.6857	5.1342	5.1055	0.56	99.44
Calcium	4.3083	14.6234	10.3703	10.3151	0.53	99.47

Sample 2

Ion	Real Concn. (mgL^{-1})	Found (mgL^{-1})	Added (mgL^{-1})	Recovery (mgL^{-1})	RSD (%) (n =3)	Recovery (%)
Lithium	---	1.0102	1.0257	1.0102	1.51	98.49
Sodium	1.6011	5.7705	4.1727	4.1694	0.08	99.92
Ammonium	---	6.1729	5.1593	6.1729	-19.65	119.65
Potassium	0.5587	10.7974	10.4008	10.2387	1.56	98.44
Magnesium	0.5802	5.6981	5.1799	5.1179	1.20	98.80
Calcium	4.3083	14.8955	10.4625	10.5872	-1.19	101.19

3.6.2 Statistical Assessment of Recovery Results of Geothermal Water Samples

The recovery results acquired with three different concentrations of standards were compared statistically in 95 % confidence level. For this purpose, pooled standard deviations, experimental difference ($|\bar{x}_1 - \bar{x}_2|$) and computed values were calculated for geothermal water samples of Bölmekaya location. Calculations made for lithium are as follows.

$$S_{pooled} = \sqrt{\frac{\sum_{i=1}^{n}(x_i - x)^2 + \sum_{j=1}^{n}(x_j - \bar{x})^2}{N_1 + N_2 - 2}}$$

$$S_{pooled} = \sqrt{\frac{(0)^2 + (0{,}0004)^2 + (-0{,}0004)^2 + (-0{,}0002)^2 + (-0{,}0001)^2 + (-0{,}0004)^2}{3+3-2}}$$

$S_{pooled} = 0.0004$

S_{pooled}: Pooled standard deviation. x_i: any measurement value. $\bar{x}$: mean value of first group of measurements. N_1 and N_2: number of replicated analysis. For 95 % confidence level t=2.78; and if

$$|\bar{x}_1 - \bar{x}_2| < t * S_{pooled} * \sqrt{\frac{N1 + N2}{N1 * N2}}$$

In our case;

$$|1.3227 - 1.3266| < 2.78 * 0.0004 * \sqrt{\frac{3+3}{3*3}}$$

$0.0039 > 0.0008$

The difference of averages of lithium for two successive months is 0.0039 and this value is larger than the critical value for 1:40 dilution ratio for 95 % confidence level.

In other terms; the experimental difference is higher than the computed value and significant ‘’difference’’ between the means has been demonstrated at 95 % confidence level for lithium measurements.

Similarly; test results of sodium, potassium, magnesium and calcium exhibited significant experimental differences between the measurements performed at different dates (See Table 3.13, 3.14 and 3.15).

These differences can be attributed to the concentrations of major cations in geothermal water samples collected from Bölmekaya in April 29, 2008 and june 26, 2008 may be altered because of seasonal effects.

Table 3.13 Statistical evaluation of geothermal water samples of Bölmekaya location. The results were acquired with 1:40 diluted standards. First and second measurements were performed at April 29, 2008 and June 26, 2008 respectively

Ion	1^{st} Measurement (Ave.) (mgL^{-1})	2^{nd} Measurement (Ave.) (mgL^{-1})	S_{pooled}	$\lvert 1st - 2nd \rvert$ Measurement (Ave.) (mgL^{-1})	$t*S_{pooled}*\sqrt{(N1+N2)/(N1*N2)}$	Statistical Results
Li^+	1.3227	1.3266	0.0004	0.0039	0.0008	DIFFERENT
Na^+	29.6020	28.7942	0.0156	0.8078	0.0355	DIFFERENT
NH_4^+	7.6040	7.5893	0.0053	0.0147	0.0121	DIFFERENT
K^+	23.8307	23.8461	0.0088	0.0154	0.0199	DIFFERENT
Mg^{2+}	80.2910	81.3916	0.0499	1.1007	0.1132	DIFFERENT
Ca^{2+}	93.4623	157.8147	0.0578	64.3525	0.1312	DIFFERENT

Table 3.14 Statistical evaluation of geothermal water samples of Bölmekaya location. The results were acquired with 1:25 diluted standards. First and second measurements were performed at April 29, 2008 and June 26, 2008 respectively

Ion	1st Measurement (Ave.) (mgL^{-1})	2nd Measurement (Ave.) (mgL^{-1})	S_{pooled}	|1st -2nd| Measurement (Ave.) (mgL^{-1})	$t*S_{pooled}*\sqrt{(N1+N2)/(N1*N2)}$	Statistical Results
Li^+	2.0851	2.1288	0.0015	0.0437	0.0033	DIFFERENT
Na^+	32.3950	31.9719	0.0109	0.4231	0.0248	DIFFERENT
NH_4^+	11.8811	12.0319	0.0426	0.1507	0.0966	DIFFERENT
K^+	31.5860	32.0274	0.0049	0.4413	0.0112	DIFFERENT
Mg^{2+}	84.0301	85.4537	0.0417	1.4236	0.0948	DIFFERENT
Ca^{2+}	101.1516	166.0328	0.0282	64.8812	0.0640	DIFFERENT

Table 3.15 Statistical evaluation of geothermal water samples of Bölmekaya location. The results were acquired with 1:20 diluted standards. First and second measurements were performed at April 29, 2008 and June 26, 2008 respectively

Ion	1st Measurement (Ave.) (mgL^{-1})	2nd Measurement (Ave.) (mgL^{-1})	S_{pooled}	|1st -2nd| Measurement (Ave.) (mgL^{-1})	$t*S_{pooled}*\sqrt{(N1+N2)/(N1*N2)}$	Statistical Results
Li^+	2.5981	2.6371	0.0012	0.0390	0.0028	DIFFERENT
Na^+	34.2844	35.2712	0.0038	0.9868	0.0086	DIFFERENT
NH_4^+	14.5528	14.7518	0.0302	0.1990	0.0687	DIFFERENT
K^+	36.7259	37.0993	0.0147	0.3735	0.0334	DIFFERENT
Mg^{2+}	86.4753	87.7349	0.1452	1.2596	0.3295	DIFFERENT
Ca^{2+}	106.1721	168.9871	0.0597	62.8149	0.1354	DIFFERENT

3.6.3 Reproducibility

Reproducibility of the method was assessed as the percentage relative standard deviation (%RSD) of both (within-day) and (between-days) at different concentrations of the certified reference standard (CRS) solutions.

Standard deviation (SD) and relative standard deviation (RSD) calculations of Calcium; as a representative example; were shown below.

$$SD = \sqrt{\frac{\sum (x_{ave} - x_i)^2}{N - 1}}$$

$$SD = \sqrt{\frac{0.001602}{6 - 1}}$$

$$SD = 0.0179$$

$$RSD = \frac{S.D.}{x_{av.}} \text{ x } 100$$

$$RSD = \frac{0.0179}{7.0979} \text{ x}100$$

$$RSD = \% \ 0.2528$$

Where N is the number of measurements. RSD is relative standard deviation. SD is standard deviation and X_{ave} is average of peak area. Calculations for other cations were performed similarly.

3.6.3.1 Reproducibility of Replicate Injection

The certified reference standard solutions were diluted 1: 25 with ultra pure water and used as test material. After 12 injections the peak areas were integrated. Standard deviation (SD) and relative standard deviation (% RSD) of peak areas were calculated. For a satisfactory reproducibility, the relative standard deviation should be less than 1 %. Except that of sodium, RSD values of six cations were found to be less than 1 % for 12 replicate measurements.

Table 3.16 Average, SD and RSD values of six cations for 12 measurements

n=12	Peak Area (µS*min) Lithium	Peak Area (µS*min) Sodium	Peak Area (µS*min) Ammonium	Peak Area (µS*min) Potassium	Peak Area (µS*min) Magnesium	Peak Area (µS*min) Calcium
I.	2.2354	2.6370	1.7760	3.8698	5.5829	7.0821
II.	2.2380	2.6393	1.7758	3.8645	5.5788	7.0936
III.	2.2358	2.6370	1.7757	3.8671	5.5772	7.1108
IV.	2.2358	2.4930	1.7781	3.8585	5.5755	7.0846
V.	2.2349	2.4868	1.7777	3.8595	5.5726	7.1017
VI.	2.2314	2.4917	1.7778	3.8659	5.5657	7.0854
VII.	2.2334	2.4878	1.7758	3.8546	5.5667	7.0790
VIII.	2.2359	2.4874	1.7761	3.8505	5.5650	7.0800
IX.	2.2323	2.4873	1.7739	3.8519	5.5684	7.0931
X.	2.2420	2.5144	1.7801	3.8815	5.5857	7.1217
XI.	2.2425	2.5131	1.7765	3.8781	5.5904	7.1355
XII.	2.2425	2.5127	1.7794	3.8773	5.5867	7.1068
AVERAGE	2.2367	2.5323	1.7769	3.8649	5.5763	7.0979
S.D	0.0038	0.0645	0.0018	0.0104	0.0088	0.0179
% R.S.D.	**0.1719**	**2.5462**	**0.0987**	**0.2687**	**0.1581**	**0.2528**

3.6.3.2 Reproducibility Studies of Intraday

Three different concentrations of two parallel standards were injected three times to the instrument within the same day. Concentrations were calculated from earlier calibration graphs. SD and RSD values were extracted from these data. The expected RSD values within intraday should be less than 2 % according to the statements of international organizations like ISO 9000. EPA (Environmental Protection Agency). FDA (Federal Drug Administration) and 17025 and EN (European Norms) 45001**.**

For dilution ratio of 1:40, 1:25 and 1:20 RSD % values were excellent. Table 3.17 reveals average SD and RSD % values of six cations for 6 replicate measurements of two parallel samples measured within the same day.

Table 3.17 Average (mgL^{-1}), SD and RSD values of 6 cations for six replicate measurements of two parallel samples measured within the same day.

1:40 dilution

n=6	Amount (mgL^{-1}) Lithium	Amount (mgL^{-1}) Sodium	Amount (mgL^{-1}) Ammonium	Amount (mgL^{-1}) Potassium	Amount (mgL^{-1}) Magnesium	Amount (mgL^{-1}) Calcium
Concentration (mgL^{-1})	1.2719	5.2753	7.3066	12.9554	6.3913	12.9154
	1.2707	5.2760	7.3041	12.9448	6.3830	12.9113
	1.2705	5.2776	7.2980	12.9360	6.3875	12.9128
	1.2703	5.2685	7.2871	12.9124	6.3852	12.9300
	1.2727	5.2822	7.2908	12.9129	6.3851	12.9475
	1.2713	5.2735	7.2762	12.9198	6.3881	12.9294
Average	1.2712	5.2755	7.2938	12.9302	6.3867	12.9244
S.D	0.0009	0.0045	0.0114	0.0179	0.0029	0.0140
%R.S.D	**0.0729**	**0.0859**	**0.1565**	**0.1386**	**0.0455**	**0.1082**

1:25 dilution

n=6	Amount (mgL^{-1}) Lithium	Amount (mgL^{-1}) Sodium	Amount (mgL^{-1}) Ammonium	Amount (mgL^{-1}) Potassium	Amount (mgL^{-1}) Magnesium	Amount (mgL^{-1}) Calcium
Concentration (mgL^{-1})	2.0385	8.4833	10.8993	20.7483	10.2250	20.7471
	2.0369	8.4801	10.9008	20.7973	10.2341	20.7923
	2.0369	8.4861	10.8911	20.7979	10.2334	20.8071
	2.0308	8.2064	10.9699	20.6854	10.1693	20.6596
	2.0305	8.2077	10.9719	20.6928	10.1769	20.6411
	2.0297	8.2105	10.9653	20.6858	10.1774	20.6836
Average	2.0339	8.3457	10.9331	20.7346	10.2027	20.7218
S.D	0.0039	0.1506	0.0396	0.0542	0.0311	0.0703
%R.S.D	**0.1942**	**1.8048**	**0.3623**	**0.2613**	**0.3052**	**0.3394**

1:20 dilution

n=6	Amount (mgL^{-1}) Lithium	Amount (mgL^{-1}) Sodium	Amount (mgL^{-1}) Ammonium	Amount (mgL^{-1}) Potassium	Amount (mgL^{-1}) Magnesium	Amount (mgL^{-1}) Calcium
Concentration (mgL^{-1})	2.5028	10.5375	13.0904	25.4349	12.5906	25.5168
	2.5047	10.5505	13.0968	25.4240	12.5805	25.5879
	2.5061	10.5407	13.1067	25.4371	12.5916	25.5185
	2.5146	10.2061	13.1550	25.5642	12.6339	25.6472
	2.5170	10.2046	13.1486	25.5971	12.6191	25.5412
	2.5158	10.2066	13.1341	25.5860	12.6230	25.6898
Average	2.5102	10.3743	13.1219	25.5072	12.6065	25.5836
S.D	0.0063	0.1847	0.0276	0.0832	0.0216	0.0719
%R.S.D	**0.2512**	**1.7804**	**0.2104**	**0.3261**	**0.1713**	**0.2810**

3.6.3.3 Reproducibility Studies between Months

Three different concentrations of two parallel standards were injected three times to the instrument at two different dates after a period of one month. Concentrations were calculated from earlier calibration graphs, SD and RSD values were extracted from these data. The expected RSD should be less than 2%.

From Table 3.18 it can be concluded that the RSD values of geothermal water samples measured between two successive months were slightly deviated from the expected value; 2%; for all of the employed dilution ratio; the RSD values of the cations were found to be within the expected values.

Table 3.18 Average SD and RSD values of six cations for two sets of measurements of two parallel samples measured after a period of one month.

1:40 dilution

n = 12	Amount (mgL^{-1}) Lithium	Amount (mgL^{-1}) Sodium	Amount (mgL^{-1}) Ammonium	Amount (mgL^{-1}) Potassium	Amount (mgL^{-1}) Magnesium	Amount (mgL^{-1}) Calcium
Concentration (mgL^{-1}) (May)	1.2719	5.2753	7.3066	12.9554	6.3913	12.9154
	1.2707	5.2760	7.3041	12.9448	6.3830	12.9113
	1.2705	5.2776	7.2980	12.9360	6.3875	12.9128
	1.2703	5.2685	7.2871	12.9124	6.3852	12.9300
	1.2727	5.2822	7.2908	12.9129	6.3851	12.9475
	1.2713	5.2735	7.2762	12.9198	6.3881	12.9294
Concentration (mgL^{-1}) (June)	1.2724	5.2762	7.3219	12.9400	6.4000	13.0018
	1.2723	5.2737	7.3142	12.9295	6.3940	12.9266
	1.2724	5.2761	7.3190	12.9343	6.3989	12.9903
	1.2697	5.2430	7.3203	12.8461	6.3790	12.9210
	1.2692	5.2325	7.3305	12.8705	6.3760	12.9903
	1.2694	5.2332	7.3391	12.8629	6.3826	12.9488
Average	1.2711	5.2657	7.3090	12.9137	6.3876	12.9438
S.D	0.0012	0.0182	0.0187	0.0352	0.0074	0.0327
%R.S.D	**0.0955**	**0.3453**	**0.2552**	**0.2725**	**0.1159**	**0.2527**

1:25 dilution

n = 12	Amount (mgL^{-1}) Lithium	Amount (mgL^{-1}) Sodium	Amount (mgL^{-1}) Ammonium	Amount (mgL^{-1}) Potassium	Amount (mgL^{-1}) Magnesium	Amount (mgL^{-1}) Calcium
Concentration (mgL^{-1}) (May)	2.0385	8.4833	10.8993	20.7483	10.2250	20.7471
	2.0369	8.4801	10.9008	20.7973	10.2341	20.7923
	2.0369	8.4861	10.8911	20.7979	10.2334	20.8071
	2.0308	8.2064	10.9699	20.6854	10.1693	20.6596
	2.0305	8.2077	10.9719	20.6928	10.1769	20.6411
	2.0297	8.2105	10.9653	20.6858	10.1774	20.6836
Concentration (mgL^{-1}) (June)	2.0265	8.1495	11.0733	20.6368	10.1864	20.7224
	2.0251	8.1457	11.0982	20.6718	10.1828	20.7305
	2.0270	8.1531	10.9398	20.6315	10.1794	20.7589
	2.0327	8.1759	10.9702	20.6653	10.1897	20.6943
	2.0316	8.1630	10.9564	20.6322	10.1882	20.7284
	2.0341	8.1736	10.9656	20.6520	10.1859	20.6361
Average	2.0317	8.2529	10.9668	20.6914	10.1940	20.7168
S.D	0.0043	0.1406	0.0633	0.0592	0.0230	0.0556
%R.S.D	**0.2130**	**1.7040**	**0.5776**	**0.2861**	**0.2255**	**0.2684**

1:20 dilution

n = 12	Amount (mgL^{-1}) Lithium	Amount (mgL^{-1}) Sodium	Amount (mgL^{-1}) Ammonium	Amount (mgL^{-1}) Potassium	Amount (mgL^{-1}) Magnesium	Amount (mgL^{-1}) Calcium
Concentration (mgL^{-1}) (May)	2.5028	10.5375	13.0904	25.4349	12.5906	25.5168
	2.5047	10.5505	13.0968	25.4240	12.5805	25.5879
	2.5061	10.5407	13.1067	25.4371	12.5916	25.5185
	2.5146	10.2061	13.1550	25.5642	12.6339	25.6472
	2.5170	10.2046	13.1486	25.5971	12.6191	25.5412
	2.5158	10.2066	13.1341	25.5860	12.6230	25.6898
Concentration (mgL^{-1}) (June)	2.5053	10.1988	13.1042	25.5851	12.5793	25.5957
	2.5076	10.2091	13.0709	25.5119	12.5848	25.6043
	2.5077	10.2036	13.0656	25.5468	12.5942	25.5783
	2.5160	10.1830	13.1480	25.4851	12.6323	25.5958
	2.5135	10.1670	13.1758	25.5204	12.6479	25.6761
	2.5226	10.1921	13.3296	25.5860	12.6605	25.7455
Average	2.5111	10.2833	13.1355	25.5232	12.6115	25.6081
S.D	0.0062	0.1570	0.0703	0.0647	0.0281	0.0702
%R.S.D	**0.2471**	**1.5269**	**0.5354**	**0.2535**	**0.2229**	**0.2740**

3.7 Analysis of Geothermal Water Samples of Pamukkale Location with Ion Chromatography

In this work, six cations (lithium, sodium, ammonium, potassium, magnesium, and calcium) in geothermal water samples that were collected daily during twelwe months (July 2007- June 2008) from Denizli Pamukkale Antique Pool, were tested and analyzed with ion chromatographic method. Lithium, sodium, potassium, magnesium and calcium were found to be major ions in Pamukkale geothermal water samples. Ammonium concentrations were found to be zero.

Table 3.19, 3.20, 3.21, 3.22 and 3.23 reveal retention time (min.), peak area (μS*min) and peak height (μS) values of lithium, sodium, potassium, magnesium and calcium of geothermal water samples collected from Pamukkale Antique Pool between May 30, 2008 and June 27, 2008, respectively.

For 29 consecutive measurements, the average value of lithium concentration was found to be 0.0950 mgL^{-1}. SD and RSD of the measurements were calculated as 0.0011 mgL^{-1} and 1.1401 % respectively.

Average concentrations of sodium, potassium, magnesium and calcium were found to be 44.135, 5.6253, 88.0932 and 425.0893 mgL^{-1} respectively. Sodium and calcium measurements were performed after 1:4 dilution.

SD and RSD values of sodium, potassium, magnesium and calcium were 1.7992 mgL^{-1} (4.0787 %), 0.0846 mgL^{-1} (1.5033 %), 1.5993 mgL^{-1} (1.8155 %) and 22.8091 mgL^{-1} (5.3657 %) respectively. Among them, calcium measurements resulted with the highest SD and RSD. In case of lithium, sodium, potassium and magnesium SD and RSD values were satisfactory (See Table 3.19, 3.20, 3.21, 3.22 and 3.23).

Table 3.19 Retention time (min), peak area (μS*min) and peak height (μS) values for lithium in geothermal water samples of Pamukkale Antique Pool, Denizli.

Sample Date	**Ret. Time (min) Lithium**	**Area (μS*min) Lithium**	**Height (μS) Lithium**	**Amount (mgL^{-1}) Lithium**
30.05.2008	3.657	0.1083	0.7988	0.1001
31.05.2008	3.657	0.1019	0.7502	0.0943
01.06.2008	3.660	0.1016	0.7477	0.0940
02.06.2008	3.664	0.1026	0.7529	0.0950
03.06.2008	3.664	0.1009	0.7386	0.0935
04.06.2008	3.667	0.1020	0.7464	0.0945
05.06.2008	3.667	0.1018	0.7470	0.0943
06.06.2008	3.667	0.1015	0.7461	0.0940
07.06.2008	3.664	0.1018	0.7503	0.0943
08.06.2008	3.667	0.1021	0.7530	0.0945
09.06.2008	3.667	0.1022	0.7552	0.0946
10.06.2008	3.667	0.1025	0.7588	0.0949
11.06.2008	3.667	0.1025	0.7594	0.0949
12.06.2008	3.667	0.1028	0.7618	0.0952
13.06.2008	3.670	0.1035	0.7648	0.0958
14.06.2008	3.670	0.1024	0.7576	0.0949
15.06.2008	3.670	0.1026	0.7583	0.0950
16.06.2008	3.670	0.1030	0.7605	0.0954
17.06.2008	3.670	0.1029	0.7585	0.0953
18.06.2008	3.674	0.1030	0.7589	0.0953
19.06.2008	3.674	0.1028	0.7559	0.0952
20.06.2008	3.674	0.1034	0.7596	0.0957
21.06.2008	3.674	0.1029	0.7567	0.0953
22.06.2008	3.673	0.1026	0.7534	0.0950
23.06.2008	3.673	0.1028	0.7551	0.0951
24.06.2008	3.674	0.1026	0.7543	0.0950
25.06.2008	3.673	0.1028	0.7535	0.0951
26.06.2008	3.673	0.1025	0.7522	0.0949
27.06.2008	3.673	0.1026	0.7512	0.0950
AVERAGE	**3.669**	**0.1027**	**0.7557**	**0.0950**
S.D	**0.005**	**0.0012**	**0.0100**	**0.0011**
% R.S.D	**0.134**	**1.1964**	**1.3230**	**1.1401**

Table 3.20 Retention time (min), peak area (μS*min) and peak height (μS) values for Sodium in geothermal water samples of Pamukkale Antique Pool, Denizli.

Sample Date	Ret. Time (min) Sodium	Area (μS*min) Sodium	Height (μS) Sodium	Amount (mgL^{-1}) Sodium
30.05.2008	4.377	3.2518	22.0870	44.2826
31.05.2008	4.377	3.2554	22.1268	44.3325
01.06.2008	4.377	3.2803	22.2483	44.6711
02.06.2008	4.380	3.3690	23.0063	45.8793
03.06.2008	4.380	3.3715	22.8883	45.9131
04.06.2008	4.377	3.4704	23.6025	47.2598
05.06.2008	4.373	3.2620	22.1952	44.4220
06.06.2008	4.373	3.3151	22.5697	45.1448
07.06.2008	4.370	3.1809	21.8105	43.3172
08.06.2008	4.377	3.2856	22.3133	44.7433
09.06.2008	4.394	3.1938	21.4474	43.4926
10.06.2008	4.417	3.1173	20.7564	42.4499
11.06.2008	4.430	3.0029	19.7457	40.8911
12.06.2008	4.443	3.0535	19.8109	41.5812
13.06.2008	4.450	2.9318	18.8872	39.9211
14.06.2008	4.453	2.9879	19.1860	40.6871
15.06.2008	4.407	3.2234	21.4953	43.8964
16.06.2008	4.410	3.3005	22.0122	44.9459
17.06.2008	4.410	3.2524	21.8266	44.2916
18.06.2008	4.410	3.1713	21.2453	43.1867
19.06.2008	4.413	3.3964	22.6394	46.2527
20.06.2008	4.417	3.4286	22.8183	46.6905
21.06.2008	4.417	3.1829	21.1219	43.3436
22.06.2008	4.414	3.2096	21.4887	43.7081
23.06.2008	4.403	3.4028	22.7715	46.3401
24.06.2008	4.397	3.1906	21.5613	43.4495
25.06.2008	4.394	3.1816	21.5454	43.3270
26.06.2008	4.394	3.4212	23.0394	46.5897
27.06.2008	4.393	3.2517	22.0712	44.2819
AVERAGE	**4.401**	**3.2394**	**21.7351**	**44.1135**
S.D	**0.024**	**0.1344**	**1.1541**	**1.7992**
% R.S.D	**0.536**	**4.1490**	**5.3100**	**4.0787**

Table 3.21 Retention time (min), peak area (μS*min) and peak height (μS) values for Potassium in geothermal water samples of Pamukkale Antique Pool, Denizli.

Sample Date	Ret. Time (min) Potassium	Area (μS*min) Potassium	Height (μS) Potassium	Amount (mgL^{-1}) Potassium
30.05.2008	6.207	1.0573	5.5628	5.6331
31.05.2008	6.207	1.0328	5.4311	5.5034
01.06.2008	6.207	1.0420	5.4769	5.5520
02.06.2008	6.207	1.0544	5.5342	5.6180
03.06.2008	6.207	1.0333	5.4280	5.5063
04.06.2008	6.200	1.0413	5.4673	5.5483
05.06.2008	6.180	1.0683	5.6363	5.6916
06.06.2008	6.157	1.0375	5.5088	5.5284
07.06.2008	6.134	1.1186	5.9681	5.9583
08.06.2008	6.117	1.0514	5.6302	5.6019
09.06.2008	6.103	1.0760	5.7860	5.7325
10.06.2008	6.090	1.0557	5.6961	5.6249
11.06.2008	6.080	1.0430	5.6464	5.5576
12.06.2008	6.077	1.0635	5.7629	5.6664
13.06.2008	6.080	1.0554	5.7092	5.6230
14.06.2008	6.084	1.0514	5.6841	5.6018
15.06.2008	6.087	1.0542	5.6830	5.6167
16.06.2008	6.090	1.0549	5.6880	5.6203
17.06.2008	6.090	1.0578	5.6978	5.6356
18.06.2008	6.097	1.0501	5.6653	5.5949
19.06.2008	6.100	1.0620	5.7134	5.6582
20.06.2008	6.100	1.0525	5.6567	5.6079
21.06.2008	6.104	1.0624	5.7119	5.6604
22.06.2008	6.103	1.0664	5.7264	5.6814
23.06.2008	6.103	1.0689	5.7331	5.6950
24.06.2008	6.107	1.0450	5.6110	5.5680
25.06.2008	6.110	1.0681	5.7217	5.6905
26.06.2008	6.113	1.0481	5.6157	5.5844
27.06.2008	6.117	1.0464	5.6025	5.5757
AVERAGE	**6.126**	**1.0558**	**5.6467**	**5.6254**
S.D	**0.047**	**0.0162**	**0.1160**	**0.0846**
% R.S.D	**0.763**	**1.5374**	**2.0543**	**1.5033**

Table 3.22 Retention time (min), peak area (μS*min) and peak height (μS) values for Magnesium in geothermal water samples of Pamukkale Antique Pool, Denizli.

Sample Date	Ret. Time (min) Magnesium	Area (μS*min) Magnesium	Height (μS) Magnesium	Amount (mgL^{-1}) Magnesium
30.05.2008	9.540	47.7162	102.4084	91.1525
31.05.2008	9.540	47.8867	103.0965	91.4976
01.06.2008	9.547	47.4525	101.5680	90.6190
02.06.2008	9.540	47.7845	101.8798	91.2907
03.06.2008	9.554	46.7288	99.3253	89.1567
04.06.2008	9.550	46.8894	99.3251	89.4810
05.06.2008	9.543	47.0323	99.5165	89.7697
06.06.2008	9.540	46.5915	98.6932	88.8796
07.06.2008	9.537	46.2854	98.0605	88.2623
08.06.2008	9.537	46.2712	97.9993	88.2336
09.06.2008	9.540	46.3316	98.1930	88.3554
10.06.2008	9.540	46.4879	98.4326	88.6707
11.06.2008	9.540	46.1671	97.6572	88.0238
12.06.2008	9.540	46.2306	97.7537	88.1518
13.06.2008	9.547	46.2388	97.6704	88.1682
14.06.2008	9.554	45.8956	96.9007	87.4767
15.06.2008	9.554	45.9002	96.6333	87.4860
16.06.2008	9.554	46.0599	96.8469	87.8077
17.06.2008	9.554	45.7441	96.0452	87.1715
18.06.2008	9.557	45.8144	96.0757	87.3133
19.06.2008	9.560	45.5921	95.5490	86.8657
20.06.2008	9.557	45.8573	95.7582	87.3995
21.06.2008	9.560	45.4267	95.0309	86.5328
22.06.2008	9.560	45.4650	95.0560	86.6099
23.06.2008	9.560	45.3585	94.8211	86.3957
24.06.2008	9.560	45.2415	94.4981	86.1604
25.06.2008	9.560	45.1721	94.2464	86.0208
26.06.2008	9.560	45.1304	94.1617	85.9370
27.06.2008	9.560	45.0686	94.0132	85.8128
AVERAGE	**9.550**	**46.2007**	**97.4902**	**88.0932**
S.D	**0.009**	**0.8069**	**2.5354**	**1.5993**
% R.S.D	**0.092**	**1.7466**	**2.6007**	**1.8155**

Table 3.23 Retention time (min), peak area (μS*min) and peak height (μS) values for Calcium in geothermal water samples of Pamukkale Antique Pool, Denizli.

Sample Date	Ret. Time (min) Calcium	Area (μS*min) Calcium	Height (μS) Calcium	Amount (mgL^{-1}) Calcium
30.05.2008	11.270	157.7266	216.6213	440.4533
31.05.2008	11.320	141.8702	199.0451	397.4437
01.06.2008	11.357	133.2110	189.2693	373.8422
02.06.2008	11.327	141.8047	198.9273	397.2656
03.06.2008	11.370	131.5097	187.0758	369.1955
04.06.2008	11.320	143.7635	201.1683	402.5933
05.06.2008	11.307	143.6497	201.8044	402.2840
06.06.2008	11.250	157.1939	217.7578	439.0127
07.06.2008	11.267	147.9055	208.2242	413.8459
08.06.2008	11.257	149.1541	210.4230	417.2342
09.06.2008	11.237	154.7861	217.5411	432.4977
10.06.2008	11.217	160.3624	224.0615	447.5770
11.06.2008	11.280	139.2535	200.7699	390.3204
12.06.2008	11.230	154.7862	218.6570	432.4980
13.06.2008	11.227	157.8958	221.9742	440.9109
14.06.2008	11.224	160.4800	224.4870	447.8945
15.06.2008	11.247	154.8142	217.4270	432.5739
16.06.2008	11.234	159.3603	222.8320	444.8696
17.06.2008	11.264	150.0355	212.1532	419.6254
18.06.2008	11.244	157.4895	220.3784	439.8122
19.06.2008	11.254	154.9809	217.4833	433.0252
20.06.2008	11.264	151.6537	213.5953	424.0127
21.06.2008	11.280	147.3887	208.5838	412.4429
22.06.2008	11.240	159.7482	222.4081	445.9177
23.06.2008	11.240	159.5589	222.1408	445.4061
24.06.2008	11.240	159.9847	222.5449	446.5565
25.06.2008	11.243	159.4452	221.8482	445.0991
26.06.2008	11.243	160.2577	222.4602	447.2942
27.06.2008	11.247	159.8100	221.9824	446.0845
AVERAGE	**11.266**	**152.0648**	**213.2291**	**425.0893**
S.D	**0.040**	**8.5524**	**10.7189**	**22.8091**
% R.S.D	**0.353**	**5.6242**	**5.0269**	**5.3657**

Lithium, sodium, potassium, magnesium and calcium concentrations were monitored during 12 months. Table 3.24 shows the gathered measurement results of SD and RSD on bases of months from July 2007 to June 2008. The statistical evaluation was performed by employing all of the acquired data. The questionable values did not sorted out employing either Q or T_n tests.

All of the acquired data between July 2007 and June 2008, exhibited parallel RSD for six different cations. Fluctuations observed between July 2007 and June 2008 can be attributed to seasonal changes of ion content of the geothermal water of Pamukkale. Concentrations of the investigated cations was within the detection range of the instrument.

SD and RSD values of lithium, sodium, potassium, magnezium and calcium were less then 5 % and in acceptable range for 320 data acquired during 12 months.

Table 3.25 reveals gathered measurement results of 12 months of averages SD and RSD values of lithium, sodium, potassium, magnezium and calcium.

Table 3.24 Concentrations in mgL^{-1}, SD (mgL^{-1}) and RSD% values of Lithium, Sodium, Potassium, Magnesium and Calcium on bases of month from July 2007 to June 2008.

DATE		Lithium				Sodium				Potassium			
		Ret.Time	Area	Height	Amount	Ret.Time	Area	Height	Amount	Ret.Time	Area	Height	Amount
		min	µS*min	µS	mgL^{-1}	min	µS*min	µS	mgL^{-1}	min	µS*min	µS	mgL^{-1}
July 07	**AVE.**	3.572	0.1033	0.7434	0.1151	4.248	3.1221	19.7428	40.3943	5.796	1.0754	5.6226	5.3823
	S.D	0.036	0.0035	0.0688	0.0049	0.017	0.0637	2.2130	1.1075	0.089	0.0505	0.6670	0.3642
	%R.S.D	**1.009**	**3.3523**	**9.2604**	**4.2687**	**0.409**	**2.0390**	**11.2093**	**2.7417**	**1.545**	**4.6916**	**11.8631**	**6.7673**
August 07	**AVE.**	3.539	0.0995	0.6471	0.1222	4.214	3.1909	17.9353	41.7114	5.778	1.0429	4.7409	5.2369
	S.D	0.005	0.0022	0.0302	0.0184	0.003	0.2997	1.3548	5.0571	0.045	0.0187	0.3074	0.2630
	%R.S.D	**0.127**	**2.1669**	**4.6621**	**15.0707**	**0.064**	**9.3920**	**7.5540**	**12.1240**	**0.771**	**1.7894**	**6.4835**	**5.0216**
Sept. 07	**AVE.**	3.539	0.0969	0.5988	0.1320	4.214	3.1912	19.0562	42.6730	5.817	1.0316	4.3261	5.5296
	S.D	0.015	0.0019	0.0093	0.0237	0.018	0.1241	1.7196	2.0339	0.047	0.0215	0.0903	0.1970
	%R.S.D	**0.425**	**2.0075**	**1.5541**	**17.9562**	**0.421**	**3.8874**	**9.0240**	**4.7663**	**0.813**	**2.0840**	**2.0862**	**3.5621**
Oct. 07	**AVE.**	3.542	0.1011	0.6263	0.1004	4.042	3.1506	16.7056	40.3500	5.814	1.0321	4.4423	5.3374
	S.D	0.009	0.0009	0.0050	0.0008	0.122	0.1335	0.8908	1.7409	0.017	0.0160	0.0638	0.0832
	%R.S.D	**0.241**	**0.8854**	**0.8048**	**0.8032**	**3.017**	**4.2360**	**5.3324**	**4.3145**	**0.297**	**1.5456**	**1.4354**	**1.5587**
Nov. 07	**AVE.**	3.580	0.1012	0.6846	0.1002	4.203	3.0606	20.1611	39.2464	5.913	1.0704	5.1223	5.5402
	S.D	0.012	0.0060	0.0445	0.0055	0.048	0.1442	0.9817	2.0344	0.027	0.0955	0.4307	0.4993
	%R.S.D	**0.339**	**5.9602**	**6.5032**	**5.5221**	**1.151**	**4.7118**	**4.8692**	**5.1836**	**0.461**	**8.9229**	**8.4081**	**9.0120**
Dec. 07	**AVE.**	3.547	0.1050	0.6598	0.0955	4.233	3.2261	18.5441	43.3275	5.845	1.1580	4.9457	6.0932
	S.D	0.004	0.0014	0.0087	0.0012	0.077	0.1097	1.1405	1.4684	0.004	0.0590	0.2770	0.3054
	%R.S.D	**0.109**	**1.3336**	**1.3142**	**1.2801**	**1.813**	**3.4010**	**6.1503**	**3.3891**	**0.064**	**5.0937**	**5.6018**	**5.0120**

DATE		Magnesium				Calcium			
		Ret.Time	Area	Height	Amount	Ret.Time	Area	Height	Amount
		min	µS*min	µS	mgL^{-1}	min	µS*min	µS	mgL^{-1}
July 07	AVE.	8.998	43.5735	98.0893	79.6142	10.542	157.9616	249.7597	467.7517
	S.D	0.256	1.9986	6.7674	2.9526	0.282	12.8595	18.8579	47.7389
	%R.S.D	**2.849**	**4.5867**	**6.8992**	**3.7086**	**2.673**	**8.1409**	**7.5504**	**10.2060**
August 07	AVE.	8.769	44.3762	97.9378	80.8079	10.284	168.9328	257.9634	494.3179
	S.D	0.094	1.0074	2.1425	3.1424	0.156	29.1278	43.7618	84.3149
	%R.S.D	**1.079**	**2.2701**	**2.1876**	**3.8887**	**1.520**	**17.2422**	**16.9644**	**17.0568**
Sept. 07	AVE.	8.793	43.8247	93.2986	80.7520	10.399	140.3797	210.8113	422.4603
	S.D	0.195	0.8303	2.3938	2.8111	0.182	24.3486	18.3586	101.1565
	%R.S.D	**2.223**	**1.8946**	**2.5657**	**3.4812**	**1.746**	**17.3448**	**8.7085**	**23.9446**
Oct. 07	AVE.	8.701	42.7647	95.1213	76.9185	10.356	114.2024	191.8079	299.6749
	S.D	0.054	0.4241	1.2782	0.7661	0.074	10.8187	14.8097	26.1635
	%R.S.D	**0.624**	**0.9917**	**1.3438**	**0.9959**	**0.713**	**9.4733**	**7.7211**	**8.7306**
Nov. 07	AVE.	9.027	42.8849	96.5318	77.4117	10.634	152.8910	234.0329	392.4815
	S.D	0.088	2.3603	5.4165	4.9460	0.081	16.8508	21.7563	43.0347
	%R.S.D	**0.969**	**5.5038**	**5.6111**	**6.3893**	**0.758**	**11.0214**	**9.2963**	**10.9648**
Dec. 07	AVE.	8.889	49.3613	104.0340	89.6468	10.486	157.7265	240.9375	459.7362
	S.D	0.286	21.1751	26.8878	1.0075	0.439	29.2960	44.6152	85.4445
	%R.S.D	**3.217**	**42.8983**	**25.8452**	**1.1238**	**4.190**	**18.5739**	**18.5173**	**18.5855**

DATE		Lithium				Sodium				Potassium			
		Ret.Time	**Area**	**Height**	**Amount**	**Ret.Time**	**Area**	**Height**	**Amount**	**Ret.Time**	**Area**	**Height**	**Amount**
		min	**µS*min**	**µS**	**mgL^{-1}**	**min**	**µS*min**	**µS**	**ppm**	**min**	**µS*min**	**µS**	**mgL^{-1}**
Jan. 08	**AVE.**	3.547	0.1022	0.6785	0.0930	4.429	3.1352	20.6154	42.2826	5.843	1.1908	5.4174	6.2627
	S.D	0.002	0.0006	0.0039	0.0006	0.002	0.0849	0.5635	1.1292	0.005	0.0886	0.4048	0.4585
	%R.S.D	**0.055**	**0.6123**	**0.5678**	**0.5986**	**0.041**	**2.7074**	**2.7336**	**2.6707**	**0.080**	**7.4386**	**7.4717**	**7.3216**
Febr. 08	**AVE.**	3.678	0.1044	0.7500	0.1013	4.426	3.3154	22.0865	43.9875	6.296	1.0988	5.6405	5.8099
	S.D	0.008	0.0004	0.0012	0.0004	0.013	0.1015	0.6504	1.3503	0.028	0.0695	0.3624	0.3562
	%R.S.D	**0.208**	**0.3699**	**0.1609**	**0.3651**	**0.284**	**3.0622**	**2.9447**	**3.0697**	**0.446**	**6.3234**	**6.4255**	**6.1312**
March 08	**AVE.**	3.671	0.1038	0.7461	0.0991	4.410	3.2414	21.5478	43.3850	6.259	1.1585	5.9688	6.1286
	S.D	0.005	0.0018	0.0118	0.0035	0.006	0.0576	0.3973	1.0860	0.006	0.1592	0.8141	0.8088
	%R.S.D	**0.128**	**1.7097**	**1.5817**	**3.5415**	**0.138**	**1.7761**	**1.8439**	**2.5032**	**0.103**	**13.7387**	**13.6401**	**13.1972**
April 08	**AVE.**	3.677	0.1026	0.7373	0.0950	4.392	3.1474	21.0809	42.8602	6.269	1.0691	5.5488	5.6956
	S.D	0.002	0.0008	0.0054	0.0007	0.011	0.0388	0.2752	0.5293	0.002	0.0368	0.1924	0.1952
	%R.S.D	**0.055**	**0.7915**	**0.7367**	**0.7457**	**0.255**	**1.2341**	**1.3053**	**1.2351**	**0.037**	**3.4467**	**3.4676**	**3.4275**
May 08	**AVE.**	3.661	0.1053	0.7719	0.0974	4.386	3.2663	22.0585	44.4805	6.214	1.0652	5.5826	5.6753
	S.D	0.008	0.0032	0.0247	0.0029	0.016	0.0221	0.0861	0.3005	0.012	0.0370	0.1623	0.1964
	%R.S.D	**0.205**	**3.0567**	**3.2002**	**2.9986**	**0.355**	**0.6757**	**0.3903**	**0.6757**	**0.186**	**3.4774**	**2.9074**	**3.4602**
June 08	**AVE.**	3.669	0.1025	0.7544	0.0949	4.403	3.2383	21.7076	44.0992	6.120	1.0566	5.6578	5.6296
	S.D	0.004	0.0006	0.0058	0.0005	0.024	0.1394	1.1929	1.8994	0.043	0.0162	0.1109	0.0859
	%R.S.D	**0.106**	**0.5702**	**0.7636**	**0.5541**	**0.534**	**4.3051**	**5.4953**	**4.3071**	**0.696**	**1.5337**	**1.9606**	**1.5263**

DATE		Magnesium				Calcium			
		Ret.Time	**Area**	**Height**	**Amount**	**Ret.Time**	**Area**	**Height**	**Amount**
		min	**µS*min**	**µS**	**mgL^{-1}**	**min**	**µS*min**	**µS**	**mgL^{-1}**
Jan. 08	**AVE.**	8.807	43.2316	96.6688	84.4495	10.369	155.9019	244.2178	453.5812
	S.D	0.004	0.7542	1.9916	1.6694	0.011	4.1581	5.2153	12.5792
	%R.S.D	**0.049**	**1.7445**	**2.0602**	**1.9768**	**0.103**	**2.6671**	**2.1355**	**2.7733**
Febr. 08	**AVE.**	9.662	47.8893	101.4546	91.7110	11.514	142.6440	196.3501	406.7770
	S.D	0.083	0.6062	0.8303	1.2629	0.139	20.3362	22.3379	58.2082
	%R.S.D	**0.862**	**1.2659**	**0.8184**	**1.3771**	**1.207**	**14.2566**	**11.3766**	**14.3096**
March 08	**AVE.**	9.565	46.7702	100.0699	89.3224	11.336	155.7667	213.5391	441.1367
	S.D	0.037	0.7578	1.5963	1.4948	0.041	7.4714	8.0628	20.6249
	%R.S.D	**0.386**	**1.6203**	**1.5952**	**1.6735**	**0.363**	**4.7965**	**3.7758**	**4.6754**
April 08	**AVE.**	9.611	46.0964	97.8977	87.8817	11.395	153.4523	209.3539	428.8255
	S.D	0.004	0.3469	0.9318	0.6992	0.038	10.8711	11.9210	29.5663
	%R.S.D	**0.039**	**0.7525**	**0.9518**	**0.7956**	**0.337**	**7.0843**	**5.6942**	**6.8947**
May 08	**AVE.**	9.547	47.6777	101.5798	91.0747	11.306	150.7219	208.4081	421.4632
	S.D	0.012	0.2306	2.0601	0.4666	0.031	8.0879	8.8443	21.9415
	%R.S.D	**0.121**	**0.4837**	**2.0280**	**0.5124**	**0.275**	**5.3661**	**4.2438**	**5.2060**
June 08	**AVE.**	9.551	46.0821	97.1004	87.8538	11.263	152.2327	213.6288	425.5441
	S.D	0.009	0.6993	2.1508	1.4098	0.039	8.5738	10.7418	23.2722
	%R.S.D	**0.091**	**1.5174**	**2.2150**	**1.6048**	**0.354**	**5.6320**	**5.0283**	**5.4688**

Table 3.25 Gathered measurements results of 12 months of averages, SD and RSD values of Lithium, Sodium, Potassium, Magnesium and Calcium.

	Lithium				Sodium				Potassium			
	Ret.Time	**Area**	**Height**	**Amount**	**Ret.Time**	**Area**	**Height**	**Amount**	**Ret.Time**	**Area**	**Height**	**Amount**
DATE	**min**	**µS*min**	**µS**	**mgL^{-1}**	**min**	**µS*min**	**µS**	**ppm**	**min**	**µS*min**	**µS**	**mgL^{-1}**
July 07	3.342	0.1193	0.7232	0.1117	4.038	3.1174	19.7212	39.9833	5.577	1.0313	5.2655	5.1926
Augu. 07	3.252	0.1240	0.7129	0.1163	3.929	3.1334	19.6077	39.5155	5.436	1.0237	5.1392	5.0681
Sept. 07	3.292	0.1220	0.7177	0.1143	3.979	3.1200	19.5831	39.6332	5.497	1.0271	5.1960	5.1230
Oct. 07	3.292	0.1220	0.7177	0.1143	3.979	3.1200	19.5831	39.6332	5.497	1.0271	5.1960	5.1230
Nov. 07	3.256	0.1238	0.7134	0.1161	3.934	3.1321	19.6054	39.5267	5.441	1.0240	5.1446	5.0733
Dec. 07	3.256	0.1238	0.7134	0.1161	3.934	3.1321	19.6054	39.5267	5.441	1.0240	5.1446	5.0733
Jan. 08	2.988	0.1372	0.6849	0.1295	3.624	3.0633	18.3636	36.5795	5.021	1.0029	4.7928	4.7149
Febr.08	3.198	0.1267	0.7073	0.1190	3.868	3.1119	19.2894	38.8165	5.350	1.0195	5.0695	4.9961
Marc. 08	3.234	0.1249	0.7113	0.1172	3.911	3.1163	19.4199	39.1518	5.408	1.0224	5.1185	5.0455
Apr. 08	2.741	0.1497	0.6605	0.1420	3.346	2.9774	16.9312	33.5560	4.627	0.9840	4.4830	4.3876
May 08	3.058	0.1338	0.6930	0.1261	3.708	3.0685	18.5468	37.1748	5.128	1.0087	4.8904	4.8098
June 08	2.966	0.1384	0.6828	0.1307	3.599	3.0456	18.1594	36.1695	4.985	1.0005	4.7622	4.6815
AVE.	3.156	0.1288	0.7032	0.1211	3.821	3.0948	19.0347	38.2722	5.284	1.0163	5.0169	4.9407
S.D	0.179	0.0091	0.0188	0.0090	0.207	0.0474	0.8605	1.9801	0.283	0.0142	0.2341	0.2406
R.S.D%	**5.693**	**7.0316**	**2.6731**	**7.4595**	**5.412**	**1.5308**	**4.5206**	**5.1738**	**5.360**	**1.3939**	**4.6660**	**4.8688**

DATE	Magnesium				Calcium			
	Ret.Time	Area	Height	Amount	Ret.Time	Area	Height	Amount
	min	µS*min	µS	mgL^{-1}	min	µS*min	µS	mgL^{-1}
July 07	8.689	41.7037	87.5822	79.4195	10.241	142.2059	199.2149	396.7593
Augu. 07	8.453	40.4294	84.7047	76.9599	9.965	139.0918	194.3855	387.8699
Sept. 07	8.557	40.9823	85.9435	78.0265	10.085	140.7346	196.8550	392.5208
Oct. 07	8.557	40.9823	85.9435	78.0265	10.085	140.7346	196.8550	392.5208
Nov. 07	8.467	40.4820	84.8227	77.0615	9.976	139.2482	194.6207	388.3129
Dec. 07	8.463	40.4820	84.8227	77.0615	9.976	139.2482	194.6207	388.3129
Jan. 08	7.759	37.0951	77.6447	70.5536	9.157	129.0542	179.7805	359.3587
Febr.08	8.310	39.7604	83.3084	75.6758	9.799	137.0713	191.4692	382.1263
Marc. 08	8.406	40.2396	84.3466	76.5981	9.910	138.4236	193.4752	385.9727
Apr. 08	7.109	34.2046	71.7154	65.0209	8.404	117.6876	164.2230	327.3366
May 08	7.942	38.0682	79.7901	72.4316	9.371	131.0608	183.0558	365.1452
June 08	7.699	36.8523	77.1672	70.0908	9.089	127.8054	178.1550	355.8642
AVE.	8.201	39.2735	82.3160	74.7438	9.672	135.1972	188.8925	376.8417
S.D	0.472	2.2346	4.7147	4.2902	0.549	7.3139	10.4349	20.7096
R.S.D%	**5.757**	**5.6898**	**5.7276**	**5.7399**	**5.673**	**5.4098**	**5.5243**	**5.4956**

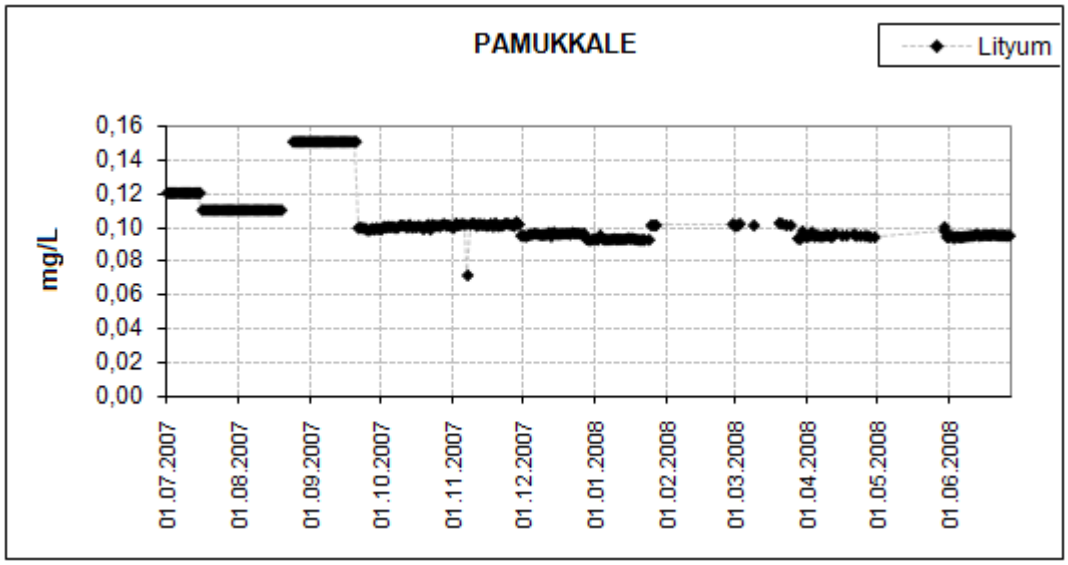

Figure 3.3 Variation of lithium concentration of geothermal water samples of Pamukkale Antique Pool from July 2007 to June 2008.

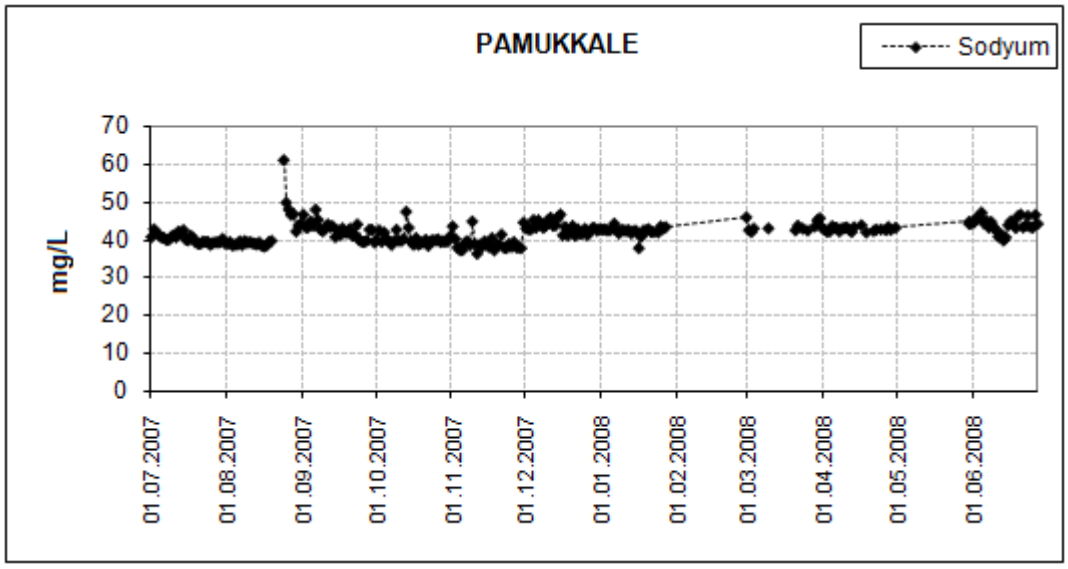

Figure 3.4 Variation of sodium concentration of geothermal water samples of Pamukkale Antique Pool from July 2007 to June 2008.

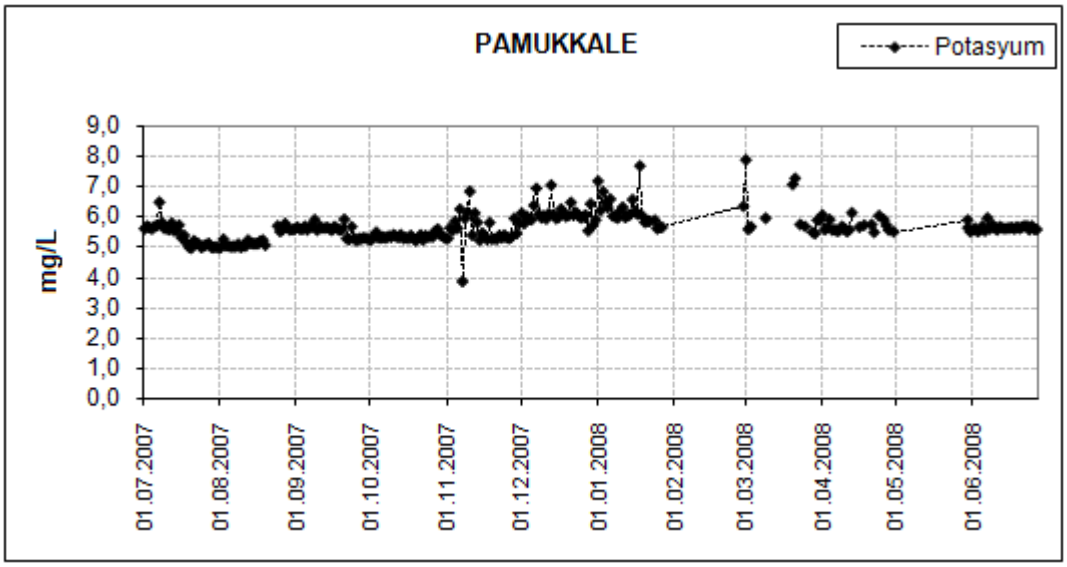

Figure 3.5 Variation of potassium concentration of geothermal water samples of Pamukkale Antique Pool from July 2007 to June 2008.

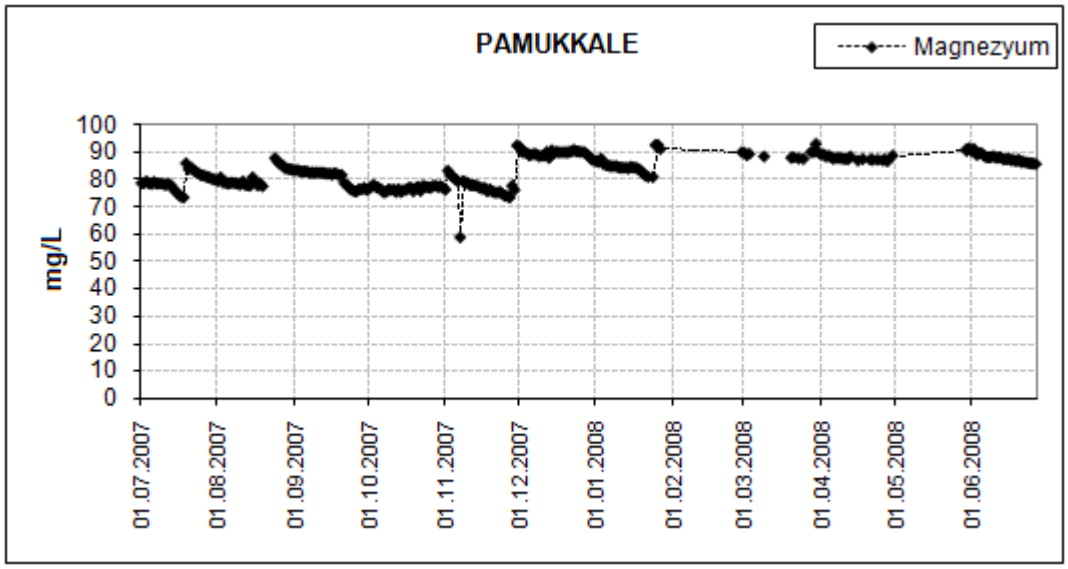

Figure 3.6 Variation of magnesium concentration of geothermal water samples of Pamukkale Antique Pool from July 2007 to June 2008.

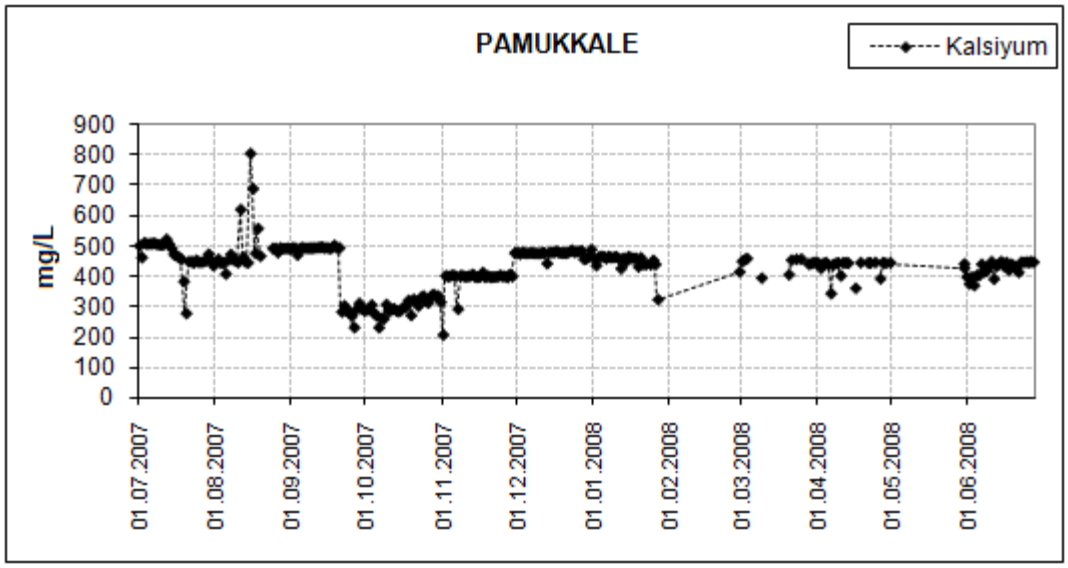

Figure 3.7 Variation of calcium concentration of geothermal water samples of Pamukkale Antique Pool from July 2007 to June 2008.

Figure 3.3, 3.4, 3.5, 3.6 and 3.7 reveal gathered daily cation concentration measurement results during 12 months. The fluctuations observed in the above mentioned figures can be attributed to the seasonal changes of the ion concentrations. It also should be noted that the statistically deviated values were kept among the recorded values.

3.8 Conclusion

In this part of the thesis, simultaneous ion chromatographic analysis of six cations (lithium, sodium, amonnium, potassium, magnezium and calcium) in geothermal water samples were performed by ion chromatography method. Some validation tests and the optimum conditions for the determination of cations were studied. Analysis of cations was performed by injection of samples to the chromatographic system after filtration and/or dilution. The precision and accuracy of the method were tested at three different concentration levels for each standard. Recovery studies were performed by adding standards in to the geothermal water and drinking water samples. For geothermal water samples recovery tests was performed between two successive months. Precision was also assessed as the percentage relative standard deviation (%RSD) of both repeatability (within-day) and reproducibility (between-day and different concentrations) for geothermal water samples. SD and RSD values of 320 real geothermal water samples acquired during 12 months were evaluated.

CHAPTER FOUR

OPTICAL SENSORS FOR THE DETERMINATION OF HEAVY METAL IONS

A few decades ago, there was a general feeling that nature could effectively handle hazardous substances. Although, nowadays human beings are more concerned of their sensitive natural environment, pollution is still a problem. Experts estimate that industrial processes introduce up to a million different pollutants into the atmosphere and the aquatic ecosystem (Förstner & Wittmann, 1981). Heavy metals are one group of these substances, although not all of them are considered harmful to humans **(**Mayr, 2002).

4.1 Conventional Methods for the Determination of Heavy Metals

The determination of heavy metals is a challenging subject for analytical chemists regarding concentration ranges set by standards and guidelines for reasons of toxicity. In addition, similar chemistry of these metals is fastidious with respect to selectivity of the determination method.

A variety of analytical methods fulfilling these demands are available. However, only some of them have found application in routine analysis. Recommended procedures for the detection of heavy metals in water samples include photometric methods, flame or graphite furnance atomic absorption spectroscopy (AAS), inductively coupled plasma emission or mass spectrometry (ICP-ES, ICP-MS), total reflection X-Ray fluorimetry (TXRF) and anodic stripping voltammetry (ASV), (Förstner & Wittmann, 1981; Merian, 1991; Fresenius& Quentin, & Schneider, 1988; Klockenkämpfer, 1997). While AAS and photometry are single element methods, ICP-ES, ICP-MS and TXRF are used for multi-element analysis, and voltammetry is an oligo-element approach (Mayr, 2002).

These methods offer good limits of detection and wide linear ranges, but require high cost analytical instruments developed for the use in the laboratories. The necessary collection transportation and pretreatment of a sample is time consuming and a potential source of error (Spichiger-Keller, 1998). However, in the last years smaller and portable and less expensive devices have been brought to the market. On the other hand, the last years have seen a growing development of chemical sensors for a variety of applications. The toxicity of heavy metals makes a continuos supervision of drinking or ground water and lentic or lotic water courses necessary. Chemical sensors enable on-line and field monitoring and therefore can be an useful alternative tool (Wolfbeis, 1991; Mayr, 2002).

4.2 Optical Ion Sensors

A chemical sensor can be defined as **"a portable miniaturized analytical device, which can deliver real-time and on-line information in presence of specific compounds or ions in complex samples"** (Camman, Guibault, Hall, Kellner, Schmidt & Wolfbeis, 1996). Chemical sensors can be categorized into electrochemical, optical, mass-sensitive and heat-sensitive, according to the types of transducer (Cattrall, 1997).

An optical sensor device which detects and converts the change of optical properties, after amplification of the primary signal, into a unit readout. The optical properties measured can be absorbance, reflectance, luminescence, light polarization, Raman and other.

Ideally, a sensor provides adequate sensitivity or dynamic range, high selectivity towards the species of interest, a proportional (or other mathematical relationship) signal output to the amount of analyte, fast response time, good signal-to-noise ratio, no hysteresis and excellent long-term stability (Diamond, 1998).

4.3 Optical sensors for the Determination of Heavy Metal Ions

A large number of optical sensors or test strips for heavy metals were developed in the past years and extensively reviewed (Oehme & Wolfbeis, 1997).

The most significant methods are the application of quenchable fluorophores or indicator dyes, which undergo a binding reaction, biosensor assays or the combination of an ionophore with a pH-indicator. More recent publications deal with metal indicators dissolved in plasticized poly (vinyl chloride) (PVC) (Sanchez-Pedreno, Ortuno, Albero, Garcia & Valero, 2000; Chan, Yang & Wang, 2001) or immobilized to ion exchange resins (Malcik, Oktar, Ozser, Caglar, Bushby, Vaughan, Kuswandi & Narayanaswamy, 1998; Vaughan & Narayanaswamy, 1998; Mahendra, Gangaiya, Sotheeswaran & Narayanaswamy, 2002) and with ion exchange membranes (Anticó, Lerchi, Rusterholz, Ackermann, Badertscher, Valiente & Pretsch, 1999).

CHAPTER FIVE

PHOTOCHARACTERIZATION OF NEWLY SYNTHESIZED DYES (A8 and A13) AND THEIR UTILITIES AS OPTICAL SENSORS

5.1 Introduction

The goal of this work was desing of optical sensing schems for the determination of heavy metal ions in aqueous samples.

Heavy metal ions can be either essential or toxic to human beings and their determination is therefore of tremendous interest. Conventional methods require high cost analytical instruments which are insufficient for online or field monitoring. This work presents the applications of several sensing strategies for the determination of heavy metal ions based on optical sensing.

In this study, newly synthesized dyes has been characterized in different solvents of absolute ethanol (EtOH), tetrahydrofuran (THF), dichloromethane (DCM), Toluene/Ethanol (To: EtOH) mixture (80:20) and in PVC and the successful use of a dyes [5-phenylazo-8-quinolinol] (A-8) and [5-(4-clorophenylazo)-8-quinolinol] (A–13) in construction of selective poly vinyl chloride (PVC)-based optical metal sensing have been reported. Typical sensor characteristics such as dynamic working range, sensitivity and selectivity have been investigated.

The interferences of various cations on the response of Mn^{2+}, Zn^{2+} and Cu^{2+} also have been studied. The dyes A8 and A13 has been used for the first time as sensing agent in the optical sensor membrane design.

5.2 Experimental Method and Instrumentation

5.2.1 Instrumentation

Absorption spectra were recorded using a Shimadzu 1800 UV-Visible spectrophotometer.

Steady state fluorescence emission and excitation spectra were measured using Varian Cary Eclipse Spectrofluorometer with a xenon flash lamp as the light source.

pH measurements were recorded with a orion pH meter.

5.2.2 Chemicals and Solution

5.2.2.1 Chemicals

All solvents used in this thesis were of analytical grade and purchased from Merck, Johnson and Mathey, Acros, Fluka and Riedel. Solvents for the spectroscopic studies were used without further purification. Tetrabutylammonium hydroxide for titration (in nonaqueous medium) was standard 0.1 M solution in isopropanol/methanol (0.1 N) from Fluka. The solution was concentrated to 1 M with vacuum evaporator before use for the titrations in ethanol (EtOH).

The polymer polyvinyl chloride (PVC) was high molecular weight and obtained from Fluka. The plasticiser, dioctyl phtalate (DOP) was 99 % from Aldrich. The additive potassium tetrakis (4-chlorophenyl) borate was selectophore, 98 % from Fluka.

The heavy metal sensitive dyes; A8 and A13 were synthesized in our laboratories' according to literature method (Sağlam, 2006). Chemical structures of the employed indicator dyes were shown in Figure 5.1.

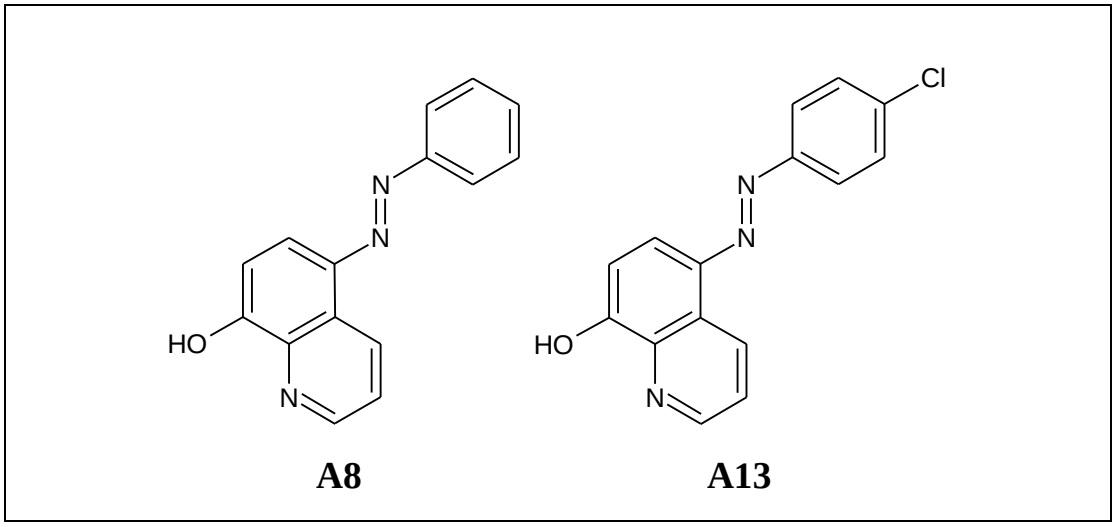

A8 **A13**

Figure 5.1 Chemical structures of the employed indicator dyes.

The standard metal solutions were prepared from their 0.1 M stock solutions by using the metal salts of $CuCl_2$, $Co(NO_3)_2$, $NiCl_2.6H_2O$, $Pb(NO_3)_2$, $Hg_2(NO_3)_2$, $Hg(NO_3)_2$, $CrCl_3$, $CdCl_2$, $Fe(NO_3)_3$, $Zn(NO_3)_2$, $CaCl_2$, $SnCl_2$, $MnCl_2$, $MgSO_4$ and ammonium-iron(II) sulphate, $Al(SO_4)_3$. N-N-Bis-(2-hydroxyethyl)-2-aminoethansulfonic acid (BES buffer) was purchased from Merck.

Calibration standards of Mn, Cu and Zn were prepared freshly from 1.10^{-1} mol L^{-1} stock solutions prior to measurements and diluted with BES buffer (1.0×10^{-2} M) up to pH 7.0.

5.2.2.2 Buffer Solutions

The pH of the solutions were monitored by use of a digital pH-meter (ORION) calibrated with standard buffers of pH 12.00, 7.00 and 4.00 at 25±1 °C.

In all of the studies ultra pure water of Millipore was used. Deionised water, generated by a Milli-Q deionised water unit, which had a resistance better than 18.2 MΩcm, was used for the preparation of all the solutions.

Preparation of 0.01 M acetic acid/acetate buffer; 0.572 mL of acetic acid (d=1.05 and 17.48 Molar) were dissolved in 950 mL ultra pure water. The solution was titrated to pH 5 at the lab. temperature of 20 °C either with 0.1 M HNO_3 or 0.1 M NaOH as needed. The resulting solution was made up to 1000 ml with ultra pure water in a volumetric flask. The buffer solutions in the range of pH 4.0-6.0 were prepared by the same way by adjusting to the desired pH.

Preparation of 0.005 M acetic acid / acetate buffer; 0.286 mL of acetic acid (d=1.05 and 17.48 Molar) were dissolved in 950 mL ultra pure water. The solution was titrated to pH 5.0 at the lab temperature of 20°C either with 0.1 M HNO_3 or 0.1 M NaOH as needed. The resulting solution was made up to 1000 ml with ultra pure water in a volumetric flask. The buffer solutions in the range of pH 4.0-6.0 were prepared by the same way by adjusting to the desired pH.

Preparation of 0.005 M H_3PO_4 buffer; 0.285 mL (d=1.71 and 14.83 Molar) of phosphoric acid were dissolved in 950 mL ultra pure water. The solution was titrated to pH 5.0 at the lab temperature of 20°C either with 0.1 M HNO_3 or 0.1 M NaOH as needed. The resulting solution was made up to 1000 ml with ultra pure water in a volumetric flask. The buffer solutions in the range of pH 2.0-3.0 were prepared by the same way by adjusting to the desired pH.

Preparation of 0.005 M NaH_2PO_4 / Na_2HPO_4 buffer; 0.78 g of $NaH_2PO_4.2H_20$ (MA=156.01) and 1.79 g of $Na_2HPO_4.12H_20$ (MA=358.14) were dissolved in 950 mL ultra pure water. The solution was titrated to pH 7.0 at the lab temperature of 20 °C either with 0.1 M HNO_3 or 0.1 M NaOH as needed. The resulting solution was made up to 1000 ml with ultra pure water in a volumetric flask. The buffer solutions in the range of pH 7.0-9.0 and 10-12 were prepared by the same way by adjusting to the desired pH.

Preparation of 0.01 M BES buffer; 2.1325 g of BES sodium salt (N,N-Bis(2-hydroxyethyl)-2-aminoethanesulfonic acid sodium salt, MW = 213.25, pKa of free acid = 7.1) was dissolved in approx. 950ml of ultra pure water. The solution was

titrated to pH 7.0 at the lab temperature of 20 ^{o}C either with 0.1 M HNO_3 or 0.1 M NaOH as needed. The resulting solution was made up to 1000 ml with ultra pure water in a volumetric flask.

5.2.3 Membrane Preparation

5.2.3.1 Preparation of the Sensor Membrane Films

The optode PVC membranes were prepared to contain 120 mg of PVC, 240 mg of plasticizer, 1.0 mg of dye (25 mmol dye/kg polymer), equivalent amount of potassium tetrakis (4-chlorophenyl) borate and 1.5 ml of THF. The prepared cocktails contained 33% PVC and 66% plasticizer by weight which is quite common (Seiler & Simon, 1992; Bakker & Simon, 1992; Lerchi, Bakker, Rusterholz, & Simon, 1992; Morf, Seiler, Rusterholz & Simon, 1990). The chemical structures of PVC, DOP and PTCPB were shown in Figure 4.3.

The mixture was dissolved in the solvent of tetrahydrofuran (THF) and mixed by several hours by the help of a magnetic stirrer.

The resulting cocktail was spread on a 125 μm polyester support (Mylar from Du Pont) and dried in a desicator which was saturated with the solvent vapour. The polyester support was optically fully transparent, ion impermeable and exhibited good adhesion to PVC. The most important function of the polyester was to act as a mechanical support because the thin silicon films were impossible to handle. Once dried, the film was insoluble in water and could be cut into pieces of appropriate size. The approximate thickness of the film was 5 μm. The films were kept in a desiccator in the dark. This way, the photostability of the membrane was ensured and the damage from the ambient air of the laboratory was avoided. For absorbance and steady state fluorescence measurements each sensing film was cut to 1.2 cm width and 2.5 cm length and fixed diagonally into the sample cuvette (See Figure 4.2) and the absorption or emission spectra were recorded.

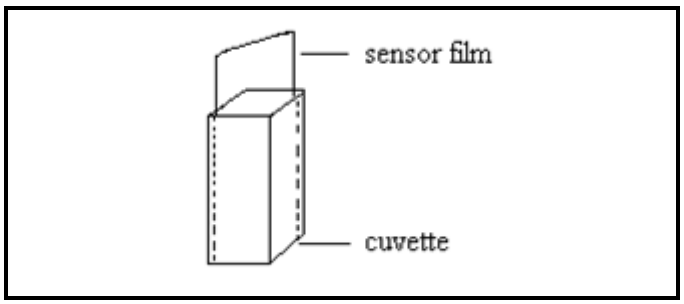

Figure 5.2 The placement of the sensor film in the sample cuvette

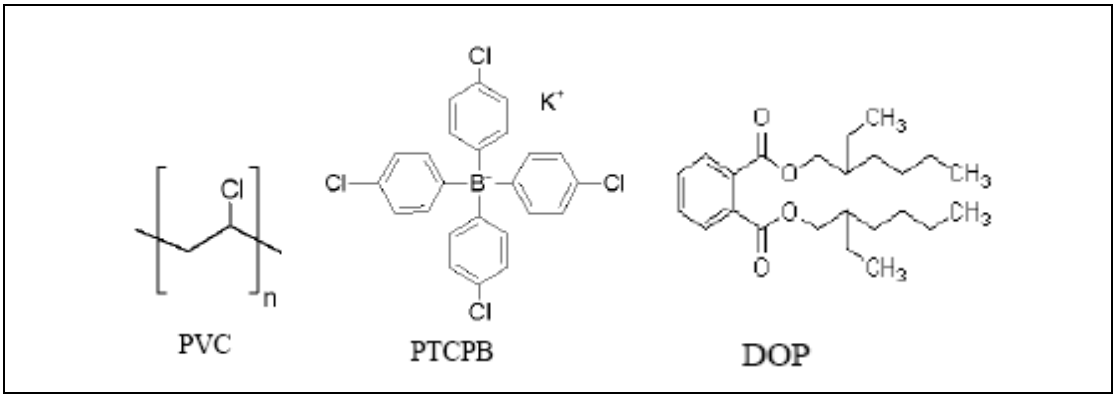

Figure 5.3 Structures of PVC, PTCPB and DOP

5.3 Spectral Characterization of the Employed Indicator Dyes

For spectral characterization, two different indicator dyes A8 and A13 were studied in the different solvents of ethanol (EtOH), dichloromethane (DCM), tetrahydrofurane (THF) and Toluene/Ethanol (To: EtOH) mixture (80:20)) and in solid matrix of PVC. Maximum absorption wavelength (λ_{abs}) and molar extinction coefficients (ε) of the indicators were determined with UV-Vis spectrophotometer in all of the employed matrices.

The dyes exhibited excellent photostability in the employed PVC matrix. The absorption, emission and excitation spectra of the A8 and A13 dyes were recorded in PVC matrix.

5.3.1 Spectral Characterization Studies in Solution Phase

In order to perform the spectral characterization of the A8 and A13 in the solition phase, absorption spectra were recorded in the solvents of DCM, EtOH, THF and Toluene/Ethanol (To: EtOH) mixture (80: 20)).

In the employed solvents (DCM, EtOH, THF and toluene) the A8 and A13 was excited at 380, 384, 385, 385 nm and 391, 393, 394, 394 nm, respectively and the spectra were recorded. Table 5.1 reveals UV/Vis spectra related data of A8 and A13 in the solvents of EtOH, DCM, THF, Toluene/Ethanol mixture (80:20) and in solid matrix of PVC.

Table 5.1 UV/Vis spectra related data of A8 and A13 in the solvents of EtOH, DCM, THF, Toluene/Ethanol mixture (80:20) and in solid matrix of PVC. (A-8, $1x10^{-5}$ M; and A-13, $1x10^{-5}$ M)

Compound	Solvent/Matrix	n (refractive index)	λ^1_{abs} (nm)	λ^2_{abs} (nm)	ε_{max} (λ^1_{abs})	ε_{max} (λ^2_{abs})
A8	EtOH	1.3590	384	--	66000	--
A8	DCM	1.4241	380	--	86800	--
A8	THF	1.4070	385	--	24900	--
A8	Tol: EtOH	1.4694	385	--	92600	--
A8	PVC	1.5200	370	500	79234	8253
A13	EtOH	1.3590	393	--	29700	--
A13	DCM	1.4241	391	--	91900	--
A13	THF	1.4070	394	--	34400	--
A13	Tol: EtOH	1.4694	394	--	31000	--
A13	PVC	1.5200	390	480	46104	6967

Figure 5.4 and 5.5 show UV-Vis spectra of the studied indicator dyes (A8 and A 13) in four different solvents (EtOH, DCM, THF and Toluene/Ethanol mixture (80:20)).

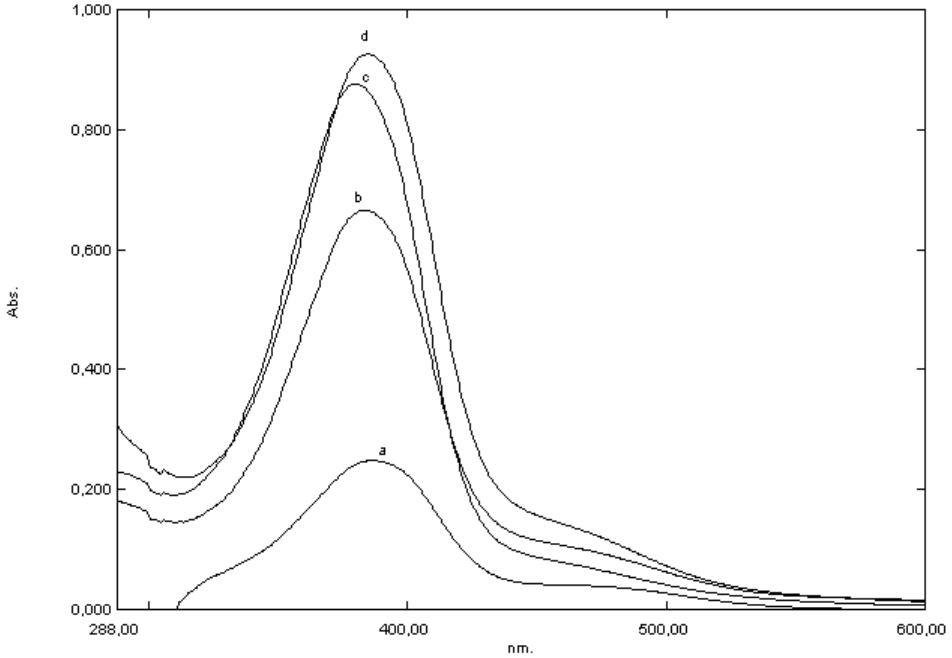

Figure 5.4 UV/Vis spectra of A8 (1.10^{-5} M) in the solvents of EtOH, DCM, THF and Toluene/Ethanol mixture (80:20) (a) THF (b) EtOH(c)DCM (d) To:EtOH

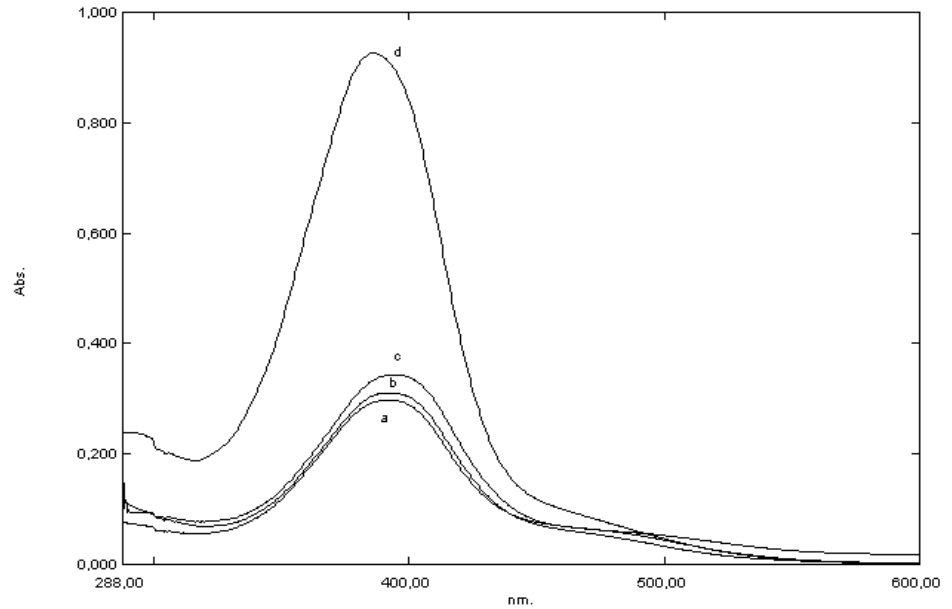

Figure 5.5 UV/Vis spectra of A13 (1.10^{-5} M) in the solvents of EtOH, DCM, THF and Toluene/Ethanol mixture (80:20) (a) EtOH (b) To: EtOH (c) THF (d) DCM

5.3.1.1 Acidity Constant Calculations (pKa) of A8 and A 13 in the Solvent of EtOH

The knowledge of acidity constant (p*K*a) of the employed indicator dye (A8 and A13) is of fundamental importance in order to provide information on chemical reactivity range of them. Therefore, to evaluate the availability of A8 and A13 for heavy metal sensing purposes, the acidity constants were determined. For this purpose, the pKa values of A8 and A13 were determined in EtOH and PVC.

pH induced absorption characteristics of A8 and A13 were monitored after addition of 1 M TBAOH solution in EtOH. A8 and A 13 exhibited a pH dependent response between pH 6.5–11.0 and pH 6.0–10.0 in the direction of a signal increase respectively. The signal intensities of A8 and A 13 were monitored at 457 nm and 460 nm from absorption spectrum, respectively. p*K*a values of A8 and A13 in EtOH were found to be 9.40 and 8.60 from the inflection points of the insert plots of Figure 5.6 and 5.7 respectively. The p*K*a values were also calculated as 9.66 and 8.68 by using non- linear fitting algorithm of Gauss–Newton–Marquardt equation (Oter, 2007);

$$\mathrm{p}K_{\mathrm{a}} = \mathrm{pH} + \log\left[\frac{(I_x - I_b)}{(I_a - I_x)}\right]$$

Where I_a and I_b are the absorption intensities of acidic and basic forms and I_x is the intensity at a pH near to the p*K*a.

The original pale yellow color of A8 and A13 dyes were turned to orange upon exposure to hyroxside ions.

Figure 5.6 and 5.7 reveal pH dependent UV-Vis spectra of A8 and A13 in EtOH respectively.

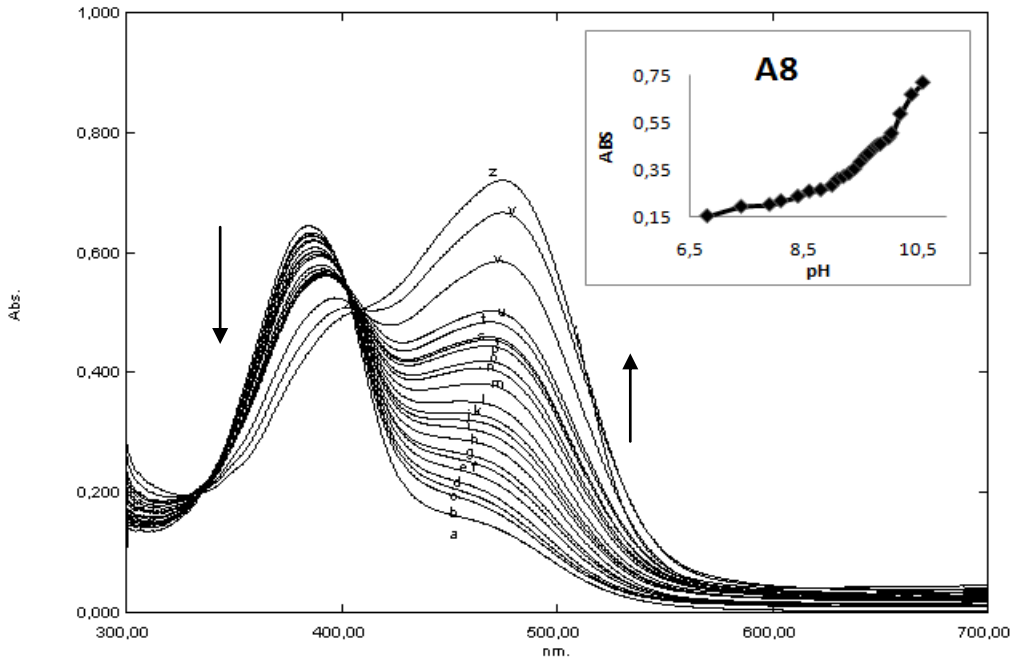

Figure 5.6 pH induced absorption characteristics and sigmoidal calibration curve of A8 (1.10^{-5} M). After titration with 1 mol L^{-1} tetrabutylammonium hydroxide in EtOH at 457 nm in the pH range of 6.80 and 10.60 (pH= (a)6.80 (b)7.40 (c)7.90 (d)8.10 (e)8.40 (f)8.60 (g) 8.80 (h) 9.00 (ı) 9.10 (j) 9.20 (k) 9.30 (l) 9.40 (m) 9.50 (n) 9.60 (o) 9.65 (p) 9.75 (r) 9.80 (s) 9.85 (t) 10.00 (u) 10.05 (v) 10.20 (y) 10.40 (z) 10.60

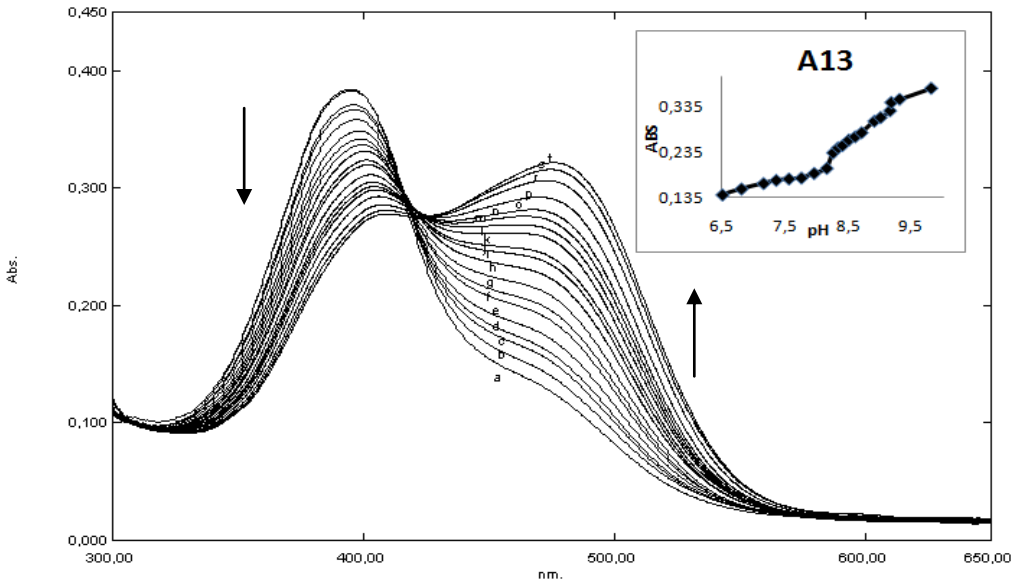

Figure 5.7 pH induced absorption characteristics and sigmoidal calibration curve of A13 (1.10^{-5} M). After titration with 1 mol L^{-1} tetrabutylammonium hydroxide in EtOH at 460 nm in the pH range of 6.50 and 9.60 (pH = (a)6.50 (b)6.80 (c)7.15 (d)7.35 (e)7.55 (f)7.75 (g) 7.95 (h) 8.15 (ı) 8.25 (j) 8.40 (k) 8.50 (l) 8.65 (m) 8.80 (n) 8.90 (o) 9.00 (p) 9.20 (r) 9.35 (s) 9.50 (t) 9.60

5.3.2 Spectral Characterization Studies in Solid Phase

For spectral characterization of the PVC doped A8 and A13 absorbsion, excitation and corrected emission spectra of the films were recorded.

5.3.2.1 Acidity Constant Calculations (pKa) of A8 and A13 in PVC Matrix

In order to calculate the pKa values of the PVC doped indicator dyes the thin films of A8 and A13 were exposed to buffered solutions at different pH values. The pH dependence of the dye doped membrane was investigated in buffered solutions in the pH range of 2.0-12.0. Buffer solutions were prepared with 0.005 M CH3COOH, 0.005 M NaH2PO4, 0.005 M Na_2HPO4 and 0.005 M H_3PO_4.

The sensor membranes reversibly responded in the acidic and alkaline region of the pH scale. The relative signal changes of absorption spectra of A8 and A13 were monitored after addition of certain concentrations of buffered solutions (between 2-12 pH). A8 and A13 exhibited the best response to pH between pH 2-12.

5.3.2.1.1 Absorption Based Spectra of the PVC Doped Indicator Dyes. Figure 5.8, 5.9, 5.10 and 5.11 reveal pH dependent absorption characteristics and sigmoidal calibration curves of PVC doped A8 and A13 in the pH range of 7.00-2.5; 7.50-12.00 and pH 7.00-2.5; 7.5–11.50 respectively.

p*K*a values of A8 and A13 were found to be 5.5, 11.5 and 6.00, 10.00 from the inflection points of the insert plots of Fig. 5.8, 5.9, 5.10 and 5.11 respectively. The p*K*a values were also calculated as, 5.68, 11.51 and 6.07, 10.53 by using non- linear fitting algorithm of Gauss–Newton–Marquardt method, respectively.

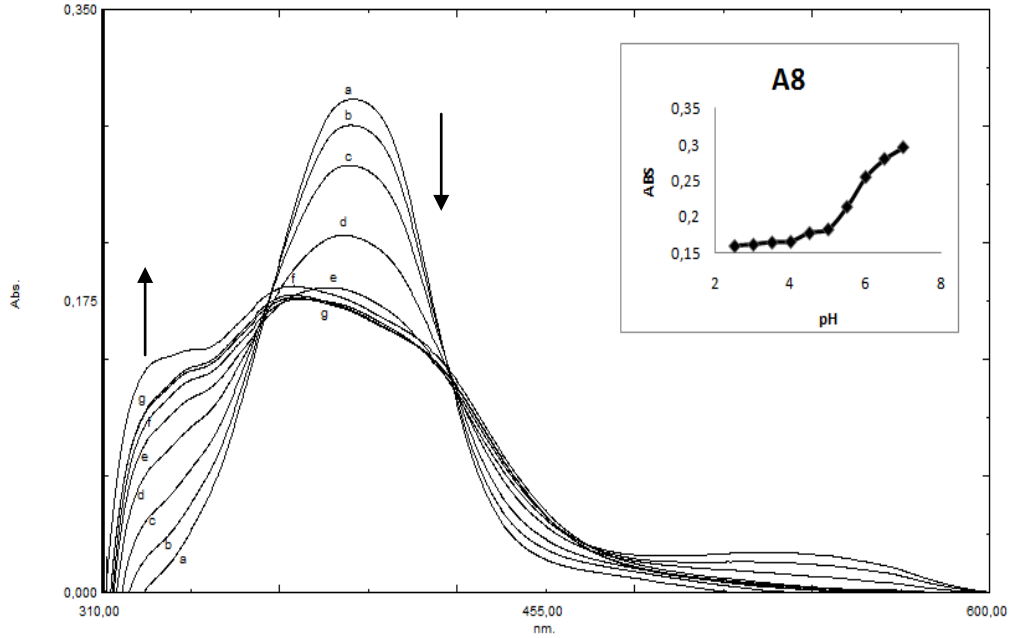

Figure 5.8 pH induced absorption spectra and sigmoidal calibration curve of PVC doped A8 in the pH range of 7.00-2.50. pH (a)7.00 (b)6.50 (c)6.00 (d)5.50 (e)5.00 (f)4.50 (g)4.00; 3.50; 3.00; 2.50

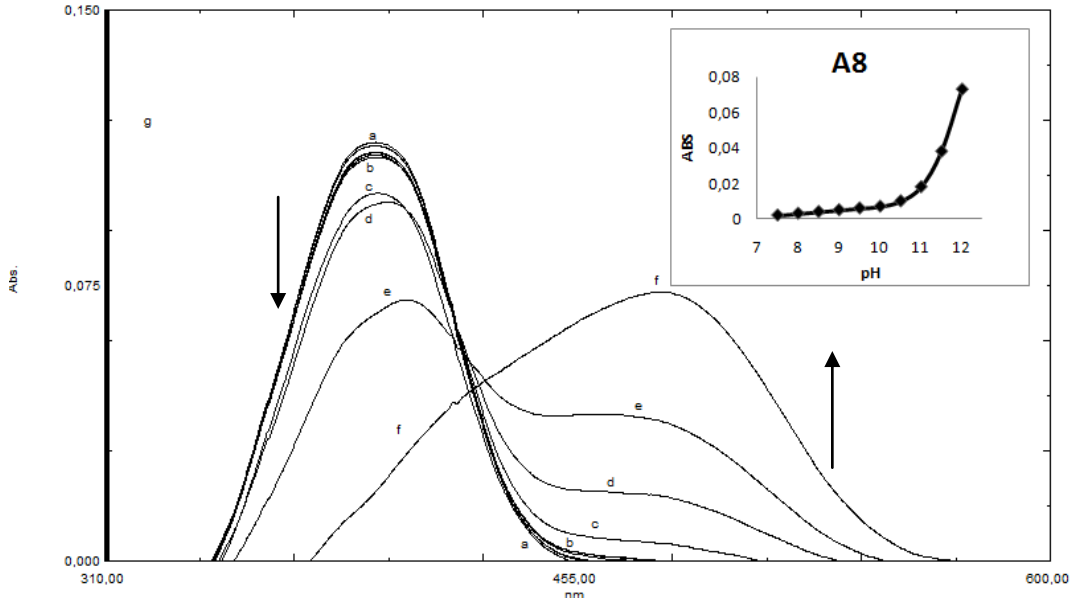

Figure 5.9 pH induced absorption spectra and sigmoidal calibration curve of PVC doped A8 in the pH range of 7.50-12.00. pH: (a)7.50; 8.00 (b)8.50; 9.00; 9.50; 10.00 (c) 10.50 (d)11.00 (e)11.50 (f)12.00

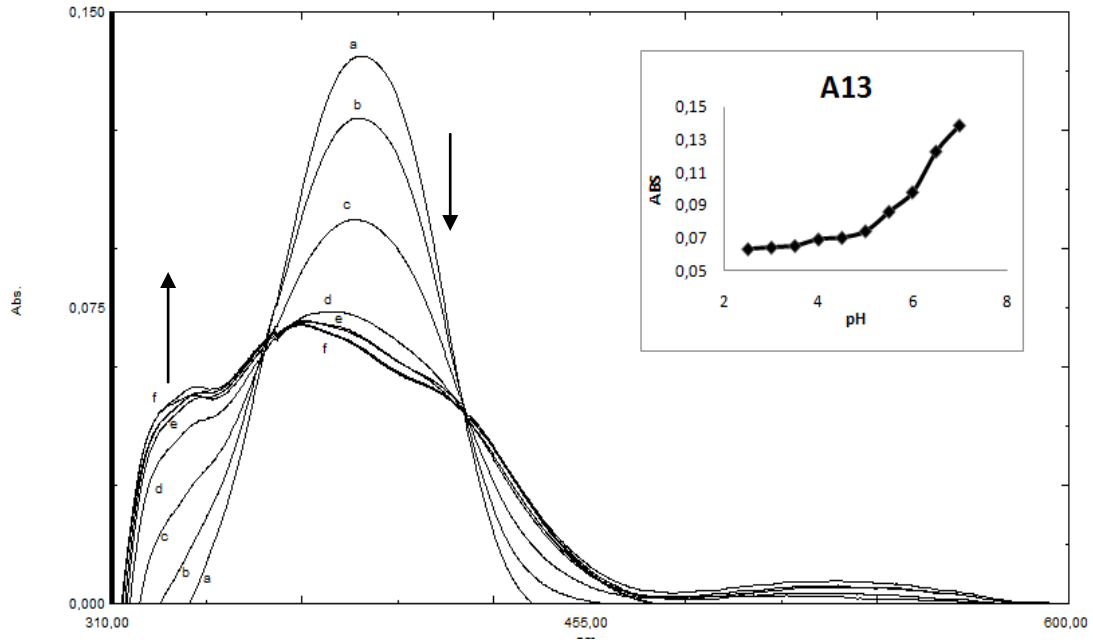

Figure 5.10 pH induced absorption spectra and sigmoidal calibration curve of PVC doped A13 in the pH range of 7.00-2.50. pH :(a)7.00 (b)6.50 (c)6.00 (d)5.50 (e)5.00; 4.50; 4.00 (f)3.50; 3.00; 2.50

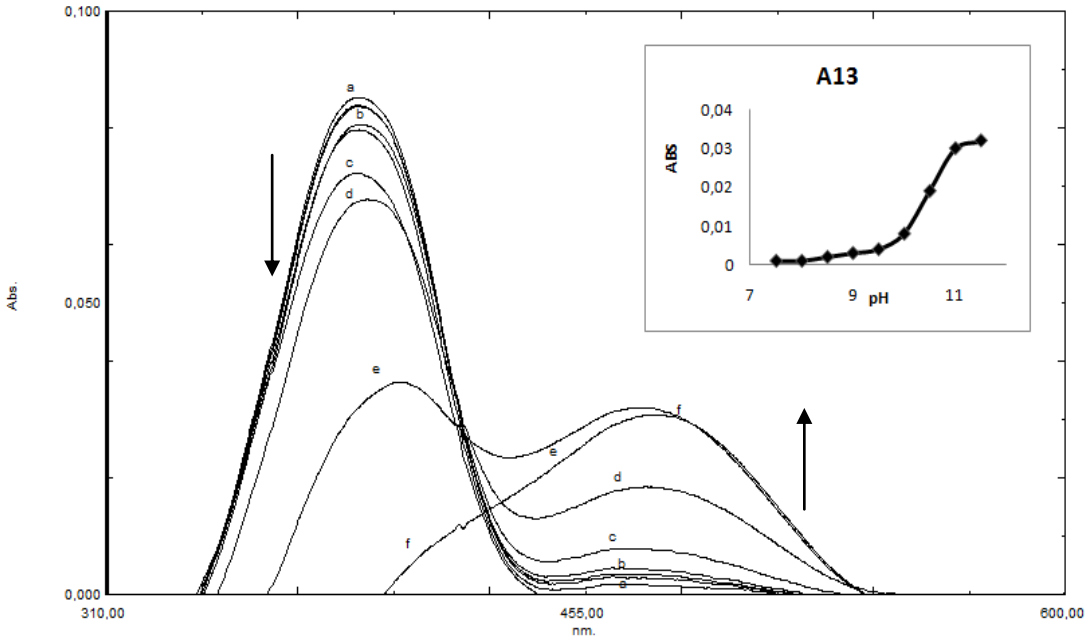

Figure 5.11 pH induced absorption spectra and sigmoidal calibration curve of PVC doped A13 in the pH range of 7.50-11.50. pH: (a)7.50; 8.00 (b)8.50; 9.00; 9.50 (c)10.00 (d)10.50 (e)11.00 (f)11.50.

5.3.2.1.2 Emission Based spectra of the PVC Doped Indicator Dyes. Emission and excitation spectra of A8 and A13 were recorded with Fluorescence spectrophotometer.

The emission based relative signal changes of A8 and A13 were shown in Figure 5.12, 5.13, 5.14 and 5.15 in the pH range of 7.0-2.5; 7.50-12.00 and pH 7.0-2.5; 7.5–11.50 respectively.

Emission based test results of A8 exhibited a decrease in signal intensity upon exposure to proton in the pH range of 7.00-2.5 (See Figure 5.12). In contrast upon de-protonation the same dye exhibited an increase in the fluorescence intensity (See Figure 5.13). The A13 dye exhibited similar emission based response to pH (See Figure 5.14 and 5.15).

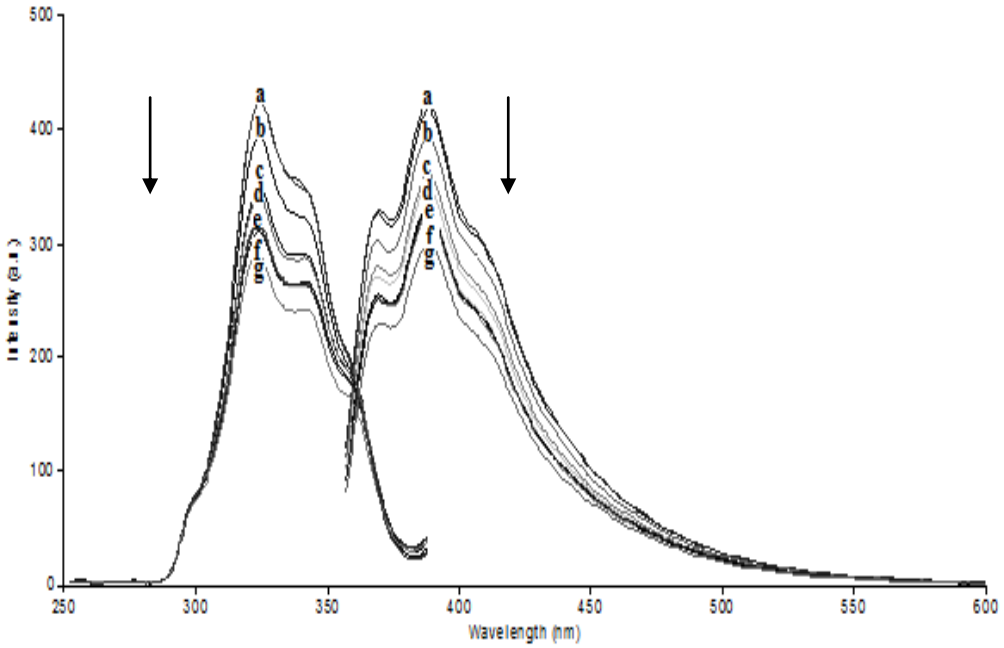

Figure 5.12 pH induced emission characteristics PVC doped Y A8 in the pH range of 7.00-2.50. Emission spectra: ex 345nm; em 355–600 nm; Excitation spectra: em 399nm; ex 250–389nm; pH (a)7.00 (b)6.50 (c)6.00 (d)5.50 (e)5.00 (f)4.50 (g)4.00; 3.50; 3.00; 2.50.

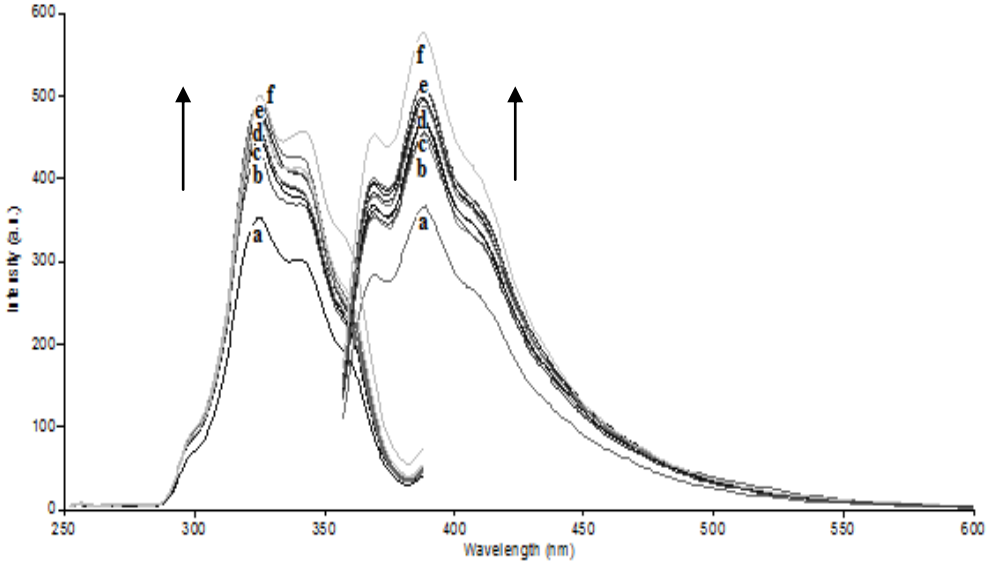

Figure 5.13 pH induced emission characteristics PVC doped A8 in the pH range of 7.50-12.00. Emission spectra: ex 345nm; em 355–600 nm; Excitation spectra: em 399nm; ex 250–389nm; pH: (a)7.50; 8.00 (b)8.50; 9.00; 9.50; 10.00 (c) 10.50 (d)11.00 (e)11.50 (f)12.00

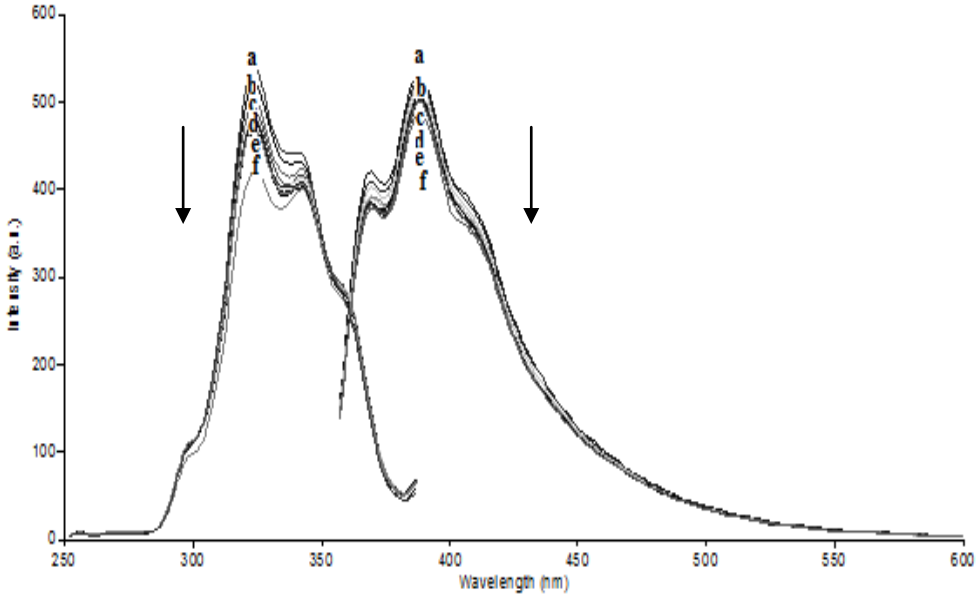

Figure 5.14 pH induced emission characteristics PVC doped Y A13 in the pH range in the pH range of 7.00-2.50. Emission spectra: ex 345nm; em355–600 nm; Excitation spectra: em 400nm; ex 250–390nm; pH (a)7.00 (b)6.50 (c)6.00 (d)5.50 (e)5.00; 4.50; 4.00 (f)3.50; 3.00; 2.50

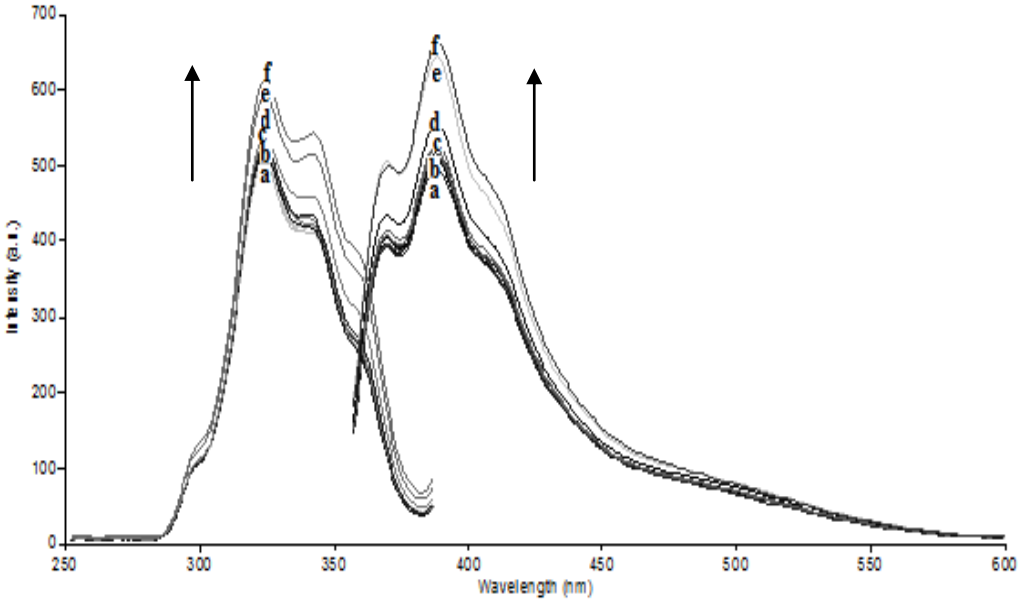

Figure 5.15 pH induced emission characteristics PVC doped A13 in the pH range of 7.50-11.50. Emission spectra: ex 345 nm; em 355–600 nm; Excitation spectra: em 400 nm; ex 250–390nm; pH: (a)7.50; 8.00 (b)8.50; 9.00; 9.50 (c)10.00 (d)10.50 (e)11.00 (f)11.50

Emission based relative signal changes of PVC doped A8 and A13 dyes were not as good as absorption based ones. Absorption based response of A8 and A13 dyes were resulted with 100 % relative signal change in the basic region of the pH scale. However, the highest atteined emission based relative signal changes for the same dyes were around 40-45%.

5.3.3 Response of PVC Doped A8 and A13 to Different Cations and Anions

Response of PVC doped A8 and A13 to polyvalent metal ions was investigated by exposure to 10^{-5} M solutions of Ca^{2+}, Ag^{+}, Ni^{2+}, Al^{3+}, Mn^{2+}, Bi^{2+}, Co^{2+}, Hg^{+}, Hg^{2+}, Pb^{2+}, Cd^{2+}, Zn^{2+}, Mg^{2+}, Sn^{2+}, Fe^{2+}, Fe^{3+}, Cu^{2+}, Cr^{3+}, V^{4+}, Mo^{2+}, Sb^{3+} and Y^{3+}. Response of PVC doped thin films of A8 and A13 to anions was also investigated by exposure to SO_4^{2-}, I^{-}, Cl^{-}, NO_2^{-}, Br^{-}, NO_3^{-}, PO_4^{2-}, PO_4^{1-}, HCO_3^{-} and OH^{-}. Figure 5.16 and 5.17 reveal absorption-based response of PVC doped A8 and A13 to the metal cations and some anions in BES buffered solutions at pH 7.0. Results were plotted as relative signal changes, $(A - A_o)$, where A is the absorption intensity of the sensor membrane after exposure to ion-containing solutions and A_o is the absorption intensity of the sensor slide in ion-free buffer solution.

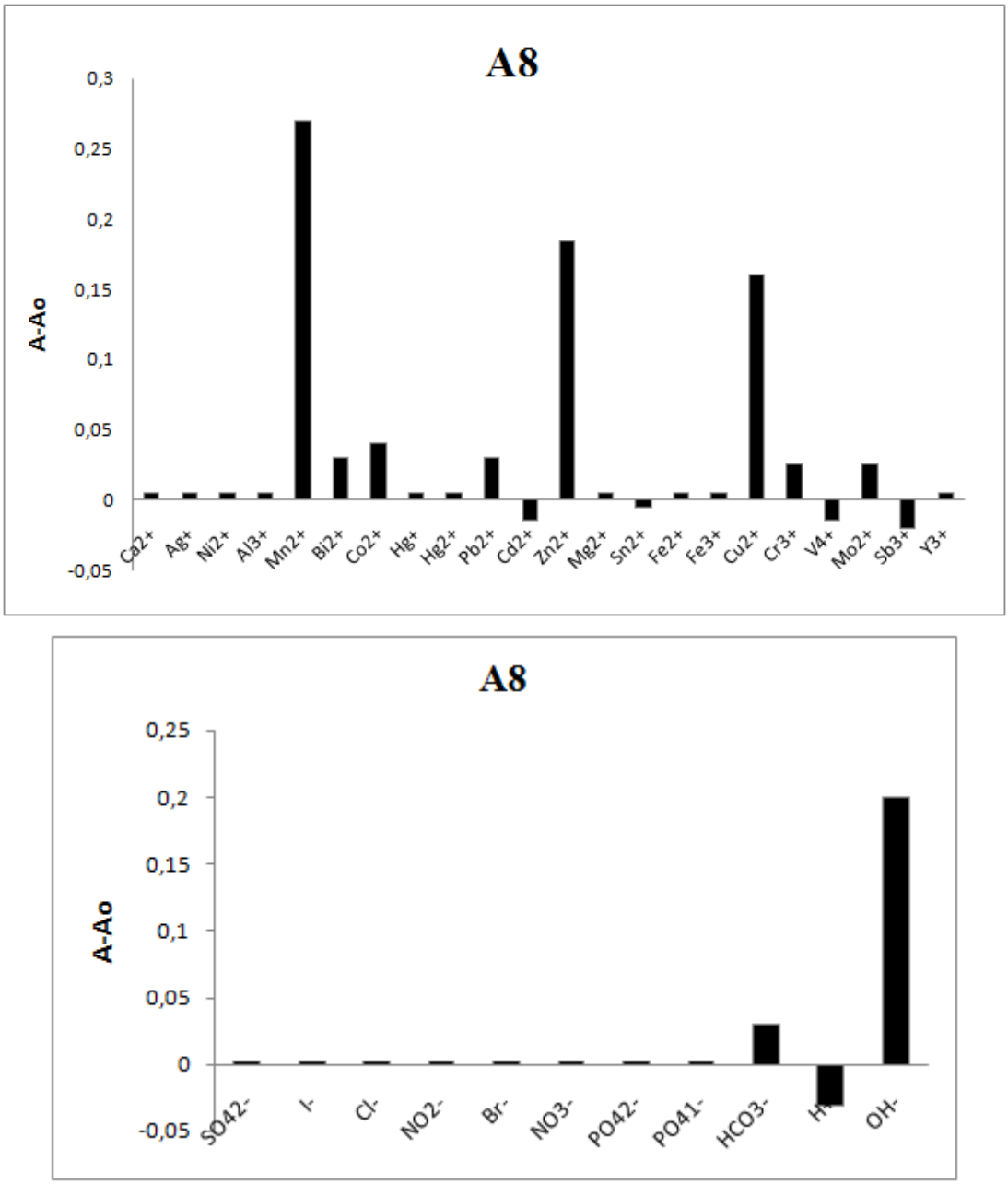

Figure 5.16 Metal-ion and anion response tests results for A8. Results are plotted in terms of signal changes, (A - A_o), where A is the absorbance intensity of the sensor membrane after exposure to ion-containing solutions and Ao is the absorption intensity of the sensor slide in ion-free buffer solution.

The PVC doped A8 dye exhibited absorption based response to Mn^{2+}, Zn^{2+} and Cu^{2+} ions at 507 nm, 530 nm and 535nm, respectively.

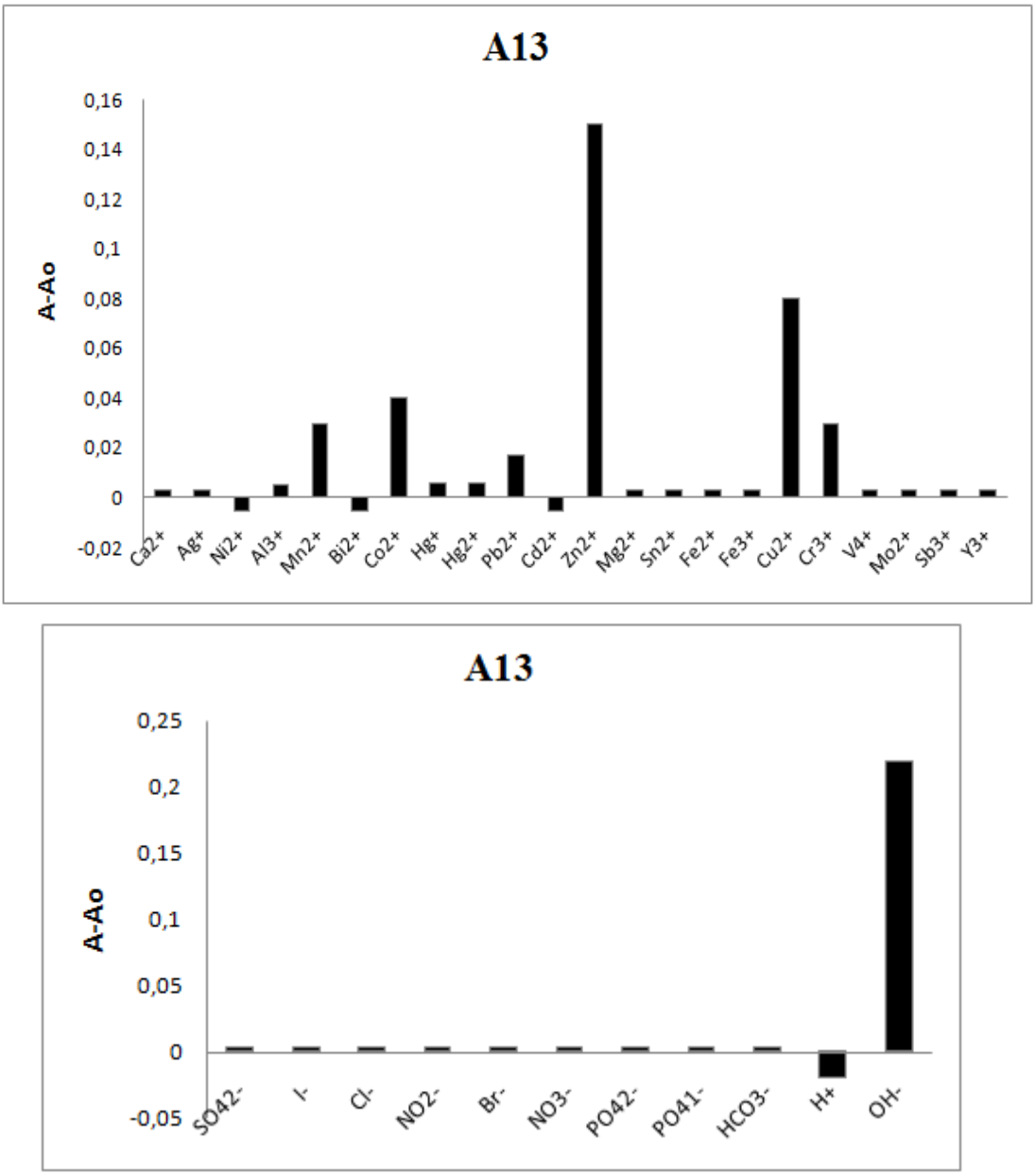

Figure 5.17 Metal-ion and anion response test results for A13. Results are plotted in terms of signal changes, (A - A_o), where A is the absorbance intensity of the sensor membrane after exposure to ion-containing solutions and Ao is the absorption intensity of the sensor slide in ion-free buffer solution.

Similarly, the PVC doped A13 dye exhibited absorption based response to Zn^{2+} and Cu^{2+} ions at 505 nm and 535nm. Except that of Mn^{2+}, Zn^{2+} and Cu^{2+}; none of the employed ions produced a significant response when interfaced with dye doped PVC membranes. Figure 5.18 and 5.19 shows metal-ion response spectra of Mn^{2+}, Zn^{2+} and Cu^{2+} for A8 and A13 at different maximum absorbsion point.

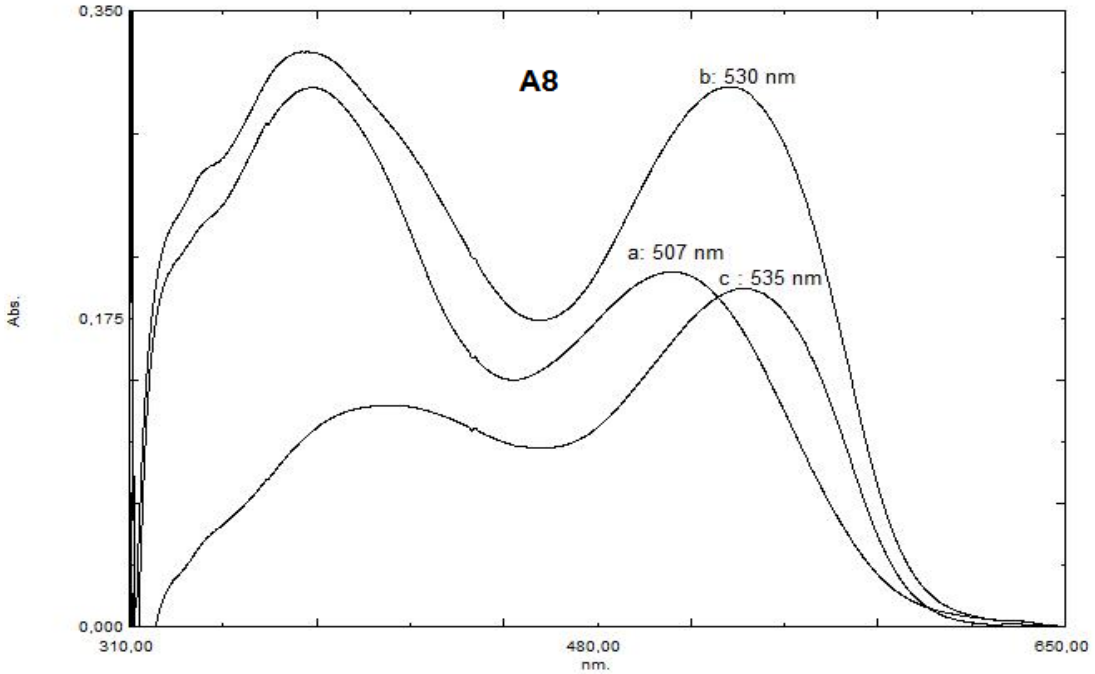

Figure 5.18 Metal-ion response spectra for A8. In presence of metal cations a: Cu^{2+} = 507 nm, b:Mn^{2+}= 530 nm and c: Zn^{2+} = 535nm.

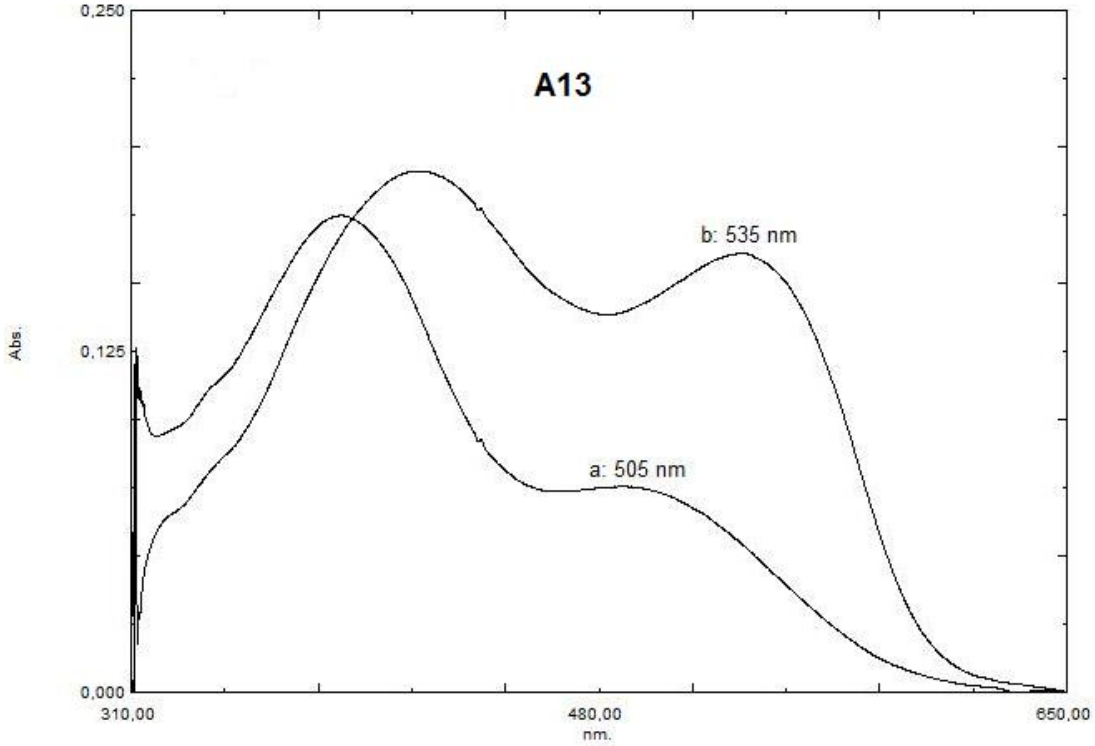

Figure 5.19 Metal-ion response spectra for A 13. In presence of metal cations a: Cu^{2+} = 505 nm and b:Zn^{2+} = 535nm.

5.3.4 Calibration Graph of PVC Doped A8 and A13 Dyes for Mn^{2+}, Zn^{2+} and Cu^{2+}

Absorption based metal response of immobilized A8 and A13 dyes were recorded after exposure to different concentrations of metal solutions. All of the employed dyes exhibited and increasing response in signal intensity in the concentration range of $1x10^{-9}$ - $1x10^{-2}$M. Different concentrations of Standard metal solutions were prepared freshly from 1.10^{-1} mol L^{-1} stock solution before the measurements and diluted with 1.0×10^{-2} M BES buffers of pH 7.0. Standard metal solutions of Mn^{2+}, $Zn^{2+}$and Cu^{2+} were added into the sensing agent-containing cuvette, and the changes in absorption intensity caused by addition of different concentrations of Mn^{2+}, Zn^{2+} and Cu^{2+} were measured.

Figure 5.20, 5.21 and 5.22 show the absorption-based response of the PVC doped A8 dyes to Mn^{2+}, $Zn^{2+}$and Cu^{2+} solutions. Figure 5.23 and 5.24 shows the absorption-based response of the PVC doped A13 dyes to Zn^{2+} and Cu^{2+} solutions.

The original pale yellow of PVC doped A8 turned to pinky red, dark yellow and pink when exposed to solutions of Mn^{2+}, Zn^{2+} and Cu^{2+} respectively. Similarly, original pale-yellow color of A13 was turned to dark yellow with $Zn^{2+}$and did not chance with Cu^{2+}.

Concentration dependent absorption based responses and calibration graphs of the above mentioned PVC doped dyes were shown in the following five Figures (See Figure 5.20, 5.21, 5.22, 5.23 and 5.24).

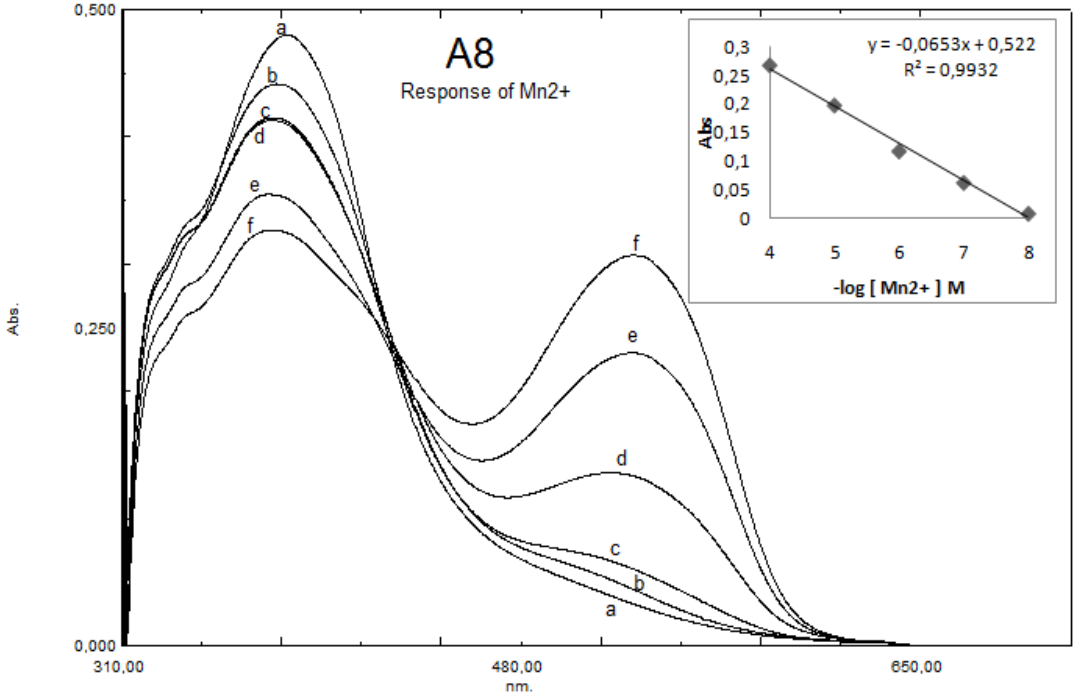

Figure 5.20 Absorption based spectra of PVC doped A8 for Mn^{2+} (a)Blank (free buffer); (b)$1x10^{-8}$ M; (c)$1x10^{-7}$ M; (d)$1x10^{-6}$ M; (e)$1x10^{-5}$ M; (f)$1x10^{-4}$ M and Absorption based calibration plot of PVC doped A8 for Mn^{2+}

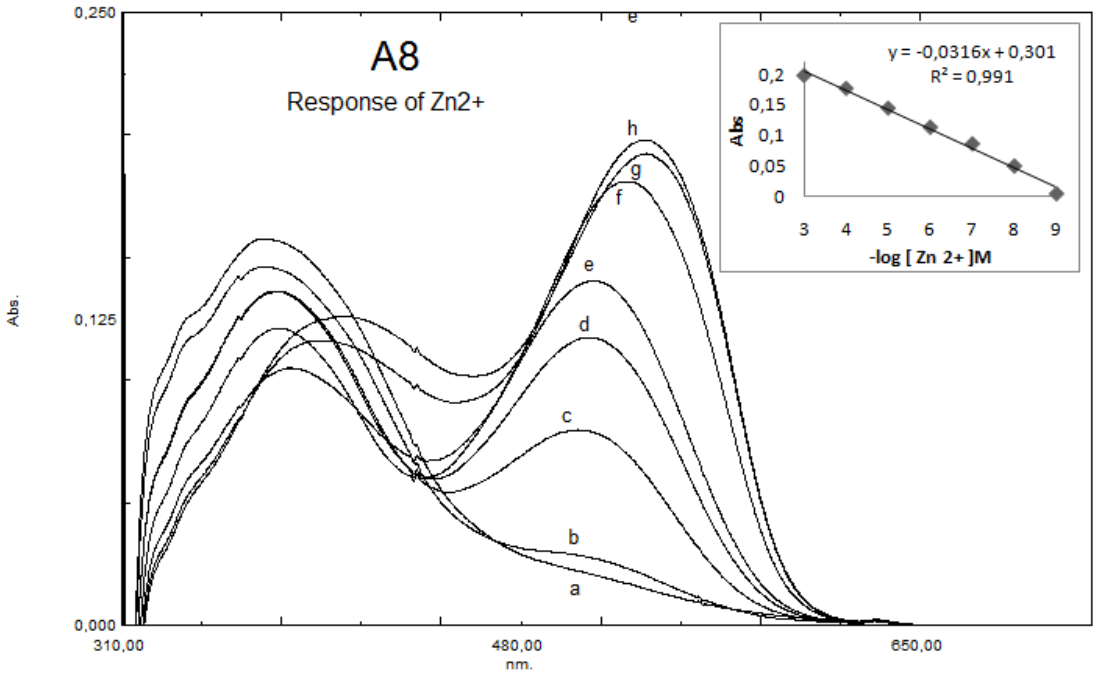

Figure 5.21 Absorption based spectra of PVC doped A8 for Zn^{2+} (a)Blank (free buffer); (b)$1x10^{-9}$ M; (c)$1x10^{-8}$ M; (d)$1x10^{-7}$ M; (e)$1x10^{-6}$ M; (f)$1x10^{-5}$ M; (g)$1x10^{-4}$ M; (h)$1x10^{-3}$ M and Absorption based calibration plot of PVC doped A8 for Zn^{2+}

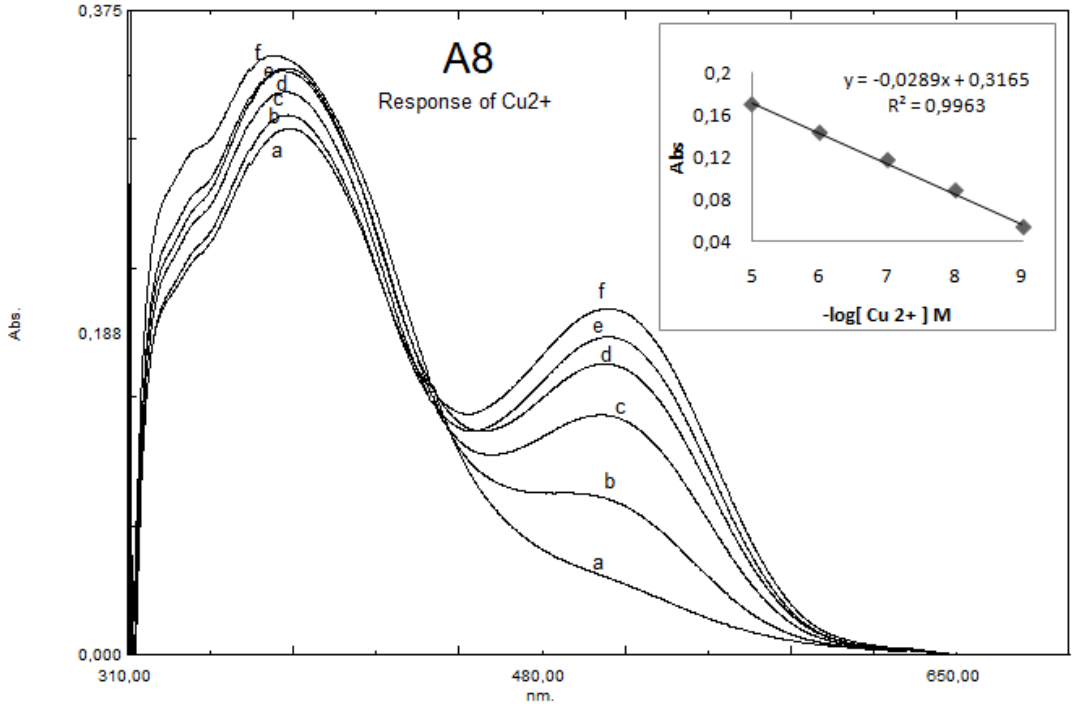

Figure 5.22 Absorption based spectra of PVC doped A8 for Cu^{2+} (a)Blank (free buffer); (b)$1x10^{-9}$ M; (c)$1x10^{-8}$ M; (d)$1x10^{-7}$ M; (e)$1x10^{-6}$ M; (f)$1x10^{-5}$ M; and Absorption based calibration plot of PVC doped A8 for Cu^{2+}

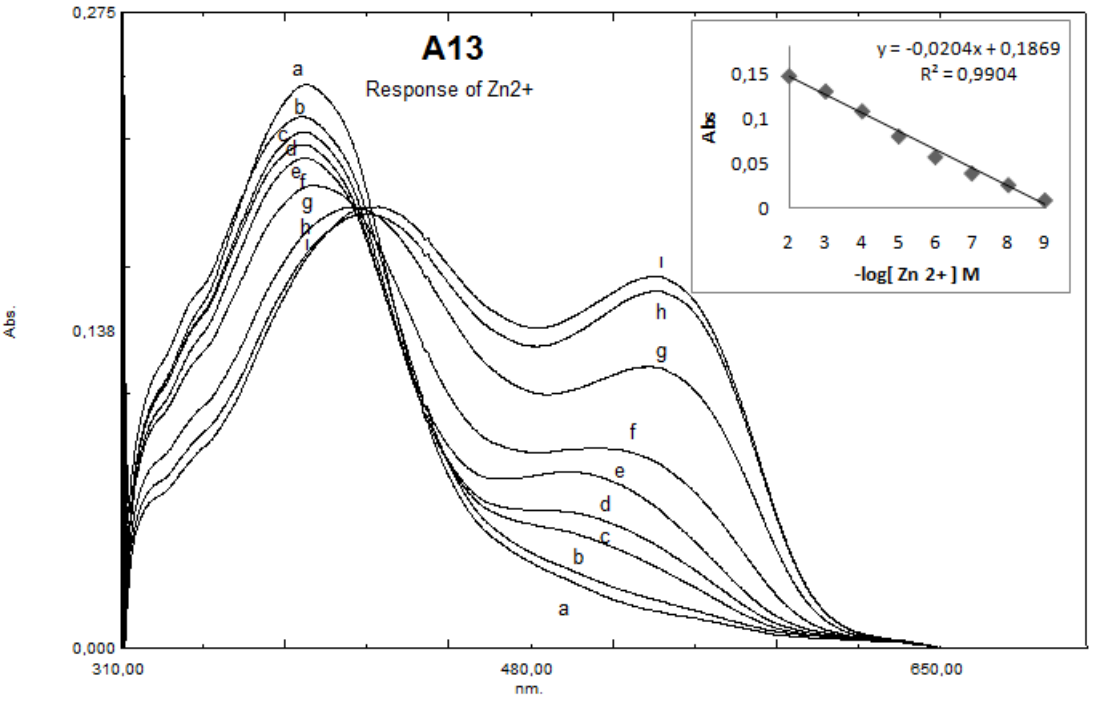

Figure 5.23 Absorption based spectra of PVC doped A13 for Zn^{2+} (a)Blank (free buffer); (b)$1x10^{-9}$ M; (c)$1x10^{-8}$ M; (d)$1x10^{-7}$ M; (e)$1x10^{-6}$ M; (f)$1x10^{-5}$ M; (g)$1x10^{-4}$ M; (h)$1x10^{-3}$ M ; (ı)$1x10^{-2}$ M and Absorption based calibration plot of PVC doped A8 for Zn^{2+}

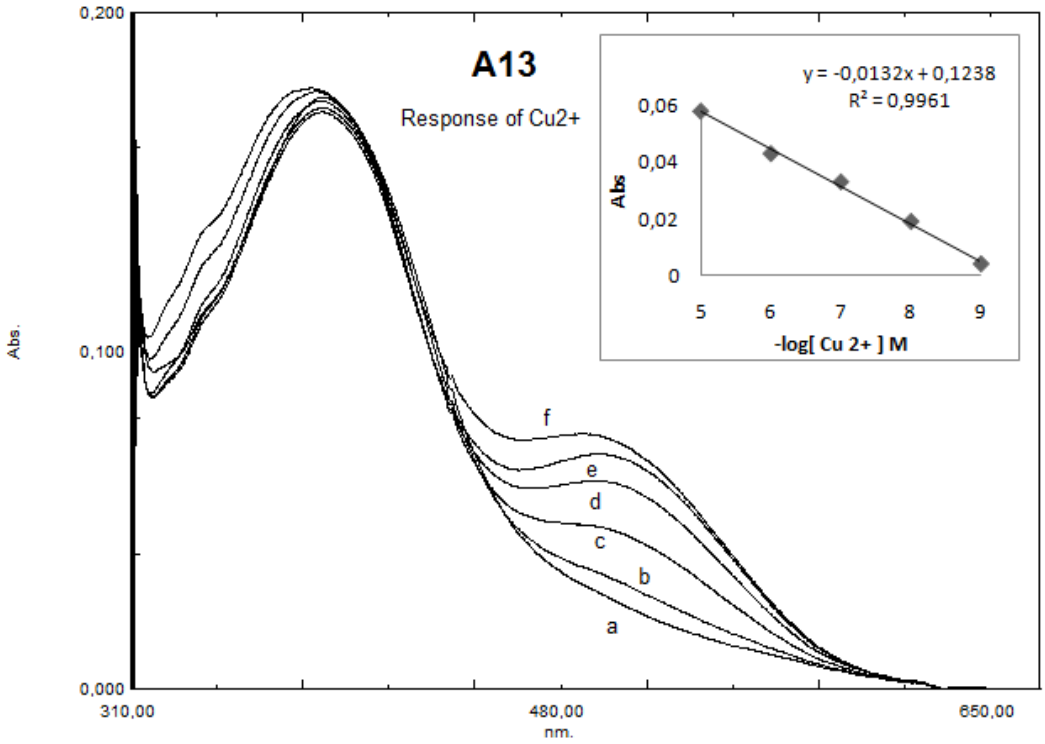

Figure 5.24 Absorption based spectra of PVC doped A13 for Cu^{2+} (a)Blank (free buffer); (b)$1x10^{-9}$ M; (c)$1x10^{-8}$ M; (d)$1x10^{-7}$ M; (e)$1x10^{-6}$ M; (f)$1x10^{-5}$ M and Absorption based calibration plot of PVC doped A8 for Cu^{2+}

5.3.5 Determination of Manganese (II), Zinc (II) and Copper (II) Ions in Geothermal Water Samples Using A8 and A13 as Selective Metal Reagent

After calibration studies, geohermal water samples were tested in the same experimental setup. The recorded absorption intensities of the geothermal water samples were employed to the calibration equations. Solution of the calibration equations was yielded the Mn ve Zn concentration of the geothermal water samples. Comparative results were shown in Table 5.2.

Figure 5.25 shows absorption based response spectra of PVC doped A8 and A13 for geothermal water samples.

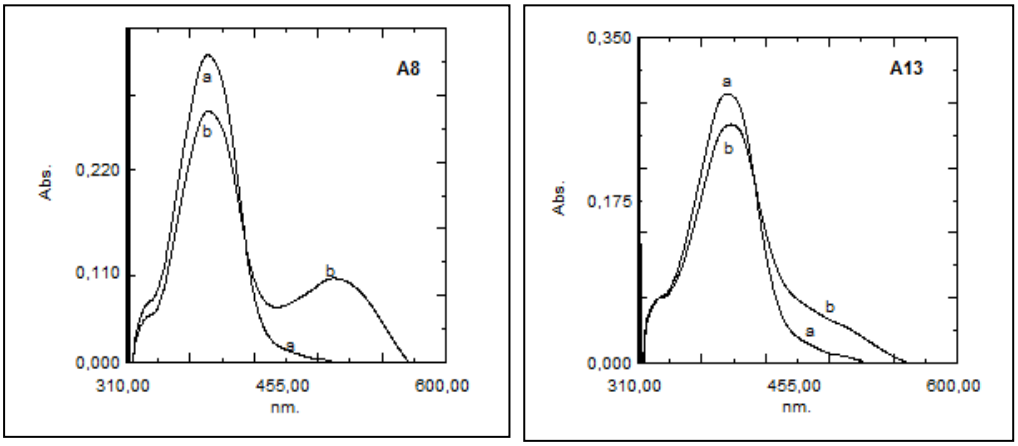

Figure 5.25 Absorption based response spectra of PVC doped A8 and A13 for geothermal water samples (a) Blank (free buffer); (b) Geothermal water Sample.

Table 5.2 Mn and Zn concentrations determined by spectral method and taken from wall of Pamukkale antique pool.

	Taken from wall of Pamukkale antique pool		**A8**	**A13**
	ppm (mgL^{-1})	M ($molL^{-1}$)	($molL^{-1}$)	($molL^{-1}$)
Mn	0.02	$3.64x10^{-7}$	$8.74x10^{-7}$	--
Zn	0.03	$4.59x10^{-7}$		$3.89x10^{-7}$
Cu	-	-	-	-

5.4 Conclusion

In this chapter, spectrophotometric metal analysis results of geothermal water samples of Pamukkale Antique Pool were given. İndicator dyes namely [5-phenylazo-8-quinolinol] (A-8) and [5-(4-clorophenylazo)-8-quinolinol] (A–13) were offered for the first time for absorption based analysis of Mn^{2+}, Zn^{2+} and Cu^{2+}**.**

The indicator dyes were characterized in the different solvents; ethanol (EtOH), dichloromethane (DCM), tetrahydrofurane (THF) and Toluene/Ethanol (To: EtOH) mixture (80:20) and in solid matrix of PVC. Maximum absorption wavelength (λ_{abs}) and molar extinction coefficients (ε) of the indicators were determined with UV-Vis spectrophotometer in all of the employed matrices.

Acidity constant values of two different indicator dyes were calculated in ethanol and polyvinylchloride. Cross sensitivities of the indicator dyes to other cations and anions was also tested and evaluated.

CHAPTER SIX

CONCLUSION

This thesis consists of two complimentary chapters. In the first part of the thesis (chapter 3), simultaneous ion chromatographic analysis of six cations (lithium, sodium, amonnium, potassium, magnezium and calcium) in geothermal water samples were performed by single cloumn ion chromatography method. Some validation tests and the optimum conditions for the determination of cations were studied. Analysis of cations was performed by injection of samples to the chromatographic system after filtration and/or dilution. The precision and accuracy of the method were tested at three different concentration levels for each standard. In order to evaluate effectiveness of the method, certified reference standards at three different dilution levels were applied initially to the ion chromatography. Subsequently, the same instrumental approach was applied to field samples. Cation concentrations of known certified reference standards (CRS), their calibration related data and results obtained from control samples are presented. The final calibration curves of CRS resulted in >99.999 % correlation coefficient values except that of calibration curve of ammonium.

Chromatographic system-suitability parameters (asymmetry (EP), resolution and plate number (N) values) were determined for six different calibration points. The asymmetry values of high concentrations of lithium and sodium exhibited an excellent peak symmetry. All other measured asymmetry values were acceptable for the employed calibration ranges. The resolution values were calculated with respect to Ca^{2+} and it can be concluded that the resolution performance of the column was very satisfactory in all cases. In our case number of plates are quite good for all calibration points.

The validation studies and accuracy of the method were tested at three different concentration levels for each standard. Recovery studies were performed by adding standards in to the geothermal water and drinking water samples. For geothermal

water samples recovery tests was performed between two successive months. The geothermal water samples were treated with added different concentrations of certified reference standards, which were diluted in the ratio of 1:40, 1:25 and 1:20.

In geothermal water samples, the deviations in recovery values (%) were less than 10 %, except that of ammonium. However, in ammonium the deviations may extend to 20 %. Drinking water samples exhibited excellent recovery values with respect to geothermal water samples. This can be referred to the rich heavy metal content of geothermal water samples, as well as similar affinities of sodium and ammonium cations when their ratio has been extremely different.

Precision was also assessed as the percentage relative standard deviation (%RSD) of both repeatability (within-day) and reproducibility (between-day and different concentrations) for geothermal water samples from Bölmekaya location.

Six cations (lithium, sodium, ammonium, potassium, magnesium, and calcium) in geothermal water samples, that were collected daily during twelwe months (July 2007- June 2008) from Denizli Pamukkale Antique Pool, were tested and analyzed with ion chromatographic method. Lithium, sodium, potassium, magnesium and calcium were found to be major ions in Pamukkale geothermal water samples. Ammonium concentrations were found to be zero. Average concentrations of lithium, sodium, potassium, magnesium and calcium were found to be 0.0950, 44.135, 5.6253, 88.0932 and 425.0893 mgL^{-1} respectively. Sodium and calcium measurements were performed after 1:4 dilution. SD and RSD values of 320 real geothermal water samples acquired during 12 months were evaluated.

The second part (Chapter 5) consists of analysis of geothermal water samples by spectrophotometric method for Mn^{2+}, Zn^{2+} and Cu^{2+}. Indicator dyes namely [5-phenylazo-8-quinolinol] (A-8) and [5-(4-clorophenylazo)-8-quinolinol] (A–13) were offered for the first time for absorption based analysis of Mn^{2+}, Zn^{2+} and Cu^{2+}. The indicator dyes were characterized in the different solvents and in solid matrix of PVC. UV-Vis spectrophotometer dependent photophysical characteristic of the indicators

were determined with in all of the employed media. Acidity constants and cross sensitivities to other cations and anions was also tested and evaluated. For both of the employed dyes the responses to Mn and Zn were excellent in PVC matrix.

REFERENCES

Afton, S., Kubachka, K., Catron, B., & Caruso, J. A. (2008). Simultaneous characterization of selenium and arsenic analytes via ion-pairing reversed phase chromatography with inductively coupled plasma and electrospray ionization ion trap mass spectrometry for detection Applications to river water, plant extract and urine matrices. *Journal of Chromatography A, 1208,* 156–163.

An introduction to ion chromatography. (n.d.). Retrieved December 8, 2008, from http://www.metrohm.com.cn/administrator/resource/upfile/ic_theory_20041011_e.pdf

Anticó E., Lerchi, M., Rusterholz, B., Ackermann, N., Badertscher, M., Valiente, M., & Pretsch, E. (1999). Monitoring Pb2+ with optical sensing films. *Anal .Chim. Acta, 388,* 327.

Antonio Jurado-Gonza´lez, J., Dolores Galindo-Rian˜o, M., & Garcı´a-Vargas, M. (2003). Factorial designs applied to the development of a capillary electrophoresis method for the analysis of zinc, sodium, calcium and magnesium in water samples. *Talanta*, *59,* 775-783.

Bakker, E. & Simon, W. (1992). Selectivity of ion-sensitive bulk optodes. *Anal. Chem., 64 (17),* 1805-1812.

Buytenhuys, F. A. (1981). Ion chromatography of inorganic and organic ionic species using refractive index detection. *Journal Of Chromatography, 218,* 57.

Camman, K., Guibault, G., Hall, E., Kellner, R., Schmidt, H. L., & Wolfbeis, O. S. (1996). The Cambridge Definition of Chemical Sensors.

Cattrall, R. W. (1997). Chemical Sensors. *Oxford University Press Inc*. New York.

Chakrapani, G., Murty, D.S.R., Mohanta, P.L., & Rangaswamy, R. (1998). Sorption of PAR-metal complexes on activated carbon as a rapid preconcentration method for the determination of Cu, Co, Cd, Cr, Ni, Pb and V in ground water. *Journal Of Gochemical Exploration, 63* (2), 145-152.

Chan, W. H., Yang, R. H., & Wang, K. M. (2001). Development of a mercury ion-selective optical sensor based on fluorescence quenching of 5,10,15,20-tetraphenylporphyrin. *Anal. Chim. Acta., 444*, 261.

Chen, Z., Adams, M. A. (1998). A metallic cobalt electrode for the indirect potentiometric determination of calcium and magnesium in natural waters using flow injection analysis. *Talanta, 47*, 779–786.

Chrompack, Inc. (1981). *Bridgewater*. New Jersey. Chrompack Topics. Vol. 8.

Diamond, D. (1998). Principles of Chemical and Biological Sensors. *Wiley & Sons.* New York.

Dionex Referance Library. (2007). [Recorded by Dionex Corporation], On [CD].

Dissolved Mass in Groundwater. (n.d.). Retrieved December 12, 2008, from faculty.kfupm.edu.sa/es/shaibani/16dissolved%20mass%20in%20gw.ppt

Eith, C., Kolb, M., Seubert, A., & Viehweger, K. H. (2001). *Practical Ion Chromatograph.* Retrieved December 28, 2008, from www.metrohmpeak.com/pdf/8_792_5003_practical. Pdf.

Fátima Barroso, M., Silva, A., Ramos S., Oliva-Teles, M.T., Delerue-Matos, C., Goreti, M., Sales, F., & Oliveira, M.B.P.P. (2009). Flavoured versus natural waters: Macromineral (Ca, Mg, K, Na) and micromineral (Fe, Cu, Zn) contents. *Food Chemistry, 116,* 580–589.

Förstner, U., & Wittmann, G. T. (1981). Metal Pollution in the Aquatic Environment. *Springer*, Berlin.

Fresenius, W., Quentin, K. E., & Schneider, W. (1988). *Water Analysis*. *Springer*, Berlin.

Fries, E., & Klasmeier, J. (2009). Analysis of potassium formate in airport storm water runoff by headspace solid-phase microextraction and gas chromatography–mass spectrometry. *Journal of Chromatography A, 1216*, 879–881.

Fritz, J.S., & Gjerde, D.T. (2000). *Ion chromatography* (3th ed.) Germany: Wiley-WHC

Gros, N., Camões, M.F., Oliveira, C., & Silva, M.C.R. (2008). Ionic composition of seawaters and derived saline solutions determined by ion chromatography and its relation to other water quality parameters. *Journal of Chromatography A, 1210*, 92–98.

Groundwater protection. (n.d.). Retrieved December 12, 2008, from http://www.bafu.admin.ch/gewaesserschutz/01338/index.html?lang=en

Gustavo Gonza´lez, A., Angeles Herrador, M., & G. Asuero, Agustı´n. (1998). Intra-laboratory testing of method accuracy from recovery assays. *Talanta, 48*, 729–736.

Haddad, P.R., & Heckenberg, A.L. (1982). High-performance liquid chromatography of inorgangic and organic ions using low-capacity ion-exchange columns with indirect refractive index detection. *Journal of Chromatography A, 252*, 177-184.

Haddad, P.R., Jackson, P.E., *«Ion Chromatography: Principles and Applications»,* 1st ed. (1990), J. Chromatogr. Library Vol. 46, Elsevier Verlag, Amsterdam

Henshall, A., Rabin, S., Statler, J., & Stilian, J. (1992). Recent development in ion chromatography detection: the self-regenerating suppressor. *American Laboratory , 24*, 20R.

Hershcovitz, H., Yarnitsky, Ch., & Schmuckler, G. (1982). Ion chromatography with potentiometric detection. *Journal of Chromatography, 252,* 113.

Inorganic Chemicals in Ground Water. (n.d.). Retrieved December 12, 2008, from http://jan.ucc.nau.edu/~doetqp-p/courses/env302/lec35/LEC35.html

International Conference on Harmonization. (2005). Validation of Analytical Procedures: Text and Methodology Q2(R1), ICH, Geneva, Switzerland.

Ion Chromatography for Electronic Assemblies & Bare Boards. (n.d.). Retrieved December 25, 2008, from http://www.residues.com/ion_chromatography.html

Ion chromatography. (n.d.). Retrieved December 25, 2007, from www.thairohs.org/index.php*?*

Ion chromatography. (n.d.). Retrieved December 25, 2008, from www.bioscreen.com/pdf/tech%20bulletin%20ionchromatographybulletin.pdf

Ion Exchange Chromatography. pdf (n.d.). Retrieved December 16, 2008, from sbio.uct.ac.za/Sbio/documentation/Ion_exchange_chromatography.pdf

Klockenkämpfer, R. (1997). Total-Reflection X-ray Fluorescence Analysis. *Wiley,* New York.

Komy, Z. R. (1993). Determination of trace-metals in nile river and ground-water by differential-pulse stripping voltammetry. *Mikrochimica Acta, 111* (4-6), 239-249.

Lerchi, M., Bakker, E., Rusterholz, B. & Simon, W. (1992). Lead-selective bulk optodes based on neutral ionophores with subnanomolar detection limits. *Anal. Chem., 64 (14),* 1534-1540.

Levin, S. *Ion Exchange Chromatography*. Retrieved December 25, 2008, from www.forumsci.co.il/hplc/ic_pharm.pdf

Liu. Y., Wu. D., Li. J., & Ga, R. (1999). Determination of trace iron(III) and molybdenum(VI) in ground water by pyrocatechol resin-phase spectrophotometry. *Spectroscopy And Spectral Analysis, 19* (5), 694-696.

Mahendra, N., Gangaiya, P., Sotheeswaran, S., & Narayanaswamy R. (2002). Investigation of a Cu(II) fibre optic chemical sensor using fast sulphon black F (FSBF) immobilised onto XAD-7. *Sens. Actuators B, 81,* 196.

Malcik, N., Oktar, O., Ozser, M. E., Caglar, P., Bushby, L., Vaughan, A., Kuswandi B., & Narayanaswamy, R. (1998). Immobilised reagents for optical heavy metal ion sensing. *Sens. Actuators B, 53,* 211.

Mascini, M. (1971). Potentiometric titrations with solid-state ion-selective electrodes, Determination of calcium and magnesium in water analysis. *Analytica Chimica Acta, 56,* 316-321.

Mayr, T. (2002). Optical Sensors for the Determination of Heavy Metal Ions. *Institut für Analytische Chemie:* Chemo- und Biosensorik an der Universität Regensburg.

Merian, E. (1991). Metals and their Compounds in the Environment, VCH, Weinheim.

Morf, W.E., Seiler, K., Rusterholz, B. & Simon, W. (1990). Design of a novel calcium-selective optode membrane based on neutral ionophores. *Anal. Chem., 62,* 738.

Morris, J. & Fritz, J.S. Ion Chromatography of metal cations on carboxylic acid. *J. Chromatography*. *602*, 111, 1992.

Motellier, S., Petit, S., & Decambox, P. (2000). Quantitative capillary electrophoretic analysis for calcium and magnesium in sodium–matrix waters. *Analytica Chimica Acta, 410,* 11–23.

Muller, J. (1999). Determination of inorganic arsenic(III) in ground water using hydride generation coupled to ICP-AES (HG-ICP-AES) under variable sodium boron hydride ($NaBH_4$) concentrations. *Fresenius Journal Of Analytical Chemistry, 363* (5-6), 572-576.

Niedzielski, P. (2005). The new concept of hyphenated analytical system: Simultaneous determination of inorganic arsenic(III), arsenic(V), selenium(IV) and selenium(VI) by high performance liquid chromatography-hydride generation-(fast sequential) atomic absorption spectrometry during single analysis. *Analytica Chimica Acta, 551* (1-2), 199-206.

Nyman, J., & Ivaska, A. (*1995.)* Spectrophotometric determination of calcium in paper machine white water by sequential injection analysis. *Analytica Chimica Acta, 308,* 286-292.

Oehme, I., & Wolfbeis, O. S. (1997). Fundamental Review – Optical Sensors for Determination of Heavy Metal Ions. *Microchim. Acta, 126*, 177.

Ohta, K., & Tanaka, K. (1998). Simultaneous determination of common inorganic anions, magnesium and calcium ions in various environmental waters by indirect UV-photometric detection ion chromatography using trimellitic acid-EDTA as eluent. *Analytica Chimica Acta, 373,* 189-195.

Oter, O. (2007). Investigation of Sensor Characteristics of Some Chromoionophore Structures in Polymer and Sol-Gel Matrices. Dokuz Eylul University Graduate School of Natural and Applied Sciences: Izmir

Otero-Roman´ı, J., Moreda-Pi˜neiro, A., Bermejo-Barrera, P., & Martin-Esteban, A. (2009). Inductively coupled plasma – optical emission spectrometry / mass spectrometry for the determination of Cu, Ni, Pb and Zn in seawater after ionic imprinted polymer based solid phase extraction. *Talanta.*

Ozcan. A., & Yilmaz. S. (2005). Determination of boron in the waters of Troia by inductively coupled plasma-atomic emission spectrometry (ICP-AES). *Journal Of The Serbian Chemical Society*, *70* (10), 1219-1227.

Phillip, M. *Geochemistry*. Retrieved December 8, 2008, from geoheat.oit.edu/pdf/bulletin/bi015.pdf

Rong, L., Lim, L. W., & Takeuchi, T. (2007). Determination of iodide in seawater using C30 column modified with polyoxyethylene oleyl ether in ion chromatography. *Talanta, 72*, 1625–1629.

Sağlam, A. (2006). 8-hidroksikinolinin Diazolanan Çeşitli Karbosiklik ve Heterosiklik Aminlerle Tepkimesinden Azo Bileşiklerinin Sentezi ve Bazı Özelliklerinin İncelenmesi. Gazi University Graduate School of Natural and Applied Sciences: Ankara.

Sallee, D. *Essentials of Geology*. Retrieved December 8, 2008, from www.geog.unt.edu/~sallee/geology%201610/geology%201610/chapter%2012%20groundwater.pdf

Sanchez-Pedreno, C., Ortuno, J. A., Albero, M. I., Garcia, M. S., & Valero, M. V. (2000). Development of a new bulk optode membrane for the determination of mercury (II). *Anal. Chim. Acta, 414*, 195.

Schwedt, G., & Fresenius, Z., *Anal. Chem.* 320 (1985) 423.

Seiler, K. & Simon, W. (1992). Theoretical aspects of bulk optode membranes. *Anal. Chim. Acta*, 266, 73-87.

Skoog, D.A., & Leary, J.J. (1992). *Ion Chromatography in Principles of instrumental analysis.* (4th. ed.) (654–655–656) USA: Saunders College

Small, H. (1989*). Ion chromatography*. New York: Plenum press

Small, H., Stevens, T. S., & Bauman, W. G. (1975). Novel ion-exchange chromatographic method using conductimetric detection. *Analytical Chemistry, 47, 1801.*

Spichiger-Keller, U. E. (1998). Chemical Sensors and Biosensors for Medical and Biological Applications. *Wiley-VHC*. Weinheim.

Stevens, T. S., Davis, J. C., & Small, H. (1981). Hollow fiber ion exchange suppressor for ion chromatography. *Analytical Chemistry, 53,* 1488-1492.

Stillian, J. (1985). An improved suppressor for ion chromatography. *LC Magazine, 3,* 802-805.

Strasburg, R. F., Fritz J. S., Berkowitz, J. & Schmuckler, G. (1989). Injection peaks in anion chromatography. *Journal of Chromatography, 482* (2), 343-350.

Strong, D. L., & Dasgupta, P.K. (1989). Electrodialytic membrane suppressor for ion chromatography. *Analytical Chemistry , 61*, 939-945.

Tartari G. A., Marchetto A., & Mosello, R. (1995). Precision and linearity of inorganic analyses by ion chromatography. *Journal of Chromatography A, 706*, 21-29.

The Cation Micro Membrane Suppressor. (n.d.). http://www.dionex.com/en-us/columns-accessories/accessories-suppressors/cons5341.html

The Micro Membrane Suppressor. (n.d.). http://www.dionex.com/en-us/columns accessories/accessories-suppressors/cons5339.html

The principle of ion exchange chromatography. (n.d.). Retrieved December 10, 2007, from http://www.rmpr.cnrs.fr/j1pr/5__techniques_de_purification/ion_exchange.swf

V. Barreto, L. Bao, A. Bordunov, C. Pohl and J. Riviello, *Electrolytic suppression in ion chromatography*. Paper No. 958 Pittcon'99 Orlando, FL

Vaaramaa, K., & Lehto, J. (2003). Removal of metals and anions from drinking water by ion exchange. *Desalination, 155* (2), 157-170.

Vaughan, A. A., & Narayanaswamy R. (1998). Optical fibre reflectance sensors for the detection of heavy metal ions based on immobilised Br-PADAP. *Sens. Actuators B, 51*, 368.

Wang, P., Wu, J., Chen, H., Lin, T., & Wu, C. (2008). Purge-and-trap ion chromatography for the determination of trace ammonium ion in high-salinity water samples. *Journal of Chromatography A, 1188*, 69–74.

Weiss, J. *Handbook of Ion Chromatography*. Retrieved December 26, 2008, from http://media.wiley.com/product_data/excerpt/19/35272870/3527287019.pdf

Weiß, J. *Ion enchromatographi*, 2. Aufl. (1991). Verlag Chemie, Weinheim.

Wolfbeis, O. S. (Ed.). (1991). *Fiber Optic Chemical Sensors and Biosensors,* Vol. 1&2, CRC, Boca Raton.